GROUNDWATER FLOW AND QUALITY OF COASTAL AQUIFERS: CASE STUDY OF MOMBASA NORTH COAST, KENYA

TEMITOPE EZEKIEL IDOWU

(CE300-0005/15)

A THESIS SUBMITTED TO PAN AFRICAN UNIVERSITY, INSTITUTE FOR BASIC SCIENCES, TECHNOLOGY AND INNOVATION IN PARTIAL FULFILMENT OF THE REQUIREMENT FOR THE DEGREE OF

MASTER OF SCIENCE IN CIVIL ENGINEERING (ENVIRONMENTAL AND ARID & SEMI-ARID LANDS OPTION)

2017

DECLARATION

This thesis is my original work and has not been presented for a degree in any other University.

Signature:……. **Date: ……..**

This thesis has been submitted for examination with our approval as University Supervisors.

Signature:…….. Date:……..

Prof Maurice Nyadawa

Civil Engineering, Jaramogi Oginga Odinga University of Science and Technology

Signature:…… Date:…….

Dr M. Korowe

Department of Physics, Jomo Kenyatta University of Agriculture and Technology

DEDICATION

To God Almighty and my ever supportive parents

ACKNOWLEDGEMENTS

My deepest gratitude goes to God Almighty, for the strength and wisdom from the start to the completion of this thesis. I wish to extend my profound gratitude to African Union commission who awarded me this scholarship to pursue a masters' degree for two years. All thanks to every individual directly or indirectly linked with this thesis, my two supervisors Prof Maurice Nyadawa and Dr Maurice K'Orowe – your support and guidance cannot be quantified. You were more than Supervisors, you are Mentors indeed. I feel indebted to every other person who played one role or the other in guiding and sharpening my research skills; Prof P. Home, Prof Kanali amongst others. My heartfelt appreciation also goes to Rose Waswa Malot of Regional Centre for mapping of Resources for Development (RCMRD) for her technical guidance in the application of GIS. A big thanks to John Kimathi of Chemistry department (JKUAT) for his priceless support. I am equally grateful to the entire staff of PAUSTI, JKUAT, AICAD and WRMA Mombasa Office for their direct and indirect supports towards making the research a success. My dear colleagues in PAUSTI, words will fail me in expressing how privileged I feel to have had you as colleagues. We have learned a lot from one another, I look forward to meeting us in great places contributing our quota to the growth of humanity, Africa and our respective countries. To my wonderful family back home, my dear parents Mr & Mrs Idowu; Engr A.R Azeez; Mrs B Olaniyan; and many others whose names are not included you are the best anyone could ever wish for. Thank you all for your moral support, encouragements from time to time and your prayers. My appreciation will be incomplete without mentioning my one and only Sister Olubunmi Idowu and my ever loyal and special friend Otemuyiwa Ayomide for their contributions to the quality of this work in terms of proof reading and editing. I love you all!!!

TABLE OF CONTENTS

LIST OF TABLES

LIST OF FIGURES

LIST OF APPENDICES

LIST OF ABBREVIATIONS AND ACRONYMS

3D- Three Dimensional

DEM- Digital Elevation Model

EC- Electrical Conductivity

ESRI- Environmental Systems Research Institute

GDP- Geographic Data Processing

GIS- Geographic Information System

GMS- Groundwater Modelling System

MOC- Method of characteristics

MODFLOW- **Mod**ular Finite-Difference **Flow** Model

MSL- Mean Sea level

MT3D/MT3DMS- modular three dimensional (3D) transport model

PBM- Process-Based Modelling

SRTM- Shuttle Radar Topography Mission

SWI- Seawater Intrusion

TDS- Total Dissolved Solids

USGS- United States Geological Survey

WRMA- Water Resources Management Authority

ABSTRACT

Groundwater is the most readily available source of freshwater in the hydrologic cycle, hence the importance of aquifers. However, these groundwater resources are prone to pollution in the wake of anthropogenic activities, over-exploitation and climate change related activities. Coastal aquifers are faced with additional unique problems of seawater intrusion which may be aggravated by climate change related challenges like sea level rise and coastal flooding. The aquifer of Mombasa, a coastal city, home to East Africa's busiest seaport is not an exception to these challenges. This study investigated the groundwater flow, quality and vulnerability to seawater intrusion of the coastal aquifer of Mombasa North Coast. This is a 74.2 km^2 region bounded by the Indian Ocean on the East, by creeks on the North and South and high elevated hills on the West. The hydrogeological characteristics, salinity and extent of seawater intrusion in the study area were assessed using statistical and geospatial methods. The statistical methods include the use of correlation coefficients, cross plots and piper plots. GALDIT overlay index was used to assess the vulnerability of the study area with the aid of ArcGIS while groundwater flow and solute transport were simulated with the aid of MODFLOW, MT3D and SEAWAT packages. In addition to secondary data obtained, three phases of field data such as static water levels and water quality parameters from boreholes/shallow wells were collected at pre-monsoon, the peak of rainy season, and post-monsoon in 2016. This was followed by laboratory analysis for Na, K, Mg, Ca, Cl, HCO_3 and SO_4 concentrations in the water samples obtained from the field. The results show that the study area is characterised by shallow unconfined aquifer with groundwater heads ranging from -1 to 33m above mean sea level irrespective of the seasons. The EC and TDS values were observed to have near perfect correlations with each other and generally high, as over 94% of the water samples exceeded WHO drinking water limit of 750 µS/cm and 500mg/l respectively. The pH of the groundwater was slightly alkaline but could be slightly acidic in the rainy season. Over 90% of the water samples had pH values within 6.5 and 8.5 the acceptable limit of WHO guidelines. The groundwater is generally marine in nature while there is a wide variation of the EC, TDS, NaCl, Na, K and Cl values within the aquifer. Over 50% of the water samples also had Na concentrations exceeding the WHO and Kenya drinking water limits of 200mg/l. Hence the groundwater is generally unfit for direct drinking. The salinity of the groundwater varies with seasons and groundwater recharge heavily influences the salinity of the groundwater.The aquifer is largely experiencing a moderate impact of seawater intrusion depending on the season with only

a few regions experiencing injurious impacts. This might be because of the current groundwater abstraction rates which are easily compensated by high annual rainfall above 1000mm. Over 50% of aquifer's coverage experiences moderate vulnerability to seawater intrusion, however, the aquifer is more vulnerable in the dry season than the wet season. The direction of groundwater flow is predominantly towards the north-eastern and southern part of the study area. Finally, solute transport simulation shows that concentrations of NaCl in the groundwater slightly reduced from the centre of the study area outwards from June (peak of rainy season) to September (post-monsoon). In view of the findings made, management and modification of the pumping scheme are recommended. This includes encouraging the digging of wells and boreholes to be as shallow as possible. The recommendations will help sustain the current quality of the groundwater and prevent further pollution of the groundwater.

CHAPTER ONE- INTRODUCTION

1.1 Background of study

Coastal areas all over the world experience comparatively higher net human migration than the inland areas, due in part to their functionality as hubs of commerce, industrialisation and international trade. Six megacities are expected to emerge by 2030 in Africa, 50% of them are coastal cities (WUP, 2014). Currently, population densities of coastal areas are about three times the global average (Small & Nicholls, 2003). Coastal areas only cover 5% of the world's surface, yet 50 – 70% of the human population in the globe is estimated to be occupying these coastal zones (Benoit et al, 2007). The resulting effects of these realities are increased water usage and potential over-exploitation of coastal groundwater (Darneault & Godinez, 2008). Groundwater is a very vital source of freshwater to humans for domestic, industrial and agricultural purposes. In fact, over 90% of the world's readily available freshwater is found as groundwater (Boswinkel, 2000; UNEP, 2008). Hence, groundwater is the principal source of freshwater provisioning in many parts of the world, especially in sub-Saharan Africa where water recycling and reuse is almost none existent.

The Water Exploitation Index (WEI), which is the mean yearly overall demand for freshwater divided by the long-term mean freshwater resources available, is observed to be very high in several regions of sub-Saharan Africa (Gueye *et al.*, 2005; Boko *et al.*, 2007). Ashton (2002) also projected that population trends and patterns in water usage will cause more countries in Africa to exceed their limits of "economically usable, land-based water resources before 2025". The potential effect of over-exploitation and high WEI in coastal aquifers is not just the lowering of groundwater levels but also the peculiar adverse impact of seawater intrusion. This is due to the proximity of such aquifers to the ocean or creeks and the hydraulic pressure differences between saltwater and freshwater.

Several studies have been done on seawater intrusion with Ghyben-Herzberg principle as the most fundamental of all. Some methods and approaches previously and currently being applied in the study of salinity and seawater intrusion into fresh groundwater of coastal aquifers include Geophysical methods (Goldman *et al.*, 1991; Hwang *et al.*, 2004; Adepelumi *et al.*, 2009; Bouderbala & Remini, 2014), Geochemical and Geophysical methods (Ayolabi *et al.*, 2013;

Cimino et al. 2007; Fadili *et al.,* 2015), Hydrochemical methods (Kim & Park, 1998; Mondal *et al.,* 2010), Numerical Modelling methods (Zhou *et al.,* 2000; Javadi *et al.,* 2011), GIS methods based on chemical Indices (Santha & Syed., 2013; Trabelsi *et al.,* 2016; Balathandayutham, *et al.,* 2015), Multivariate Statistical Analysis methods (King et al, 2013; Yang *et al.,* 2015), and Estimation of pressure differences between freshwater and saltwater zones (Kim *et al.,* 2007).

Naturally, seawater intrusion is a dynamic process and it may be observed that the quality of groundwater resources vary with spatial distribution, and time-based on factors influencing the hydrological system, hence, the concept of Vulnerability of groundwater resources. This concept of groundwater vulnerability as a measure for the protection of groundwater resources can be traced to the work of Albinet & Margat (1970). The aquifer may be vulnerable to environmental influences such as surface pollutants (leachates), a high concentration of effluents in rivers through the process of diffusion and advection, as well as seawater intrusion.

Over the years, a number of overlay methods have been developed for assessing the vulnerability of aquifers to pollution. The DRASTIC Index (Aller et al, 1987); GOD index (Foster, 1987); AVI rating system (Van Stempvoort et al, 1993); SINTACS method (Civita, 1994); ISIS method (Civita & De Regibus, 1995) and EPIK method (Doerfliger & Zwahlen, 1997) are major overlay methods identified by Gogu & Dassargues (2000). More recent methods are; PI method (Goldscheider *et al.,* 2000); and the GALDIT method (Chachadi & Lobo-Ferreira, 2001). In some cases, more than one of these methods were applied in a single study (Corniello et al, 1997: Draoui et al, 2007). The names ascribed to all these methods are acronyms of the most important parameters identified for the vulnerability assessment in each case. The GALDIT method; an adaptation from the DRASTIC method for assessing the vulnerability of coastal aquifers to seawater intrusion was applied for this study. GALDIT method is essentially a method for assessing the vulnerability of coastal aquifers to seawater intrusion and it has been widely applied in several places for mapping out the vulnerability of coastal aquifers to seawater intrusion. Lobo-Ferreira *et al.,* (2005) applied the method on the coastal aquifer of Monte Gordo, southern Portugal; Sophiya & Syed (2013) studied the coastal aquifer of parts of Eastern India and assessed the vulnerability to seawater intrusion. The Rhodope aquifer system in the North Eastern part of Greece was also assessed for its vulnerability to SWI by Kallioras *et al.,* (2011). Saidi *et al.,* (2013)' work on Mahdia-Ksour Essaf

aquifer on the eastern coast of Tunisia also covered the application of GALDIT for vulnerability assessment.

The East African region has been identified as the least urbanised region in the world, howbeit, it has the shortest doubling time for its urban population (UN Habitat, 2008). Its coastline is one of the coastal regions with the least human induced modified land. I.e. minimal land reclamation, dredging and modification (UNEP, 2008). Its urban coastal population is fast increasing as evidenced in the cases of Dar es Salaam (Tanzania) and Mombasa (Kenya). However, very few groundwater pollution studies have been carried out in the coastal regions of East Africa. How seawater intrusion and seasonal changes affect the quality of water in the coastal aquifers of Dar es Salaam was studied by Sappa *et al.,* (2015). The study showed the groundwater of the coastal aquifer under study to be highly saline, while depletion of the water levels poses serious challenges for current and future freshwater provisioning from the aquifer. The Quaternary aquifer of Dar es Salaam was also investigated for the occurrence of seawater intrusion (Mtoni *et al.,* 2013) where a discussion was made on the causes, consequences, remedial actions and future likelihood of seawater intrusion in the study area.

The population growth on the north coast of Mombasa has been on a steady and progressive rise in the past four decades (GOK, 1979, 1989, 1999; KNBS, 2010). This does not only suggest an increase in the demand for groundwater, but also a higher risk of pollution. Munga et al, (2006) assessed the pollution status and the vulnerability of the coastal aquifer of Mombasa to groundwater pollution from anthropogenic activities. The study employed the use of DRASTIC index overlay method with GIS to obtain the spatial distribution of the vulnerability of the study area to surface pollution. MODFLOW groundwater model package was used to study the flow of the groundwater stream. This research focused on the saltwater intrusion pollution component of the same study area. Advanced GIS, different chemical analysis methods, and Visual MODFLOW Flex groundwater modelling package were applied extensively for the study of North coast of Mombasa's coastal aquifer. Hence, studying the seawater intrusion component of the study area provides a broader knowledge on the groundwater pollution for a more sustainable management of the groundwater.

1.2 Statement of problem

The groundwater pollution study by Munga et al, (2006) on Mombasa North Coast exposed some data and information gaps amongst which are "Physico-chemical indicators of water quality including salinity, conductivity, pH; water table data and related geohydrologic parameters; saline water intrusion; and influence of seasonal rains on aquifer recharge and groundwater quality". This research filled some of the gaps by studying the hydrogeological characteristics of the aquifer including the impact of seasonal changes on water quality status, impacts of seawater intrusion and the groundwater flow and solute transport. Similar studies have been done in many parts of the world, for instance, in sub-Saharan Africa, Ayolabi *et al.*, (2013) assessed the quality and seawater impact of a coastal region in Nigeria using geophysical and geochemical methods. In East Africa, few similar works were reported in Dar es Salaam where hydrochemical methods where used in assessing the water quality and impact of seawater on the coastal and quaternary aquifers of the area (Sappa *et al.*, 2015; Mtoni *et al.*, 2013). However, very few related studies have been reportedly done on the coastal aquifer of Kenya vis a vis seawater intrusion. This work, therefore, utilised the understanding of chemistry, geology, GIS, remote sensing and groundwater modelling in establishing knowledge on the hydrogeological condition of the study area and observing changes in the flow and quality of the fresh groundwater to enhance sustainable management of the groundwater resource.

1.3 Justification

In Kenya, a good number of studies have been carried out on groundwater resources and aquifers. However, very few empirical studies have been carried out on coastal aquifers of Kenya. The salient truth is that the coastal aquifers require a lot more attention due to the unique challenges affecting them such as sea water ingression, coastal erosion, and other climate change related phenomena. In many parts of Mombasa, domestic water is supplied by a central water corporation agency. However, with the increasing trend in population, it becomes increasingly difficult for every part of the city to be served, especially the informal settlements. This leads to a higher dependence on groundwater. The only slightly comprehensive groundwater study on the study area was reported ten years ago, in which groundwater pollution from surface sources was assessed while several gaps were identified (Munga et al, 2006). With an ever increasing impact of climate change and the surge in population in the past decade, ten years is too wide an interval for

groundwater studies and monitoring for effective management. This research thereby aimed to provide a more recent, detailed and inclusive assessment of the groundwater resource in the study area. The seawater intrusion component of the groundwater pollution, water quality changes across the seasons not covered in earlier studies were duly covered in this study. The work, therefore, did not just assess the extent of seawater intrusion in the study area but also mapped out the vulnerability of the study area to the phenomenon. Widespread saltwater intrusion inland does more harm than good in that freshwater ecosystems are threatened due to high salinity of water and provision of potable drinking water becomes more challenging. The outcomes of this work, therefore, provides sound background knowledge for managing the coastal aquifer in terms of the siting of boreholes/wells, potentially stressed areas and general groundwater management.

Invariably, the work has proven that similar studies can be done in the coastal areas of other parts of sub-Saharan Africa. The challenge had always been the availability of data and the complexity involved in employing data and knowledge from different sources and disciplines in an interdisciplinary manner in one single study within a limited scope, time and resources.

1.4 Objective of Study

1.4.1 General Objective

To investigate the groundwater quality and flow of the coastal aquifer of Mombasa North coast.

1.4.2 Specific Objectives

i. To assess the hydrogeological characteristics, salinity and extent of seawater intrusion in the aquifer of the study area.
ii. To undertake the vulnerability mapping of the aquifer to sea water intrusion
iii. To assess and simulate the groundwater flow and solute transport in the study area

1.5 Research Questions

1. What is the quality of groundwater and extent of seawater intrusion in the study area
2. What is the vulnerability of different parts of the study area to seawater intrusion
3. What is the direction of flow of the groundwater in the coastal aquifer under study

1.6 Scope of Study

The study was carried out on the north coast of Mombasa covering the populated regions of Nyali, Bamburi and Kisauni. The study area was mapped out based on hydrological boundaries and covered a total land area of 74.2 km^2. The field data collection took place between the months of March and September 2016 with field visits done in March, June and September. Fourteen boreholes/wells strategically located across the study area were identified for sampling of static water levels, field water quality parameters and water sample collection. Samples were also taken at different points in the Indian Ocean. Laboratory tests were conducted for four cations (Na, K, Ca, Mg) and three anions (Cl, HCO_3, SO_4). Secondary data such as Topo maps, Geological Maps, SRTM 30m DEM, and historical borehole data obtained from different sources complemented the field data. ArcGIS10.3 software from ESRI was used alongside statistical packages such as Grapher and Eviews for the processing and analysis of data. Finally, Groundwater Modelling System (GMS) software package containing MODFLOW, MT3DMS and SEAWAT was utilised in assessing the groundwater flow and solute transport.

1.7 Limitation of Study

The major limitations to the scope of the study were;

- Due to time constraints, the field data collection only covered the peak of dry season, the peak of long rains season and the peak of dry season before the short rains within a hydrologic cycle. A full hydrologic cycle of one calendar year was not covered.
- The entire administrative area of Mombasa could not be covered due to the constraints of time, budget and complexities in the siting of available boreholes for data collection.
- The few historical borehole data available were scanty and lacked cohesion, therefore it was not sufficient to establish a database on which long-term groundwater studies could be done.

CHAPTER TWO- LITERATURE REVIEW

2.1 Introduction

This chapter is divided into four parts: coastal aquifers; application of GIS and groundwater modelling in coastal aquifer studies; GALDIT Index and groundwater flow models; MODFLOW, MT3D, SEAWAT and GMS.

2.2 Coastal Aquifers

The voids in which groundwater is stored are found in the geological formations called *aquifers*. By definition, an aquifer is a rock layer which stores and allows the movement of water within its pores. About 30.1% of the world's freshwater exists as groundwater (Shiklomanov, 1993), and its importance for the sustenance of life cannot be overestimated. Groundwater from aquifers commands the highest demand for readily available freshwater in the world (Boswinkel, 2000). This demand is expected to escalate in the future, mainly due to rise in water use globally and a pressing need to counterbalance the diminishing availability of surface water due to increasing variability in precipitation (Kundzewicz et al, 2007). Coastal aquifers are unique for their closeness to saltwater bodies such as Oceans, creeks and lagoons. Hence, they are prone to effects of dynamic processes such as seawater intrusion, and sea level rise.

2.2.1 Challenges of Coastal Aquifers

Many coastal aquifers around the world are constantly being over-exploited, leading to serious challenges of land subsidence in a number of cases due to aquifer-system compaction. Some instances of land subsidence reported such as Vietnam, Mekong Delta and Cambodia (Ingebritsen & Galloway, 2014); *Chesapeake Bay* (Boon et al, 2010) are prime examples. In the wake of annual increasing mean sea levels and sea level rise, the secondary effects of land subsidence such as increasing storm surges and flooding are inevitable. Another challenge facing coastal aquifers is groundwater pollution from surface pollutants (leachates), effluents discharged into rivers which may find their way into the aquifer through the process of diffusion and advection as seen in the case of Mombasa (Munga et al, 2006). However, the chief source of freshwater coastal aquifer pollution is salt water intrusion.

Several methods have been devised and studies documented to address or manage these challenges. Kumar (2006), suggests extraction of saline groundwater, infiltration of surface water

(artificial recharge), physical barriers, inundation of low-lying areas, and an increase in natural recharge as countermeasures to addressing the decrease in groundwater resources and saltwater intrusion in coastal aquifers. However, detailed site-specific studies are highly essential before an approach or set of approaches are adopted for managing the challenges facing a coastal aquifer. For instance, Lin et al, (2013) opine that the study of abstraction rates will better inform decision makers in the management of land subsidence, restoration of groundwater and sustainable use in multi-aquifer systems.

2.2.2 Seawater Intrusion

When saltwater encroaches or seeps into a freshwater aquifer it is called *saltwater intrusion* but when the source of the saltwater is the sea or an adjourning Ocean, it is called *Seawater intrusion*. Seawater intrusion is a complex dynamic process in which several causative factors come into play. Darnault & Godinez, (2008) highlights the main phenomena contributing to the ingress of saltwater and affecting coastal aquifer systems as;

- " Encroachment of saltwater in coastal Aquifers;
- Characteristics of the aquifer formations;
- Anthropogenic activities producing saline waste;
- Tidal effects and;
- Fluctuations of the freshwater heads"

Two key components of climate change – Sea level rise and increased evapotranspiration have also been identified to have probable strong impacts on groundwater salinization and seawater intrusion into coastal aquifers (Kundzewicz et al, 2007). Seawater intrusion can be considered as the major concern of coastal aquifers. Kumar, (2006), notes that when addressing exploitation, restoration and management of the fresh groundwater, the major issue is saltwater intrusion in most cases of coastal aquifers. Arguably, the most fundamental empirical relationship aimed at studying the dynamics of the interaction between seawater and freshwater in a coastal aquifer is the Ghyben-Herzberg principle as illustrated in Figure 2.1.

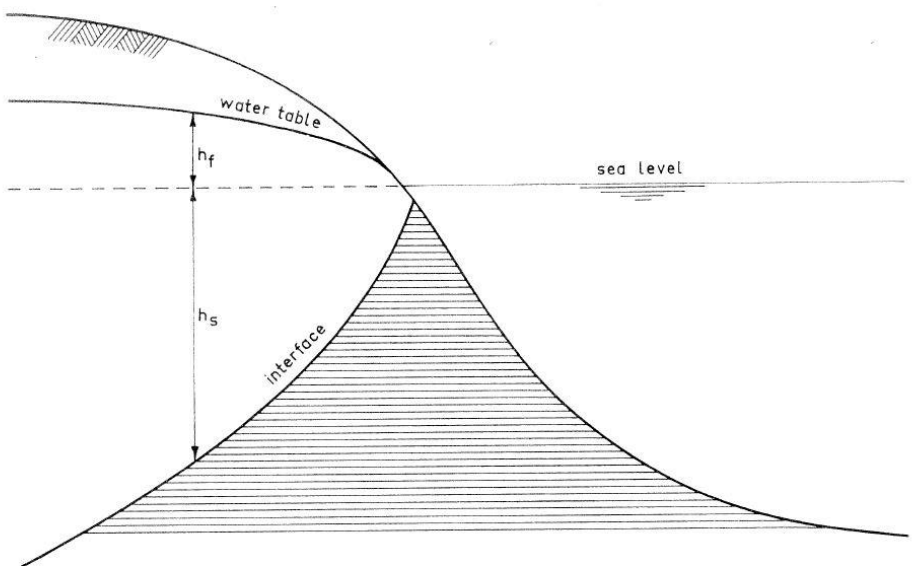

Figure 2. 4: Illustration of the fresh and seawater interface of a coastal aquifer (Roger, 1998)

Ghyben-Herzberg principle is based on the density differences between saltwater and freshwater and it states that 1/40 unit of fresh water is required above sea level for each unit of fresh water below sea level to maintain hydrostatic equilibrium with the adjourning saltwater (Roger, 1998).

The principle is mathematically represented as;

$$\boldsymbol{h_s = \frac{\rho_f}{\rho_s - \rho_f} \approx 40 h_f} \qquad \textit{1}$$

Where;

h_f = height of water table above mean sea level

h_s = height of freshwater zone below sea level

ρ_s and ρ_f are densities of saltwater and freshwater respectively.

This principle assumes the existence of hydrostatic equilibrium between the saltwater and freshwater zones, horizontal flow in the freshwater zone and a lack of progressive movement of saline water in a homogenous, unconfined coastal aquifer (Figure 2.1).

Lusczynski (1961) modified the Ghyben-Herzberg equation for non-static equilibrium conditions where seawater is constantly experiencing progressive movement with heads above and below mean sea level. It was applied to pumping wells with the condition that they are close to each other (Figure 2.2). This modified equation is given as;

$$Z = \frac{\rho_f}{\rho_s - \rho_f} h_f - \frac{h_f}{\rho_s - \rho_f} h_s \qquad 2$$

Where;

Z = depth from water level measurements in observation wells to the saline-freshwater interface

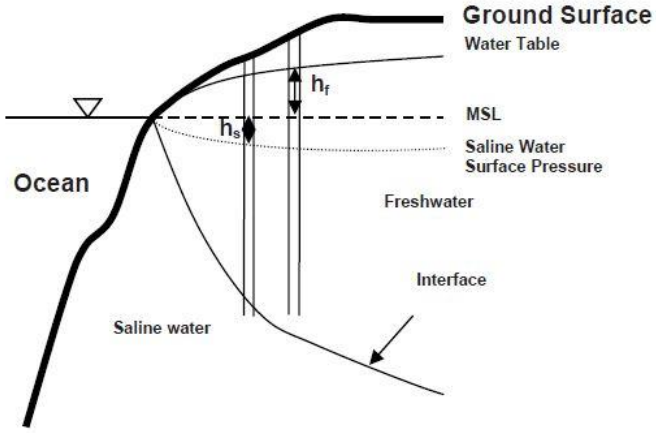

Figure 2. 5: Unconfined coastal aquifer with non-equilibrium conditions between freshwater and saltwater (Darnault & Godinez, 2008)

Several factors contribute to the dynamics of this freshwater-saltwater interaction in coastal aquifers, the significant ones are; aquifer characteristics (e.g. thickness, permeability), the characteristics of underlying rocks (unconfined) as well as the overlying rocks(confined) (Barlow, 2003).

2.2.3 Review of Coastal Aquifer Research

Only a few of the globe's coastlines are not within the influence of anthropogenic pressures even though not all Coasts are occupied (Buddemeier *et al.,* 2002). In Africa, human influence on coastal regions is quite substantial. A massive 66.6% of Senegal's national population reside within Dakar and about 90% of Senegal's industries are situated in the Dakar coastal zone, 22.6% of Nigeria's population reside in Coastal zones, while in Ghana, Togo, Benin, Sierra Leone, economic activities within the coastal zones form the backbone of their national economies (IPCC, 1997). In the East African region, most of the principal cities are inland, however, coastal cities like Mombasa and Dar es Salaam are experiencing yearly population growths of 5% and 6.75% respectively (World Bank, 1995). All these play massive roles in affecting the water usage and aquifer dynamics in coastal regions. On a regional scale, the aquifer in Africa vary significantly from one area to another and occur as "alluvial, lacustrine, basaltic and sedimentary aquifers in

coastal zones (Steyl & Dennis, 2009). Of the 32 mainland countries along the 40,000km long African coastline, only a handful have done detailed researches on their coastal aquifers. In several coastal aquifer studies, the most widely used approaches are the geophysical, hydrochemical, GIS Overlay, numerical modelling or a hybrid of two or more of the approaches.

Adepelumi et al, (2009) carried out a vertical electrical resistivity sounding survey on the coastal zones of Lekki Peninsula, Lagos Nigeria, in order to provide information on subsurface lithology and delineate the groundwater salinity. A similar work was executed by Oladapo et al (2014) where 52 borehole logs were obtained within Lagos Municipality using natural gamma and electrical resistivity and interpreted to delineate vulnerable zones and extent of seawater intrusion. The two instances are one of the few studies on coastal aquifers using geophysical approaches in sub-Saharan Africa. In the coastal region of East Africa, hydrochemical approaches (Mtoni et al, 2013; Sappa et al, 2015) were widely applied in Dar es Salaam (Tanzania). Mtoni et al, (2013) obtained log data from boreholes/wells dug between 1997 and 2009 while their field and Laboratory data comprised EC, Na, Mg, Ca, K, Cl, SO_4, and HCO_3. Piper plots were also used to illustrate the characteristics of the groundwater with almost 50% considered brackish or saline. Sappa et al, (2015) widely applied Person's correlation matrix to understand the nature of the groundwater. They recommended a more controlled exploitation of the groundwater in the study area.

The last decade has seen an increase in the application of GIS overlay in groundwater studies for carrying out vulnerability analysis. Application of GIS in groundwater studies is also known as *geographic data processing (GDP)* (Gogu et al, 2001). One of such GDP approaches is the "DRASTIC Index" introduced by Aller et al, (1987), and has been widely used in mapping out the vulnerability of an aquifer to pollution. DRASTIC is an acronym with each letter representing the following; D- Depth to the water table; R- Recharge of the aquifer; A- Aquifer media; S-Soil media; T-Topography; I- Impact of the vadose zone; C- hydraulic Conductivity. DRASTIC is best used for groundwater pollution from surface sources such as leachates from active dumpsites, pit latrines etc. The drastic method was applied in the vulnerability of Mombasa County, Kenya, to surface pollution by Munga et al, (2006).

Numerical modelling, also known as *Process-based modelling (PBM)* (Gogu et al, 2001) has also been widely applied in groundwater studies. PBM can be carried out independent of geographic

data processing, however, GDP significantly reduces the hassles inherent in process-based modelling. For instance, Gaaloul et al, (2012) modelled and analysed the seawater intrusion phenomenon in the eastern coastal aquifer of North East Tunisia using GIS-based data for the 3D numerical modelling of the aquifer.

2.3 Application of GIS and Groundwater Modelling in Coastal Aquifer Studies

Models are a representation of some parts of the real world and they can be *static or dynamic*. Geographic Information Systems is a powerful tool which involves the use of software to capture, manipulate, view and analyse geographic information or spatial data to achieve a specific goal. GIS is "a system of hardware, software, and procedures to facilitate the management, manipulation, analysis, modelling, representation, and display of geographically referenced data to solve complex problems regarding planning and management of resources" (Goodchild & Kemp, 1990). In other words, GIS comprises five major components; hardware, software, data, procedures and most importantly people. In recent times, there has been an increase in the application of GIS in the field of Environmental sciences and engineering as well as numerous other fields. Groundwater models usually take the form of numerical models. Numerical models emerged over the past 40 years as one of the primary tools that hydrologists use to understand groundwater flow and saltwater movement in coastal aquifers (Gaaloul, 2012). Numerical models are mathematical representations (or approximations) of groundwater systems in which the important physical processes that occur in the systems are represented by mathematical equations.

2.3.1 Geographic Information Systems (GIS)

GIS as a concept covers the two descriptors that represent our real world; location, and the attributes found in the location. In GIS, geographic information is usually represented as either *objects or fields*. Geographic objects are what populates a study area, and they are usually well-distinguishable, discrete, bounded entities with the spaces between them potentially empty (Rolf, 2001). Objects symbolise the real world with simple vector formats such as points, lines and polygons. Some examples of spatially represented objects in hydrogeology are boreholes, piezometers and protected zones. Attributes attached to these objects may be the Well number, point data of the static water level, chloride concentration.

On the other hand, *fields* represent real world in terms of attribute data without defining the objects. A geographic field is a geographic phenomenon in which a value can be determined for every point in the study area (Rolf, 2001) e.g. a raster. A raster model comprises rectangular arrays of cells with each cell being assigned an attribute. In terms of representation, spatial representation of data may be 1.) In discrete values for each point (well-defined values for each location), and 2.) Kernel (spatially continuous functions). The six model methods for digitally representing spatial data in fields are the raster model, grid model, point model, contour model (Isolines), polygon model and triangulated irregular network (TIN). In the GIS environment, the most familiar model is the "Map". A map is a miniature representation of some parts of the real world. Another form of the model in GIS is a "database". A database stores a significant amount of data and provides numerous functions to operate on the stored data (Rolf et al, 2001). Data modelling is the general term for the design effort of structuring a database. Maps and the database are both categorised as static models.

A foremost software for GIS-based data processing that has seen tremendous improvements over the years is the ArcGIS software, a trademark GIS software of ESRI, the leading organisation for Geographic Information Systems. It is built with a diverse range of capabilities including cartography, network analysis, spatial and 3D analysis.

2.3.2 Groundwater Modelling

The Groundwater flow modelling and its different approaches have evolved over the years. Groundwater modelling is a *dynamic* model which is highly essential in understanding and analysing groundwater dynamics. Groundwater simulation is the building of a model whose behaviour closely resembles the actual behaviour of the aquifer under study. Broadly speaking, a groundwater model can be physical, electrical analogue or mathematical (Mercer, 1980). Each of these model types has different sub-divisions. However, Mathematical models seem to be the most widely used of all. Mathematical models may be statistical, deterministic or some combination of the two. Purely Statistical models are very useful for classifying data and describing systems that are not well understood but generally offer little physical insights. Deterministic models are the ones that define relationships between cause and effects based on the understanding of the physical system. The procedure for developing a mathematical model is shown in figure 2.3.

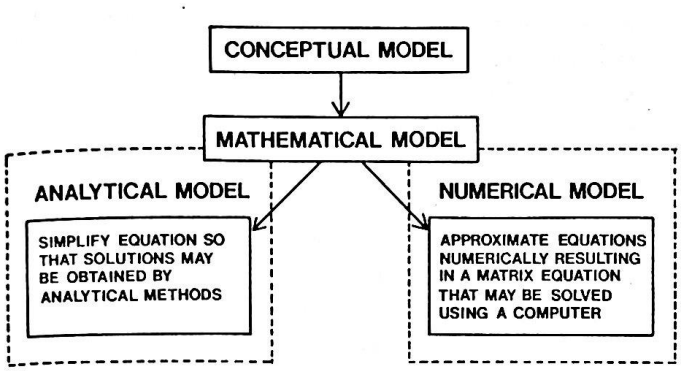

Fig 2. 6: Logic diagram for the development of a mathematical model (Source: Mercer, 1980).

The conceptual model helps in understanding the nature of the physical system under study. It forms the foundation for one or more numerical models. The numerical model gives the real time simulation of the properties of the aquifer being studied. It involves defining the objectives of the model such as the desired flow and transport simulation options, and the boundary conditions. The mathematical model consists of the initial conditions, appropriate boundary, and a partial differential equation over the study area. It must also contain phenomenological laws to describe the fluid behaviour in the system such as Darcy's Law of conservation of momentum, Fick's law of chemical diffusion and Fourier's Law of heat conduction. The boundaries for the mathematical model has to be clearly defined. Afterwards, the region is subdivided into grids. Two main discretion approaches for two-dimensional griding are the finite-difference method and finite-element method (Figure 2.4).

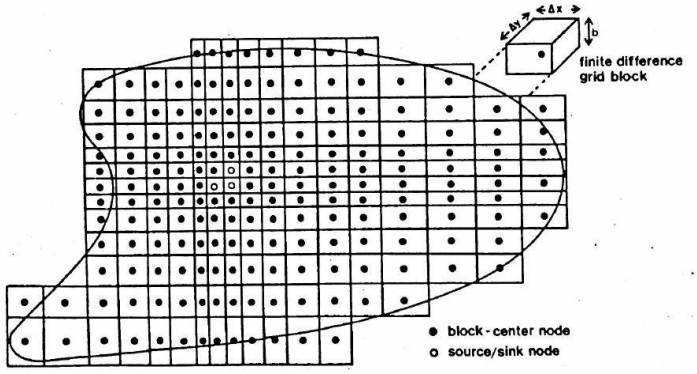

Figure 2.4 c: Finite- difference grid configuration for the study of an Aquifer (Source: Mercer, 1980).

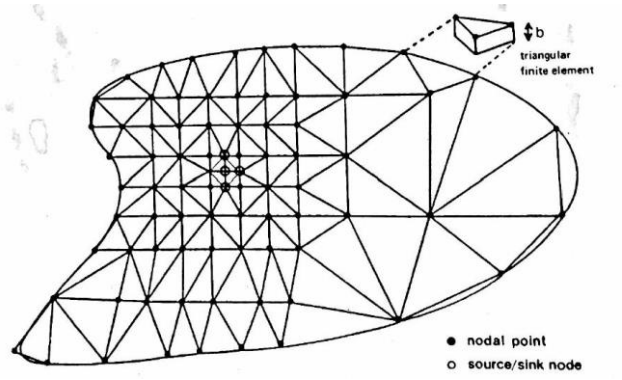

Figure 2.4 d: Finite- Element grid configuration for the study of an Aquifer (Source: Mercer, 1980).

Data used in groundwater modelling are in 4 categories;

1. The Aquifer - system stress factors
2. The Aquifer- system and strata geometry
3. The hydrogeological parameters of the simulated process
4. The main measured variables.

The stress factors in groundwater flows are; effective recharge, pumping volumes, water-surface flow exchanges input and output contaminant mass flows. Stress factors are imposed through the boundary conditions or source/sink terms. These boundary conditions are determined through the geological information such as topographic maps, contour maps of the upper and lower limits of the aquifer strata.

The hydrogeological data parameters are derived from raw data interpretations and the major ones are; hydraulic conductivity, storage coefficient, initial heads, and dispersivity.

2.3.3 Integrating of GIS with Groundwater Modelling

As expressed in Figure 2.3, the first step in achieving a numerical model for groundwater studies is the creation of the conceptual model. GIS database has made the creation of conceptual model extremely easy. Hence, integrating GIS with numerical models does not only save time but also reduces the drudgery of building conceptual models from scratch. Developers of advanced Groundwater modelling software packages like Visual MODFLOW flex and GMS have helped make the building of conceptual models from GIS data more relatively stress-free.

Techniques for integrating GIS with groundwater models have been identified to be three; namely *loose coupling, tight coupling, and embedded coupling* (Gogu et al, 2001).

a. Loose coupling- This is when independent software packages are used for the GIS and the GW model components. The data transfer of predefined files from one software package to the other is made through input and output model. The advantage is that potential future changes can be facilitated in an independent manner since each software is distinct on its own.

b. Tight coupling- In this case, data is exported from the GIS to the model but the GIS tools are able to interactively access the input subroutines of the GW model package. There is a shared user interface between the GIS and the modelling system, while data exchange is also automatic. A good example of tight coupling is ArcGIS-SWAT data model developed by Olivera et al (2006). Another example is the PIHMgis package developed by (Bhatt et al, 2014) which is integrated with QGis as a plugin based toolbar.

c. Embedded coupling- This occurs when the hydrogeological model is created using GIS programming language or when a complex modelling system assimilates a simple GIS. In this case, the user interface, data and method base are not just shared between the GIS and the model but also, intra-simulation model modification, query and control are also very possible. A good example of embedded coupling is the AVTOP- a topography-based hydrological model built with the macro language interface of ArcView (Huang & Jiang, 2002). However, it requires very complex programming and data management.

Both the tight coupling and embedded coupling require considerable investment in programming and data management which are not always justifiable.

2.4 GALDIT Overlay Index

GALDIT overlay index is an open-ended model which utilises a numerical ranking system for evaluating the saltwater intrusion potential of a coastal aquifer within the framework of the hydrogeological settings using certain established factors (Lobo Ferreira et al, 2005). These factors also known as GALDIT factors, have been identified as the most important map-able factors controlling seawater intrusion (Chachadi & Lobo-Ferreira 2001; Chachadi & Lobo-Ferreira 2005; Lobo Ferreira et al, 2005). The factors include;

- G- Groundwater occurrence (Aquifer type; confined, unconfined, leaky confined)
- A- Aquifer hydraulic conductivity
- L- Level of the Groundwater depth above sea level

- D- Distance from shore (distance inland perpendicular from shoreline)
- I- Impact of existing status of seawater intrusion in the area
- T- Thickness of the mapped aquifer

The acronym GALDIT was derived from the first letter of each parameter. The parameters are drawn up into map layers which are then overlaid based on weightages, ranges and importance rankings. The weights were derived from the analysis of the data obtained from opinion surveys, experts' opinions, focused groups and several academic forums on what are considered to be the most important factors contributing to the intrusion of seawater into coastal aquifers (Table 2.1). The weights are therefore considered as constants that are not expected to be altered by subjective opinions. The importance rating factors are put on a scale of 2.5 to 10. The higher the value of the importance rating, the higher the vulnerability of the aquifer to Saltwater Intrusion. The total sum of all the individual scores is referred to as the Decision Criterion. This is obtained by multiplying the values of the importance ratings with the corresponding Indicator weights.

Table 2. 2: Standardised weightages for GALDIT factors (Chachadi & Lobo-Ferreira, 2005)

Factors		Weights
1.	Groundwater occurrence (aquifer type)	1
2.	Aquifer hydraulic conductivity	3
3.	Height of groundwater above sea level	4
4.	Distance from the shore	4
5.	Impact of existing status of seawater intrusion	1
6.	Thickness of Aquifer being mapped	2

The final vulnerability maps derived from the overlay and spatial analysis of the GALDIT indices provide useful information on areas which are more susceptible to the intrusion of saltwater than the others.

The GALDIT index has been widely applied in several studies to map out the vulnerability of coastal aquifers to seawater intrusion (Chachadi & Lobo-Ferreira 2001; Chachadi & Lobo-Ferreira 2005; Lobo Ferreira et al, 2005; Kallioras et al. 2011; Sophiya & Syed 2013; Gontara, et al, 2016).

2.5 MODFLOW, MT3D, SEAWAT and GMS

2.5.1 Brief Description on MODFLOW

MODFLOW is a finite-difference ground water model. Groundwater flow is simulated using a block centred finite-difference approach (Modflow: USGS, 2013). Layers can be simulated as confined or unconfined. The newest main version of MODFLOW is the MODFLOW-2005. Prior to the development of MODFLOW, two and three-dimensional finite difference models were used extensively by US Geological Survey (USGS) and others for computer simulation of ground-water flow. Therefore, the first version of MODFLOW was the result of the need to consolidate all the commonly used simulation capabilities into a single code that was easy to understand, use and modify. This was developed using Fortran Computer Language- Initially Fortran 66 then Fortran 77. This first version of MODFLOW was called MODFLOW-88. Originally MODFLOW was conceived solely as a ground-water flow model, but its application has expanded beyond ground water flow into transport and parameter estimation (Banta *et al.*, 2005).

Principles of MODFLOW

MODFLOW uses a modular structure wherein similar program functions are grouped together, and specific computational and hydrologic options are constructed in such a manner that each option is independent of other options. Because of this structure, new options can be added without the necessity of changing existing options. The model may be in two or three-dimensional forms. When the model is visualised in terms of a three-dimensional assemblage of cells, each cell contains a point called a node at which head is to be calculated. The size of the model grid is specified by the user in terms of the number of rows (NROW), the number of columns (NCOL), and the number of layers (NLAY); these terms define a three-dimensional grid of cells in the form of a rectangular box. Input procedures have been designed so that each type of model input data may be stored and read from separate external files. User-specified formatting allows input data for the grid to be read in almost any format without modification to the program. The output of model results is also flexible; the user may select which data to output, the frequency of output, and for some data, the format of the output. MODFLOW is not necessarily a single program, but all MODFLOW programs include the Groundwater Flow Process (Banta *et al.*, 2005).

Operations of MODFLOW

MODFLOW utilises iterative methods to obtain the solution to the system of finite-difference equations for each time step. In these methods, the calculation of head values for the end of a given time step is started by arbitrarily assigning a trial value, or estimate, for the head at each node at the end of that step. A procedure of calculation is then initiated that alters these estimated values, producing a new set of head values that are in closer agreement with the system of equations. These new, or interim, head values then take the place of the initially assumed heads, and the procedure of calculation is repeated, producing a third set of head values (Harbaugh *et al.*, 2000). Currently, it has been made possible for MODFLOW models to be successfully coupled with ArcGIS. This extension called *Arc Hydro Groundwater* can be downloaded freely from Aquaveo (2016). Furthermore, several MODFLOW-related programs have been developed with capacities to simulate, solute transport, parameter estimation, coupled surface-water / groundwater systems, variable- density flow (including saltwater), aquifer-system compaction, and land subsidence, and groundwater management.

MODFLOW code is based on the fundamental laws of continuity of mass and motion which are solved for the partial differential equation as expressed in Figure 2.5.

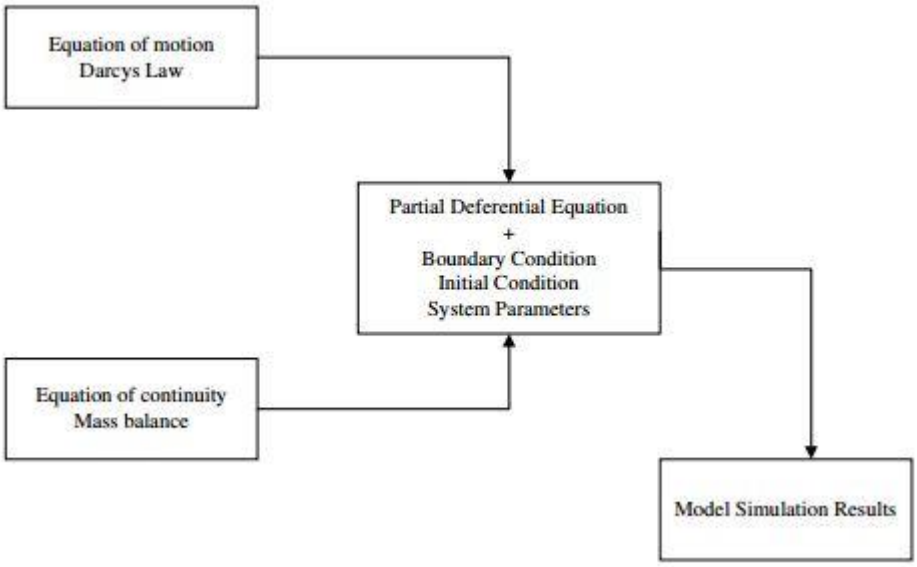

Fig 2. 5: Component of Groundwater flow approach (Source: Rientjes, 2006)

The governing equation used in MODFLOW, describing the three-dimensional groundwater flow through the aquifer is the given by Freeze & Cherry, (1979) as:

$$\frac{\partial}{\partial x}\left(K_x \frac{\partial h}{\partial x}\right) + \frac{\partial}{\partial y}\left(K_y \frac{\partial h}{\partial y}\right) + \frac{\partial}{\partial z}\left(K_z \frac{\partial h}{\partial z}\right) - w = S_s \frac{\partial h}{\partial t} \qquad 3$$

Where;

K_x, K_y, K_z are the hydraulic conductivity values along the x, y and z coordinates

h- is the hydraulic head values

w- is the volumetric flux per unit volume and represents sources and sinks of water per unit time (t^{-1})

Ss- is the specific storage of the porous material and

t - is the time

The first part of the simulation runs a steady state solution which takes the form:

$$\frac{\partial}{\partial x}\left(K_x \frac{\partial h}{\partial x}\right) + \frac{\partial}{\partial y}\left(K_y \frac{\partial h}{\partial y}\right) + \frac{\partial}{\partial z}\left(K_z \frac{\partial h}{\partial z}\right) - w = 0.0 \qquad 4$$

The steady state solution is then solved for the transient state in order to solve for storage coefficient.

2.5.2 Brief description of MT3D

MT3D is a modular three-dimensional (3D) transport model having its first version developed by Chunmniao Zheng in 1990 and released as a public domain code from U.S. Environmental Protection Agency (Zheng, 1990). MT3D is based on a modular structure which enables the simulation of transport components independently or jointly (Aquaveo, 2006). MT3DMS is the second generation of MT3D, developed under the strategic Environmental Research and Development Program (SERDP). MT3D code has a wide range of solution options such as; method of characteristics (MOC); modified method of characteristics (MMOC), a hybrid of MOC and MMOC (HMOC); and the standard finite-difference method (FDM).

MT3DMS supports all the discretization and hydrologic features of MODFLOW. It is a modular three-dimensional transport model for simulating dispersion, advection, and chemical reactions of dissolved constituents (Zheng & Wang, 1999). It is used with MODFLOW in a 2-step flow and transport simulation. In the first step, MODFLOW computes the heads and cell-by-cell flux and are written in a formatted file. The second step involves the reading of the formatted file by MT3DMS and used as the flow field for the solute transport component of the simulation process.

The differences between MT3DMS and MT3D are that the former enables multi-species transport, support additional solvers, and make allowances for cell-by-cell input of all model parameters.
The partial three-dimensional equation used in MT3D for the solute transport is equally highlighted in Freeze & Cherry, (1979) and expressed as:

$$\frac{\partial C}{\partial t} = \frac{\partial}{\partial x_i}\left[D_{ij}\frac{\partial C}{\partial x_i}\right] - \frac{\partial}{\partial x_i}(v_i C) + \frac{q'_s}{\theta}C_s + \sum_{k=1}^{N} R_k \qquad 5$$

Where;

C is the concentration of dissolved contaminant in groundwater [ML^{-3}];

X_i is the distance along the Cartesian co-ordinate axis

D_{ij}: is the hydrodynamic coefficient of dispersion [L^2T^{-1}];

vi: the seepage or linear pore water velocity;

q'_s: the volumetric flux of water per unit volume of aquifer's sources and sinks [T^{-1}];

C_s: the concentration of the sources or the sinks[ML^{-3}];

θ: the porosity of the porous medium [-]; and

R_k: chemical reaction term

The solute transport equation was slightly modified by Zheng & Wang (1999) for the running of MT3D module and given in equation 6 as;

$$\frac{\partial(nC)}{\partial t} = \nabla.(nD.\nabla C) - \nabla.(qC) - q'_s C_s \qquad 6$$

Where:

n is the porosity of the medium, **q** is the specific discharge [LT^{-1}].

2.5.3 A brief description of SEAWAT

SEAWAT is a generic MODFLOW/MT3DMS-based computer program designed to simulate 3D variable density groundwater flow coupled with multispecies solute and heat transport, focused mainly on brine migration in continental aquifers as well as the saltwater intrusion in coastal aquifers (Langevin et al, 2003). It is designed to simulate three-dimensional variable-density groundwater flow coupled with multispecies solute and heat transport, first documented by Guo and Bennett (1998) and based on the concept of the freshwater head, or equivalent freshwater head, in a saline ground-water environment. The SEAWAT code follows a modular structure and was developed by combining MODFLOW and MT3DMS into a single program that solves the coupled

flow and solute-transport equations. The program can read and write standard MODFLOW and MT3DMS data sets, although some extra input may be required for some simulations. For the convenience of hydrologists and modellers familiar with MODFLOW and MT3DMS, the changes in input files for MODFLOW and MT3DMS were kept to a minimum for use in SEAWAT. Thus, existing input files for the standard versions of MODFLOW and MT3DMS can be revised for SEAWAT with minor modifications. Temporally and spatially varying salt concentrations are simulated in SEAWAT using routines from the MT3DMS program equally generated from MODFLOW. SEAWAT uses either an explicit or implicit procedure to couple the ground-water flow equation with the solute-transport equation. With the explicit procedure, the flow equation is solved first for each time step, and the resulting advective velocity field is then used in the solution to the solute-transport equation (Guo & Langevin, 2002). This procedure for alternately solving the flow and transport equations is repeated until the stress periods and simulation are complete. With the implicit procedure for coupling MODFLOW and MT3D, the flow and transport equations are solved multiple times for the same time step until the maximum difference in fluid density between consecutive iterations is less than a user-specified tolerance (Langevin, Shoemaker & Guo, 2003). The modified flow equation incorporating concentration of solute and specific storage (Langevin & Guo, 2006) is given in equations 7 as;

$$\nabla\left[\rho K_f\left(\nabla h_f + \frac{\rho-\rho_f}{\rho_f}\nabla z\right)\right] = \rho S_{sf}\frac{\partial h_f}{\partial t} + n\frac{\partial \rho}{\partial C}\frac{\partial C}{\partial t} - \rho_s q'_s \qquad 7$$

Where;

S_{sf} is the specific storage (L^{-1}) defined as the volume of water released from storage per unit volume per unit decline of fresh water head

C is the concentration of solute mass per unit volume of fluid [ML^{-3}].

ρ is the fluid density

K_f is the freshwater hydraulic conductivity"

Equation 6 reduces to flow equation solved by MODFLOW for a constant-density system.

The solute transport equation (equation 7) solved by MT3DMS program is used for the solute transport solution in the SEAWAT interface.

2.5.4 A brief description of GMS

GMS- which is an acronym for *Groundwater Modelling System* is an intuitive, complete and capable software platform for creating groundwater and subsurface simulations in a 2D and 3D environment. It was first developed in Environmental Modelling Research Laboratory (EMRL) in the late 1980s. Its development was funded primarily by the United States Army Corps of Engineers. In 2007, the developers of the package at EMRL became a private enterprise as Aquaveo, LLC and has continued developing GMS as well as other products like SMS (Surface-water Modelling System) and WMS (Watershed Modelling System). It supports GIS data formats and numerous other formats such as vectors, raster, topographic maps, MODFLOW files, borehole data, ArcGIS geodatabases and shapefiles, CAD files amongst others. GMS also supports a wide range of models such as MODFLOW, MODPATH, MT3DMS, RT3D, SEAWAT, FEMWATER, SEEP2D, and UTEXAS. GMS is fully equipped for both Conceptual model approach and Numerical model approach.

CHAPTER THREE- METHODOLOGY

3.1 Introduction

In carrying out this research work, a series of activities were embarked upon. The activities included; obtaining of secondary data from agencies, three rounds of field data collection, laboratory analysis of collected samples, statistical and geospatial analysis of the obtained data and groundwater modelling. ArcGIS 10.3 version under ArcInfo license was used for this research. The spatial analyst extension and other tools were used for various activities such as tables editing, clipping, joins, conversion from one dataset type to another, projection, digitisation, georeferencing, spatial Interpolation, vulnerability analysis, and cartography. For the groundwater model and solute transport simulation, this research employed the use of GMS10.1 software package using the MODFLOW component for the groundwater flow simulation and MT3DMS and SEAWAT for the 3D solute transport model. Loose coupling of GDP and PMB approach was employed for this research. All these activities contributed to achieving the set objectives.

3.1.1 Study Area

Physical Background

The location, topography, climate, hydraulic boundary, geology, and socio-Economic conditions of the study area are described in this section.

i. Location

The study area is located on the North thrust of Mombasa Coast lying between latitudes 3° 95" and 4° 07" South of the equator and between longitudes 39° 68" and 39° 72" East of the Greenwich meridian. The area, 74.2 km^2 in size is the most populated area in Kisauni Sub-county of Mombasa County. There are four administrative sub-counties and six parliamentary constituencies in Mombasa. The administrative sub-counties are the Island, Likoni in the South, Changamwe in the west and Kisauni in the North. The parliamentary constituencies include Changamwe, Likoni, Mvita, Jomvu, Nyali and Kisauni.

The study area covers Nyali and parts of Kisauni parliamentary constituencies within the division of Kisauni. Major areas such as Kongowea, Nyali, Mwakirunge, Bamburi, and Shanzu are located within this study area. Based on the 2009 Census, Nyali and Kisauni constituencies had a

population of 185,990 and 194,065 respectively (KNBS, 2010). This makes them the highest and second highest populated constituencies of the six constituencies in the county of Mombasa. The area under study is the uniquely carved out area running from Nyali Bridge up to the edge of Mtwapa Creeks (Figure 3.1). It is bounded on the north and south by creeks, on the east by the Indian Ocean and on the west by Nguu Tatu Hills.

ii. Topography

Site visits and the DEMs of the study area shows Kisauni sub-county is a low-lying coastal plain. The most elevated part of the study area is Nguu-Tatu Hills whose peak is about 124m above sea level. Nguu Tatu Hills is located some 6.5km to 7km to the ocean front. The elevation of other parts of the study area mostly ranges from Sea level to 50m above sea level. The general low-lying characteristics of the study area influences surface runoff, as infiltration and deep percolation makes possible quick recharge of the aquifer.

iii. Climate

The region can be described as hot, humid, and tropical. South Eastern and North Eastern Monsoon winds play decisive roles on the seasons in the study area. There are two rainy seasons – the long rains and the short rains both influenced by the Monsoon winds. The SE Monsoon winds blow between April and September coinciding with the long rains while the NE Monsoon winds blow between October and March influencing the short rains. The long rains occur between the months of March and July while the short rains fall between September and December. The total annual rainfall is usually above 1000mm (Climatemps, 2015). The highest amount of precipitation is usually experienced in May and the least in February.

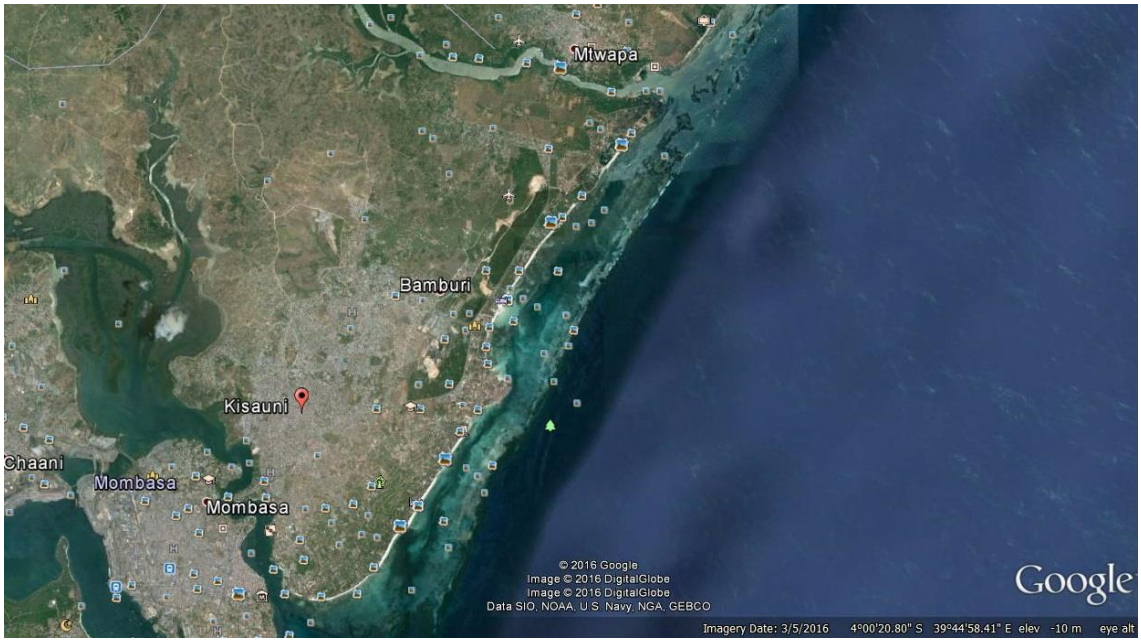

Figure 3. 10: Satellite Imagery of the Study Area (Source: Google Earth)

iv. Hydraulic Boundary Conditions

The rationale for determining the area of interest is based on the hydrogeologic suitability for feasible GIS and groundwater modelling. The area is a generally low-lying area from the coastline to the hinterlands. Therefore, Nguu -Tatu hills which have the highest elevation above sea level is chosen as the western boundary to provide a zone of constant freshwater flow. Mtwapa and Tudor creeks form the Northern and Southern boundaries respectively while the Eastern boundary is the Indian Ocean. The boundaries are highlighted below;

- The seaside boundary (coastal edge) - defined as the boundary of the constant head. i.e. the hydrostatic pressure boundary where the mean seawater level is used to define the coastline
- The Western boundary- defined by the Nguu Tatu Hills which is the boundary of no flow.
- The Northern and Southern boundary is defined by the Tudor and Mtwapa Creeks which equally act as Zones of Constant Head.

v. Geology

The geological information obtained from the Ministry of Mining shows that the rocks that form the geology of this region are sedimentary in nature. They were formed during the Pleistocene period and composed mainly of alluvium, wind-blown and superficial sands, corals and coral breccia (Caswell, 1956). The rocks dip gently and become progressively younger towards the

coast. The Nguu Tatu Hills is made up of Upper Jurassic shales which are fossiliferous in nature. Wind-blown and superficial sands of Pleistocene age cover large parts of Utange and some parts of Bamburi. Most parts of Kisauni, Nyali and parts of Bamburi are made up of Coral reefs, lagoonal sands, Kilindini sands and North Mombasa Crag which all belong to Pleistocene age (Figure 3.2). The lithology is composed mainly of limestone, sandstone and shale of varying depths. The described lithology shows the aquifer of the study area is mostly unconfined.

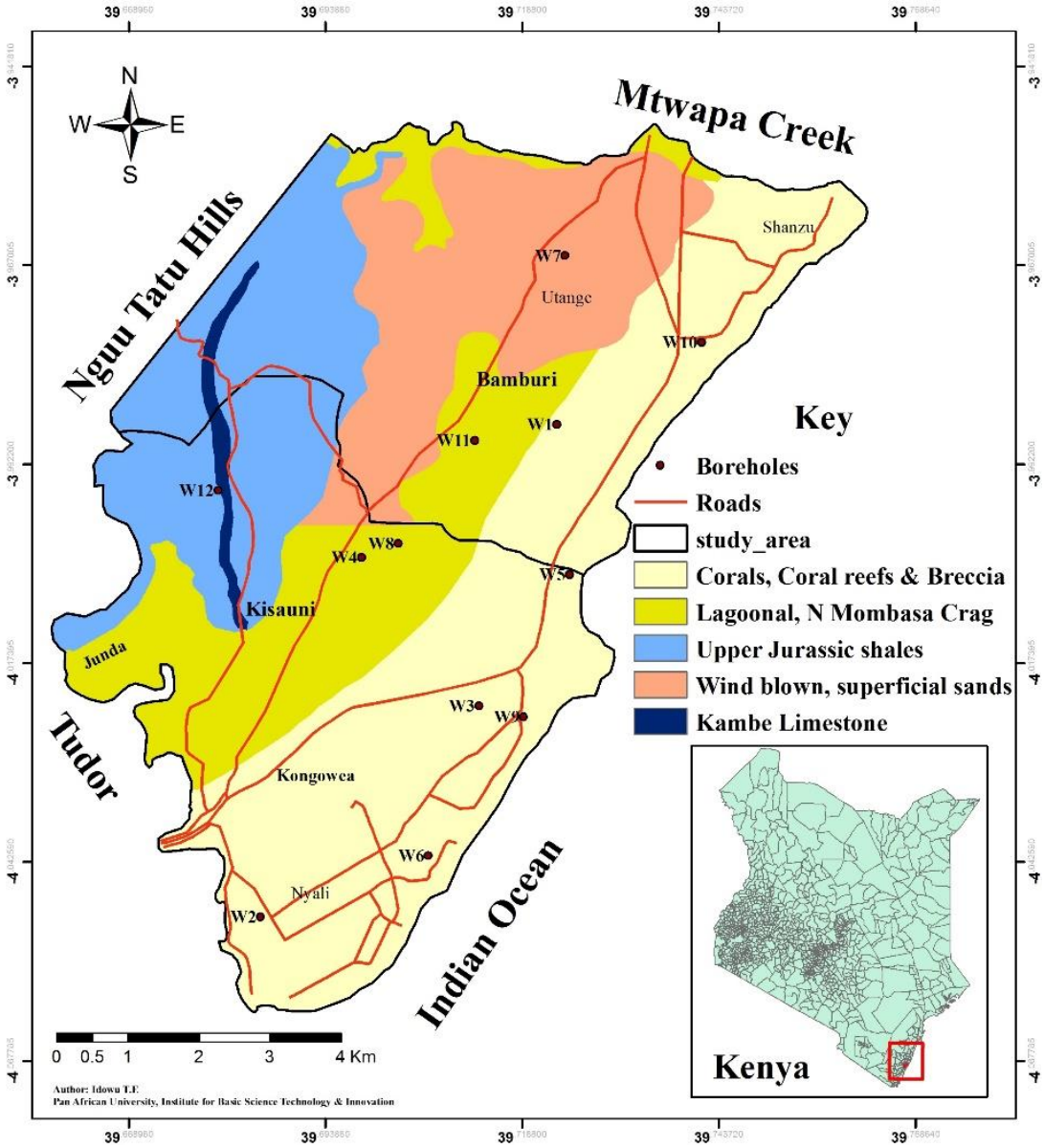

Figure 3. 11: Map of the study area
(Extracted from CASWELL 1954 geological sheets using ArcGIS)

vii. Socioeconomic Conditions

The coastlines are characterised by beautiful beaches, rich biodiversity and a variety of coastal resources. Kisauni is also an agricultural region with a wide range of cultivated crops such as cassava, cashew-nets, and coconuts. Besides being the most populated division in the county, the direction of population growth in Mombasa County is towards the north thrust of Mombasa coast. Hence, there are lots of informal settlements with poorly planned settling patterns. There are numerous low-cost areas with high densities such as Kisauni Estate, Barsheba, Mlaleo, Magogoni, Mwandoni, Mishomoroni, Bakarani, Shanzu amongst others. The significant Socio-economic activities taking place include; beef and dairy farms, tourist hotels and a few industries.

3.2 Materials and Methods

The materials used and methods of data collection completed for this research are highlighted under this section.

3.2.1 Secondary Data Collection

Prior to the actual field data collection exercise, secondary data acting as both guides and auxiliary sources of information were obtained. These data formed the basis for the field and laboratory data analysis and are highlighted in Table 3.1;

Table 3.1: Secondary data obtained and their sources

Secondary Data	Data types	Sources
Geological Data	Geological report 24 & 34, Map sheets 66,69	Mines & Geological Department, Ministry of Environment & Natural Resources, Kenya
Topographic Maps	Grid numbers 198/3, 198/4 and 201/1	Survey of Kenya, Ministry of Lands and Physical Planning, Kenya
Digital Elevation Model	SRTM 30m DEM resolution for Kenya	US Geological Service domain
Historical Data	Geophysical reports of some existing boreholes	Ministry of Water (Maji House), Nairobi, Kenya
Borehole Records	Archived borehole and geophysical survey reports	Water Resources Management Authority, Mombasa, Kenya

3.2.2 Field Data Collection

The data obtained in the field include; the GPS coordinates of the identified boreholes and wells, Electrical Conductivities, Total Dissolved Solids, pH, NaCl, static water table measurements and water samples for further tests in the laboratory. The water samples obtained were stored in cool boxes filled with ice cubes from the points of the collection in the field to the laboratory. The techniques used for obtaining the field data are highlighted in Figure 3.2.

Table 3.2: Summary of the field data obtained and the collection techniques

Field Data	Techniques for Collection
GPS coordinates	Garmin eTrex GPS receiver
Electrical Conductivity	Portable Eutech waterproof Cyberscan PC 650 & Hanna HI 99300 devices
Total Dissolved Solid	Portable Eutech waterproof Cyberscan PC 650 & Hanna HI 99300 devices
pH	Portable Eutech waterproof Cyberscan PC 650 & Hanna HI 99300 devices
NaCl	Portable Eutech waterproof Cyberscan PC 650
Static water table	Solinst water level meter (dipper)
Water samples	Sterilised 500ml transparent bottles in a cool box filled with ice

The field data collection were in phases of pre-monsoon, rainy season and post-monsoon as follows;

Pre-monsoon- 24th and 25th March 2016

Rainy season- 28th and 29th June 2016

Post-monsoon- 1st and 2nd September 2016.

Data was obtained from 12 selected boreholes and shallow wells as pre-monsoon and it expanded to 15 boreholes and shallow wells at the rainy season and post-monsoon respectively.

3.2.3 Laboratory Data Analysis

The water samples obtained from the selected boreholes and wells in the field were transported to the laboratory within 24 and 48 hours of sample collection and analysed. The procedures and health and safety precautions taken during the laboratory analysis are highlighted in Brown *et al.,* (1983). The cations tested include; Sodium (Na^+), Calcium (Ca^{2+}), Magnesium (Mg^{2+}), and Potassium (K^+) and the anions tested include; Chloride (Cl^-), Bicarbonate (HCO_3^-), and Sulphur dioxide (SO_4^{2-}). The summary of techniques used for the water sample analyses is highlighted in Table 3.3.

Table 3. 3: Techniques used for the laboratory analysis of water samples

Chemical constituents of Groundwater	Techniques used
HCO_3^-	Volumetric method (Acidimetric neutralization)
Cl-	Colorimetric Determination of Chlorine using Mercuric Thiocyanate and Ferric Ion and Spectrophotometer
SO_4^{2-}	Turbidimetric method using spectrophotometer
Na^+, K^+	Flame Emission Spectroscopy
Ca^{2+}, Mg^{2+}	Flame Atomic Absorption Spectroscopy

The secondary data, field data and results of laboratory analysis of water samples were all assembled into a geodatabase on ArcGIS software. Summary of the software packages used and their specific applications in this study are highlighted in Table 3.4.

Table 3. 4: Techniques used for the laboratory analysis of water samples

Software package	Application
ArcGIS 10.3 (ArcMap)	Creation of geodatabase, spatial analysis of parameters, vulnerability mapping
DNR Garmin	For importing coordinates data from the GPS receiver to the computer
Grapher ™	Creation of piper plots
Eviews	Correlation and regression analysis
Microsoft Excel	Data analysis to obtain minimum, maximum, mean, standard deviation, cross plots,
GMS software	Groundwater flow and solute transport simulation using the MODFLOW, MT3D & SEAWAT package embedded.

3.3 Assessment of the hydrogeological characteristics, salinity and extent of seawater intrusion

The three phases of data collection in the north coast of Mombasa coinciding with pre-monsoon, rainy season and post-monsoon formed a half-season cycle. The data obtained in each phase were statistically and spatially analysed similarly and the results compared. The water quality parameters measured in the water samples were compared with the Kenya and WHO drinking water guidelines. Hydrogeological characteristics of the coast were described by the aquifer type, geological formation, and the groundwater heads using the geological data (secondary data) and static water level measurements (field data) on ArcGIS software package. The state of salinity and extent of seawater intrusion of the region were also assessed and analysed statistically and geospatially from the field data and laboratory analyses results. Mondal et al. (2010) adopted a methodology for assessing salinity and saltwater intrusion in a coastal aquifer. From their

methodology, this research adopted the cations, anions and specific indices for assessing the characteristics of the groundwater and extent of seawater intrusion. The general workflow employed in achieving the objective is outlined in Figure 3.3.

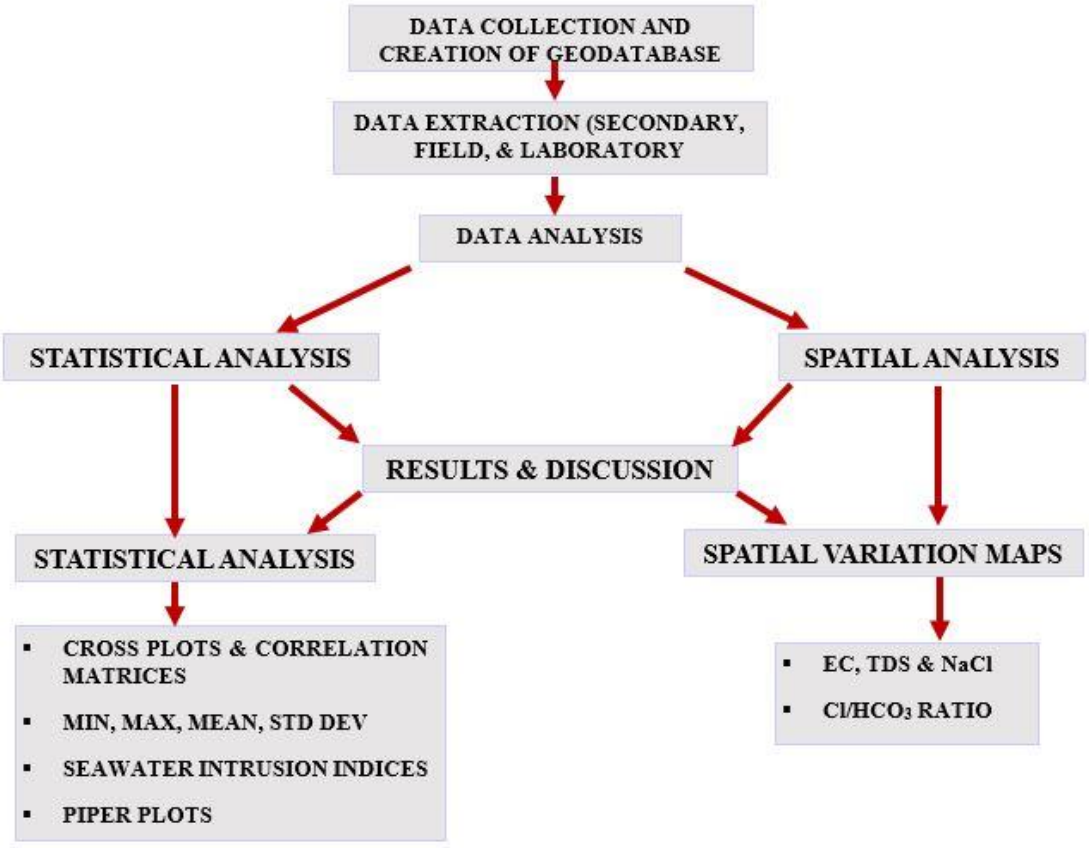

Figure 3. 12: Flowchart for the general steps in assessing hydrogeological characteristics, salinity and SWI

3.3.1 Hydrogeological Characteristics of the study area.

Hydrogeological characteristics entail the nature of the underlying rocks that constitutes the aquifer as well as the general depths or groundwater heads in the study area. The geological maps obtained were digitised, georeferenced and mosaicked together with the aid of GIS. From the large mosaicked image, the study area was clipped out to develop the geological map of the study area. Water level heads taken during the field trip were imported into ArcGIS and geostatistically interpolated to form isopleth maps of the hydraulic heads of the study area. The groundwater head contours layer was overlaid on the geological layer to form the hydrogeological map of the study area. Correlation matrices and cross plots are widely used in studying the groundwater chemistry

in aquifers (Mtoni et al, 2015; Sappa et al, 2015) and these were computed for the groundwater parameters in this study. The EC, TDS, Na, K, Mg, Ca, Cl, HCO_3 and SO_4 were all analysed for their correlational relationships to ascertain the major parameters influencing the geochemistry of the coastal aquifer. In classifying the groundwater, a piper plot was used (Piper, 1953). Piper plot is one of the most widely applied methods of characterising groundwater (Karmegam, et al 2011; Musa et al 2014). A piper plot is a graphical depiction of the chemistry of water sample(s). Two ternary plots containing normalised values of the cations and anions respectively are projected into a diamond which describes the broad nature of the groundwater (Piper, 1953). The piper plot categorises ground water as any of the following; Calcium sulphate waters, Sodium chloride waters, Sodium bicarbonate waters or Calcium bicarbonate waters. Calcium sulphate waters are typical of gypsum groundwaters and mine drainages; Calcium bicarbonate waters are indicative of shallow fresh groundwater; Sodium Chloride waters are indicative of marine and deep ancient groundwaters; while Sodium bicarbonate waters typify deeper groundwater influenced by ion exchange (Piper 1953). The cations (Na+k, Mg, Ca) and anions (Cl, SO_4, HCO_3) are normalised into 100%. These normalised values are plotted into the right and left triangles (Figure 3.4) which form points of intersections in the diamond where the groundwater chemistry is interpreted (Figure 3.5).

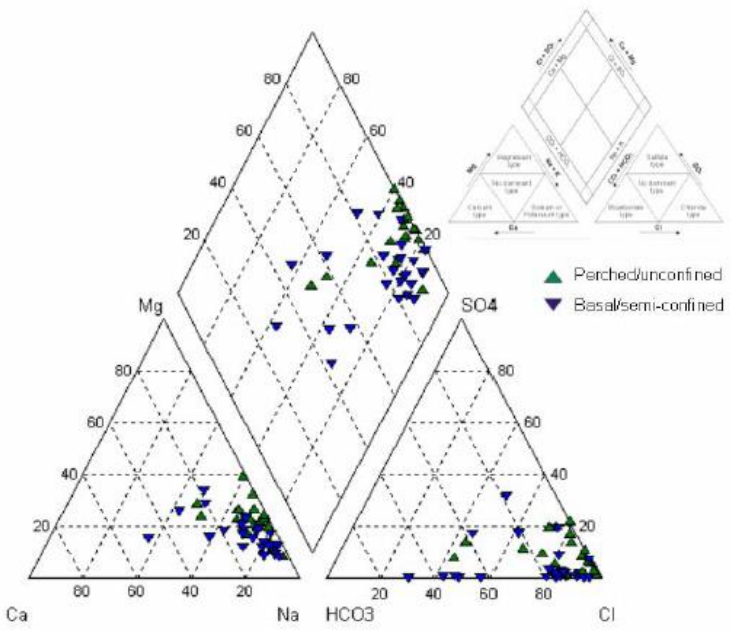

Figure 3. 13: Trilinear plots (piper) of the central catchment of Bribie Island (Source: Jackson, 2007)

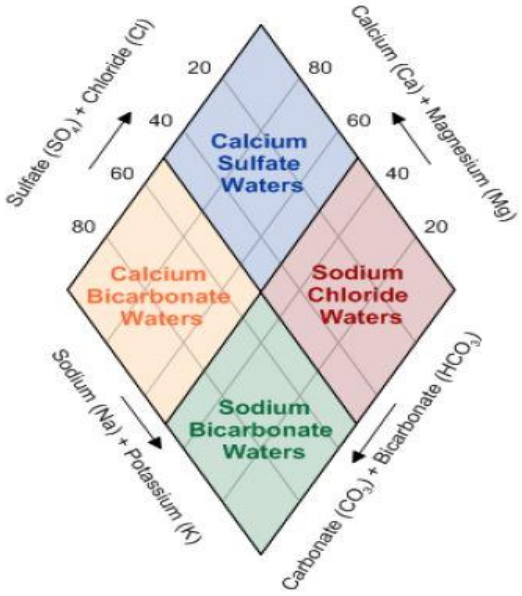

Figure 3. 14: The diamond for the interpretation of the groundwater characteristics

3.3.2 Salinity assessment of the groundwater of the study area.

Salinity in groundwater may be from several sources including, anthropogenic activities such as irrigation and saltwater bodies in proximity to the aquifer. The indicator used for assessing the salinity of the groundwater was the EC and TDS based on classifications by Saxena et. al (2003).

Saxena et al, (2003) classified groundwater based on EC values into three main classes- Fresh; Brackish; and Saline water. The ranges for each class is given as;

- Freshwater (<1,500 μS/cm);
- brackish (1,500–3,000 μS/cm);
- saline (>3,000 μS/cm)

Spatial maps of the classified EC and TDS, as well as the NaCl distribution in the groundwater across the study area, were drawn with the aid of GIS.

3.3.3 Assessment of the extent of seawater intrusion in the study area

Several approaches have been identified and widely applied in assessing the extent of seawater intrusion in a coastal aquifer. The most prominent index is the Simpson's ratio highlighted in Todd & May (2005) which was also applied in this study. This is the ratio of the chloride content to the concentration of bicarbonate in a water sample (Cl/HCO_3). El Moujabber et al. (2006), Korfali & Jurdi (2010) all adopted the range given below for classification of the extent of the impact of groundwater to seawater intrusion – Good quality (<0.5); Slightly contaminated (0.5-1.3); Moderately contaminated (1.3-2.8); Injuriously contaminated (2.8-6.6); and Highly contaminated (6.6-15.5). The groundwater samples in the study area were categorised based on this classification. These values were interpolated across the study area and the spatial maps were drawn.

Other parameters used for delineating the extent of seawater intrusion in the study are;

- Na/Cl ratio (Vengosh *et al.* (1997)
- Plots of TDS against HCO^-_3/Cl^- and Ca^{2+}/Na^+ ratios (Mondal et.al, 2010).

3.4 Spatial Vulnerability Mapping of the Coastal Aquifer to Saltwater Intrusion

This study attempted to map out the vulnerability of the coastal aquifer to seawater intrusion using the GALDIT overlay index. Lobo-Ferreira & Cabral (1991) defined the vulnerability of Groundwater to sea water intrusion as "the sensitivity of groundwater quality to an imposed groundwater pumping or sea level rise or both in the coastal belt, which is determined by the

intrinsic characteristics of the aquifer". GALDIT identified the most important characteristics of the coastal aquifer influencing the intrusion of seawater as;

- Groundwater Occurrence (aquifer type; unconfined, confined and leaky confined)
- Aquifer Hydraulic Conductivity
- Height of Groundwater Level above Sea level
- Distance to the seawater body (Inland distance perpendicular from the shoreline)
- Impact of existing Status of seawater intrusion in the area under study
- Thickness of the aquifer being mapped

3.4.1 GALDIT factors for the coastal aquifer of the study area

Based on the peculiarity of the study area, each of the factors is described below;

i. Groundwater Occurrence

Groundwater tapped from aquifers are in layers and these layers may be unconfined, confined, leaky confined or have geological boundaries. Confined aquifers may be said to be the most vulnerable due to their relatively larger cone of depression and high-pressure release of water during pumping. It, therefore, gets a rating of 10. The importance ratings for the aquifer types are all shown in Table 3.5. Groundwater in the study area is stored in an unconfined aquifer comprising limestone, coral reefs, sandstones and shales to average depths of 100m to the surface (Caswell, 1954; Caswell, 2007). The groundwater occurrence may, therefore, be given an importance rating of 7.5.

Table 3. 5: Ratings for GALDIT parameter G

Indicator	Weight	Indicator Variables	Importance Rating
Groundwater occurrence/Aquifer type	1	Confined Aquifer	10
		Unconfined Aquifer	7.5
		Leaky confined Aquifer	5
		Bounded Aquifer	2.5

ii. Aquifer hydraulic conductivity

Also referred to as the coefficient of permeability, aquifer hydraulic conductivity is a measure of the aquifer's ability to transmit water through its pores when subjected to head differences. By definition, it is the flow per unit cross-sectional area of the aquifer when subjected to a unit head (hydraulic) per unit length of flow (m/day) (Deb, 2014). Higher conductivities increase the risk of seawater intrusion and also results in wide cones of depression during pumping (Sophiya and Syed

2013). This implies hydraulic conductivity K does not only influence the influx of seawater inland but also the rate at which fresh groundwater moves seawards i.e. it plays a defining role in the freshwater-saltwater interface of coastal areas. The hydraulic conductivity of the porous media covering the study area varies from less than 4 to 12 m/day (Munga et al, 2006). Hence, the modified rating for hydraulic conductivity in the study area is expressed in Table 3.6

Table 3. 6: Ratings for GALDIT parameter A

Indicator	Weight	Indicator Variables		Importance Rating
		Class	Range	
Aquifer hydraulic conductivity (m/day)	3	High	>40	10
		Medium	12 – 40	7.5
		Low	4 – 12	5
		Very Low	<4	2.5

iii. Height of ground water above the mean sea level

This factor heavily influences the freshwater hydraulic pressure required to counterbalance the intrusion of seawater. The higher the groundwater level above sea level, the higher the hydraulic pressure and hence, the lower the risk of seawater intrusion (Chachadi & Lobo-Ferreira, 2001). The static water levels were taken both at the peak of the dry season and during the rainy season. Digital Elevation Model (DEM) for the study area was used in conjunction with static water level measurements of the selected boreholes to estimate the groundwater levels above the mean sea level. Groundwater level above mean sea level is an important factor when assessing the vulnerability of fresh groundwater sources to saltwater intrusion. The static water levels measured across the study area are relatively shallow ranging from 8m to 24m. By estimation, the groundwater levels above sea level were found to vary generally from -3m to 30m above mean sea level. Table 3.7 shows the modified ratings for the height above sea level of the groundwater in the study area.

Table 3. 7: Ratings for GALDIT parameter L

Indicator	Weight	Indicator Variables		Importance Rating
		Class	Range	
Height of groundwater above sea level (m)	4	High	<1	10
		Medium	1 – 5	7.5
		Low	5 – 10	5
		Very Low	>10	2.5

iv. Distance from saltwater body

The closer the area is to the shore or the creek, the higher the impact of the saltwater intrusion. The study area is bounded by the Indian Ocean to the east and by creeks on the north and south. This distance of each point to the saltwater body was calculated using the NEAR spatial analyst tool on ArcGIS. The modified ratings for the factor D is highlighted in table 3.8.

Table 3. 8: Ratings for GALDIT parameter D

Indicator	Weight	Indicator Variables		Importance Rating
		Class	Range	
Distance to the Shore (m)	4	Very small	<500	10
		Small	500 – 1500	7.5
		Medium	1500 – 2500	5
		Far	>2500	2.5

v. Impact of existing status of sea water intrusion

There are several indices for assessing the extent of saltwater in a study area. Base Exchange Index, Graphical methods, Na^+/Cl^-, Ca^{2+}/Na^+ and Cl^-/HCO_3^- are but a few of the widely used indices (Klassen, 2014). The ratio of chloride to bicarbonate, also referred to as Revelle's coefficient or Simpson's ratio is the most recommended (Chachadi & Lobo-Ferreira, 2001). The ratios for the study area were found to range from 1.16 to 3.97. Table 3.9 represents the modified ratings for the impact of the existing status of seawater intrusion.

Table 3. 9: Ratings for GALDIT parameter I

Indicator	Weight	Indicator Variables		Importance Rating
		Class	Range	
Impact of existing status of Seawater Intrusion	1	High	>2	10
		Medium	1.5 – 2	7.5
		Low	1 – 1.5	5
		Very Low	<1	2.5

vi. Thickness of the aquifer being mapped

The saturated thickness of an unconfined aquifer also influences the extent and magnitude of saltwater intrusion. The larger the thickness of the aquifer, the greater the likelihood of saltwater intrusion and vice versa (Chachadi and Lobo-Ferreira 2001; Najib et al. 2012; Kura et al. 2014).

From the sparse boreholes, log data gathered, the lithology of the study area is very heterogeneous in nature showing varying layers of limestone, sandstone and shales. Limestone and Sandstones are good aquifers while shale is not. However, within the study area, upper Jurassic shales lie deep below the coral reefs, North Mombasa crag, kilindini sands and the wind-blown sands in areas

close to the Ocean. The logs from a borehole sunk close to Bamburi up to a depth of 245 feet (74m) reveals intermittent layers of coral reefs, shell fragments, Sandstones, dirty white sandy clays and coral limestone (Caswell, 1957). Few other boreholes data found in the study area show the same trend. Furthermore, cross-sectional views of the lithology of the study area as shown in the geological Map show that coral reefs, kilindini sands/North Mombasa crag, and the wind-blown superficial sands extend far below 100m in most areas.

Based on this information the ratings for the aquifer thickness is given a maximum value of 10. The ratings for the aquifer thickness is expressed in Table 3.10

Table 3. 10: Ratings for GALDIT parameter T

Indicator	Weight	Indicator Variables		Importance Rating
		Class	Range	
Thickness of Aquifer being mapped	2	Large	>2	10
		Medium	1.5 – 2	7.5
		Small	1 – 1.5	5
		Very Small	<1	2.5

Decision criteria

This procedure enables the determination of numerical values of the hydro-geographical factors using an additive model. The minimum and maximum GALDIT indices are obtained by multiply the weights with the respective importance ratings as shown in Equation 8.

$$\text{GALDIT Index} = \frac{TS}{\sum_{i=1}^{6} W_i} \qquad 8$$

Where;

$TS = (W_1 \times G) + (W_2 \times A) + (W_3 \times L) + (W_4 \times D) + (W_5 \times I) + (W_6 \times T)$

W_1 to W_6 are the respective relative weights given to the six hydrogeological factors.

$\sum_{i=1}^{6} W_i = 15$

Once the GALDIT-Index has been calculated, the groundwater is then classified based on the seawater intrusion vulnerability. The minimum and maximum range of GALDIT index scores are divided into; low, moderate, and high vulnerability classes ranging from 2.5 to 10.

Based on Chachadi and Lobo-Ferreira (2005), the computation for the GALDIT indices is shown in Table 3.11;

Table 3. 11: GALDIT Index computation

SN	Indicators	Weight	Range of Importance ratings				Range of scores (weight importance)			
			Min	In- between		Max	Min	In between		Max
1	**Groundwater occurrence**	**1**	**2.5**	**5**	**7.5**	**10**	2.5	5	7.5	10
2	Aquifer hydraulic conductivity	**3**	**2.5**	**5**	**7.5**	**10**	7.5	15	22.5	30
3	**Height of groundwater above sea level**	**4**	**2.5**	**5**	**7.5**	**10**	10	20	30	40
4	**Distance from the shore**	**4**	**2.5**	**5**	**7.5**	**10**	10	20	30	40
5	**Impact of existing status of seawater intrusion**	**1**	**2.5**	**5**	**7.5**	**10**	2.5	5	7.5	10
6	**Thickness of the aquifer being mapped**	**2**	**2.5**	**5**	**7.5**	**10**	5	10	15	20
					Total Score (TS)		37.5	75	112	150
					Galdit Index		2.5	5	7.5	10

These factors were mapped into raster layers on GIS and overlaid based on their weights, ranges and importance ratings. The final vulnerability maps which bore the weighted sums of the individual layers were produced.

3.4.2 Generalised workflow for the vulnerability analysis

The general workflow for developing the spatial vulnerability map is highlighted in Figure 3.6.

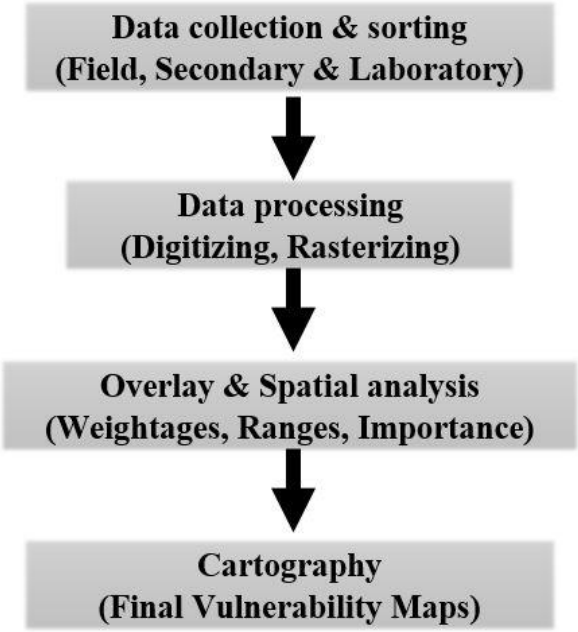

Figure 3. 15: General methodology for the vulnerability analysis

i. Data collection and sorting

The secondary, field and laboratory data obtained in the course of the study were organised into folders usable for further processing. The few borehole historical data obtained from WRMA were saved in excel database, the geological maps and topographic maps were scanned and geo-processed for further processing. The coordinates of landmarks and boreholes taken during the field trip were imported into the computer using DNR-Garmin software. Overall, a geodatabase was created where all these data are stored either as jpegs, excel, or GPS exchange format.

ii. Data processing

Thematic raster layers were created from the geodatabase for each of the factors by clipping the geological map into the area of interest, interpolating the DEM on point data in order to establish heights above sea levels of the groundwater heads, and using spatial interpolation tools to create rasters from point data. The six thematic layers created for the GALDIT factors all had uniform pixel sizes of 30m. All these were performed on the ArcGIS platform.

iii. Overlay and spatial analysis

Based on the GALDIT index computation, appropriate weightages, ranges and importance ratings as reflected in Tables 3.5 – 3.11 were assigned to each thematic layer representing each GALDIT

factor respectively. The thematic layers were then overlaid and the aggregate weighted sum derived. The final vulnerability rasters were then resized into weights of importance range of 2.5, 5, 7.5 and 10. These importance ranges were classified based on low, medium or high vulnerabilities.

iv. Cartography (final vulnerability maps)

Map elements such as the legend, north arrow, scale, geographic grids were inserted into the final vulnerability rasters to form maps which are easily understood and interpreted by any reader.

3.5 Simulation of the groundwater flow and solute transport in the study area.

Loose coupling approach was employed for the interaction between the geographic data process (GDP) and the process-based model (PBM). The PBM used include MODFLOW, MT3D and SEAWAT. All three packages are embedded in a robust software package called Groundwater Modelling System (GMS) which was used for this study.

The MODFLOW module was used for solving the steady and transient state simulation based on the modified three-dimensional groundwater flow (Equation 3&4, page 20).

The MT3D package is based on the partial three-dimensional equation for solute transport simulation given by Freeze & Cherry, (1979) as highlighted in Equation 5 (page 21). Equation 5 was slightly modified by Zheng & Wang (1999) and represented as Equation 6 (page 21) and subsequently acts as the running equation behind the MT3D used.

The SEAWAT package combined the three-dimensional groundwater flow solution from MODFLOW and the partial three-dimensional solute transport solution from MT3D. The flow and solute transport procedures in the MODFLOW and MT3D were repeatedly solved by the SEAWAT package until the provided stress periods and simulation were complete. The underlying flow equation behind the SEAWAT used is given in Equation 7 (page 22).

GIS files were independently imported into the GMS software for analysis. The general steps involved in the flow and solute transport simulation is expressed in Figure 3.7

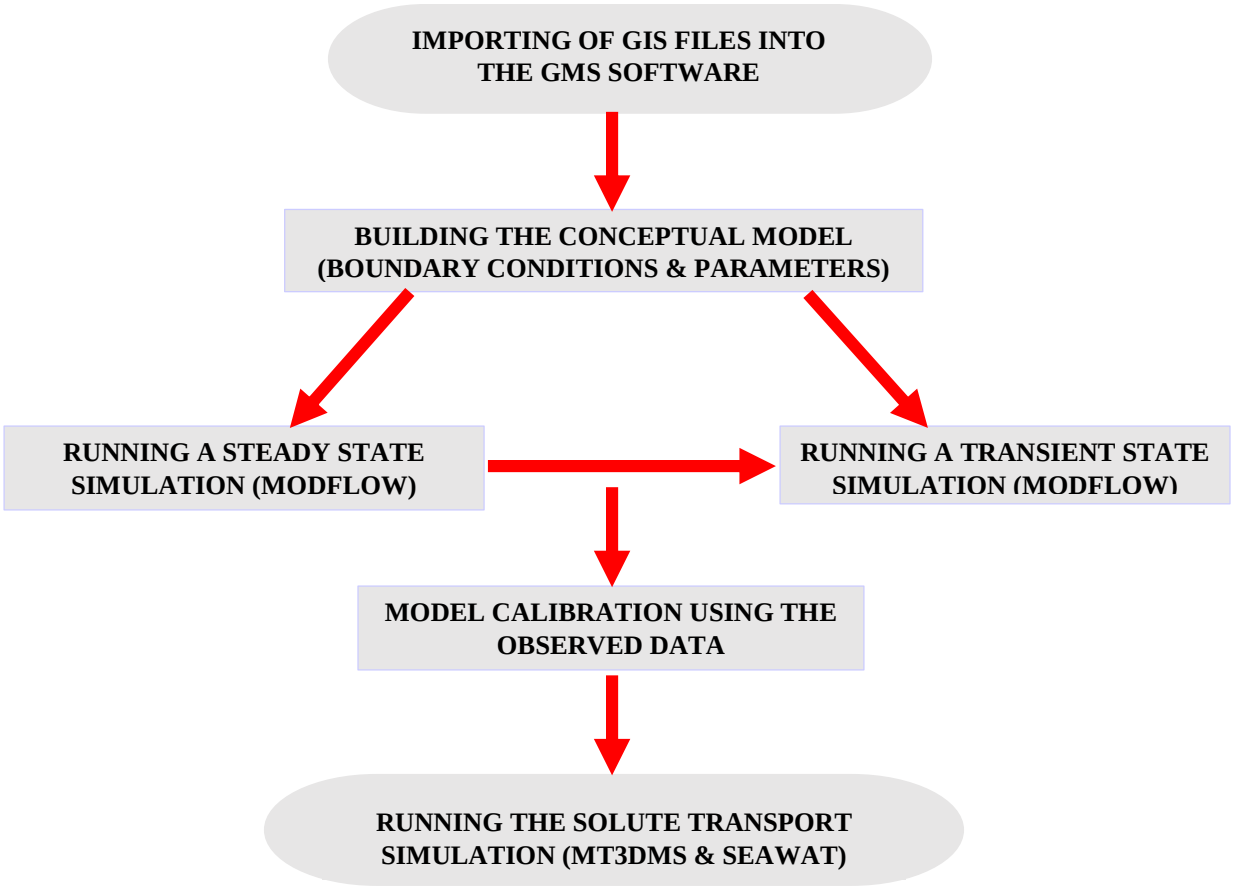

Figure 3. 16: General steps involved in the groundwater flow and solute transport simulation

3.5.1 Importing GIS Files into GMS (loose coupling)

The model inputs used for the process based modelling were independently imported from the GIS database. This approach is referred to as the loose coupling technique where independent packages are used for the GDP and PBM components of the model. The advantage is that changes are easily facilitated in an independent manner in either package since each software is distinct on its own. The following GIS files were imported into the GMS software.

- Study area boundary (shapefile)
- Hydraulic conductivity polygon (shapefile)
- Recharge polygon (shapefile
- Borehole/wells data (shapefile)
- Digital Elevation model of the study area (raster)
- Hydraulic head (raster)

These were either converted to feature objects or interpolated to the 3D grid within the GMS interface (Figure 3.8). These files were used to construct the boundary layer; Source & sink layer; Recharge layer; hydraulic conductivity and the elevations in the GMS workspace.

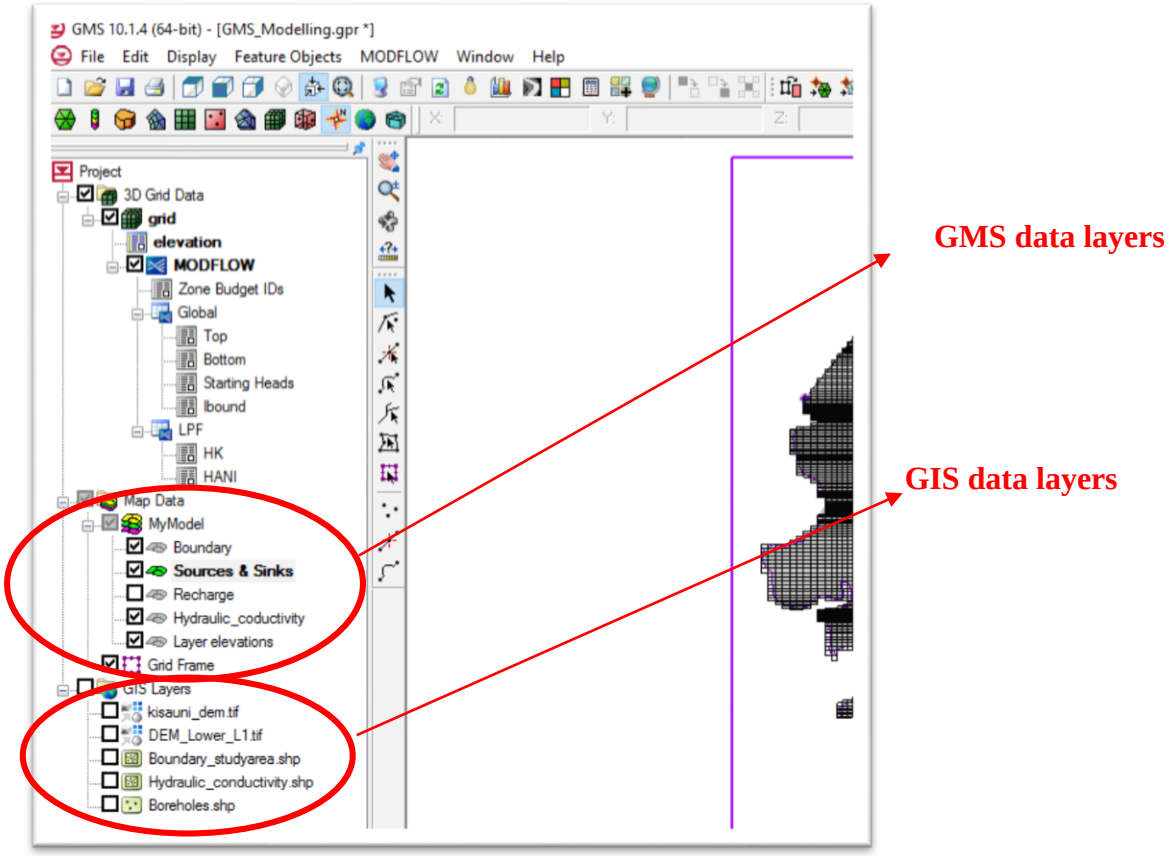

Figure 3. 17: GMS software interface showing the GIS and GMS data layers in the project explorer

3.5.2 Building the Conceptual Model for the Aquifer

This involves defining the hydraulic boundary conditions and imputing the parameters that describe the aquifer being modelled. The hydraulic boundary conditions were delineated into the no-flow boundary and the constant head boundary. The northern, southern and eastern boundaries formed the constant head boundaries (Figure 3.9). These are the boundaries bordering the creeks and the Ocean as described in section (3.2.4). The western boundary which consists of the elevated hills of Nguu-tatu formed the no-flow boundary (Fig3.9).

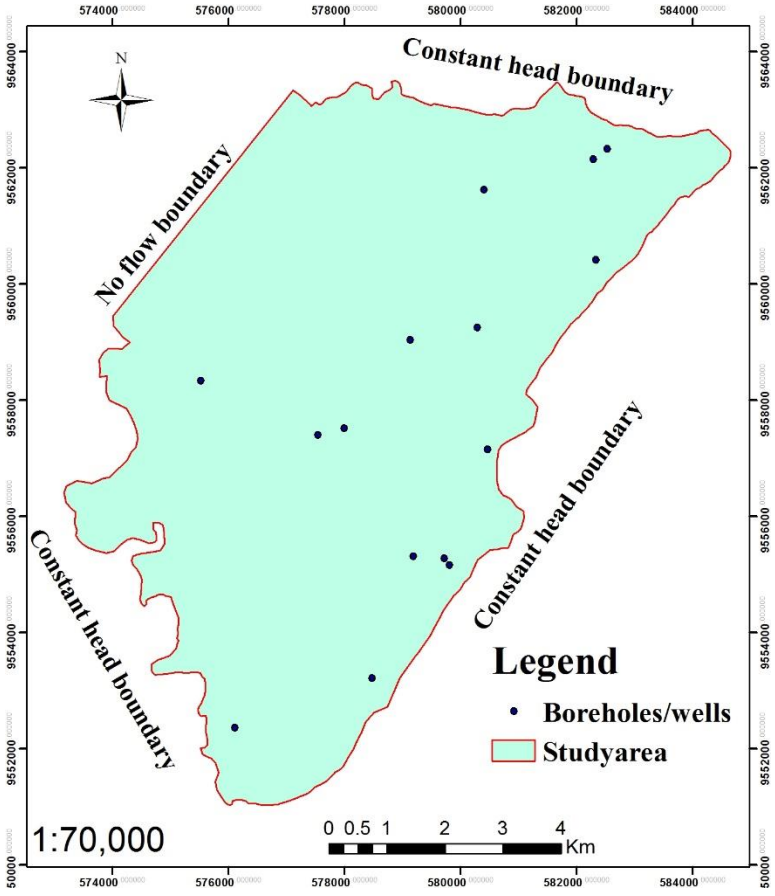

Figure 3. 18: The hydraulic boundary conditions of the study area

The parameters used in building the conceptual model were taken from secondary data, a previous study (Munga *et al.*, 2006), borehole geophysical records, as well as historical rainfall data. They are given as follows;

- Recharge: Based on the geological formation, recharge was estimated based on 5 and 10% of average monthly rainfall data for the past 10 years.
- Horizontal hydraulic conductivity (k): 4 – 12 m/day
- Vertical hydraulic conductivity: ¼ of k
- Specific yield: 0.1 – 0.2
- Specific storage: 0.0001
- Porosity (Θ): 0.3
- Coefficient of longitudinal dispersivity: 20
- Fluid density (ρ): 1000kg/m^3 for freshwater & 1025kg/m^3 for saltwater

- Transmissivity(T): k × (Aquifer thickness)
- Specific capacity- 0.6854 m^2/hr
- Flow rates/ discharges: based on specific wells
- Hydraulic heads: estimated from static water levels taken from each borehole and interpolated into a raster.

3.5.3 Steady State Flow Simulation

Steady state flow is a case where the magnitude and direction of the flow are kept constant throughout the entire hydrologic boundary. In other words, the hydraulic head remains constant with time but this does not imply a lack of movement in the groundwater. It simply implies the net flow in and out within the system is kept constant. Hence the storage term parameter in the equation is not utilised since there are no changes in head and obviously no change in the volume of water stored within the domain. From the conceptual model, the steady-state simulation was solved for the study area using the initial interpolated head raster as the starting heads. The flow direction was established at the end of the simulation.

3.5.4 Transient State Flow Simulation

Transient state flow occurs when the direction and magnitude of the flow changes with respect to time. Transient models require commencing with a steady-state stress period, establishing the starting heads equal to the solution generated from a steady state model, or allowing some time at the start of the transient model for the heads to stabilise before applying any changes in stresses (pumping rates, recharge rates, etc.). In the case of this simulation, the starting heads generated from the steady state solution were used in defining the initial stress condition of the transient state flow simulation. The subsequent stress periods were defined by incorporating the storage parameter, specific yield, and transient recharge data within the domain, abstraction rates from boreholes at different times. These parameters were incorporated into the conceptual model and enabled for transient state simulation. The subsequent stress periods were chosen to coincide with the data collection periods i.e., 29th June 2016, 1st September 2016, and 15th September 2016.

3.5.5 Model Calibration

Model calibration is essential in validating the behaviour of the model as representative as possible of the actual aquifer being modelled. Calibration is a process in which certain parameters in the model such as the recharge and hydraulic conductivity are altered systematically and repeatedly until the computed solution matches the field observed values within an acceptable level of accuracy.

The model was calibrated using observed heads taken from boreholes/wells over the period of simulation. The acceptable observation head interval used was 1m. The Hydraulic conductivity values and transient recharge data were iteratively altered until the observed errors were within the acceptable intervals.

3.5.6 Solute Transport Simulation (MT3DMS and SEAWAT)

MT3D simulations are either constructed from the grid approach or the conceptual model approach. In both cases, solutions from the groundwater flows are required for it to run. This study employed the conceptual model approach where data were entered via points, arcs and polygons. Using the solutions for the calibrated transient state simulation, the solute species was defined (salt) and initial concentrations of the salt imputed based on the field data. The MT3D packages needed for SEAWAT simulation are the advection and source/sink mixing packages. Here the porosity and longitudinal dispersivity components of the aquifer characteristics were defined in the conceptual model. The MT3D module was run and the results viewed before creating a new simulation for the SEAWAT.

Solutions from the MODFLOW and MT3D were incorporated into the SEAWAT module for simulating the intrusion of seawater within the GMS software package.

CHAPTER FOUR- RESULTS AND DISCUSSION

4.1 Hydrogeological Characteristics, Salinity and Extent of Seawater Intrusion

4.1.1 Hydrogeological Characteristics and Groundwater Chemistry

The nature of the aquifer in which ground water occur in the study area was found to be unconfined based on the lithological and geological information from Caswell (2007). The geology of the study area comprise mainly corals, coral reefs, lagoonal sands, limestone and sandstone occurring intermittently in sedimentary layers to a minimum depth of 100m to the surface in most portions of the aquifer (Cawell 1954). The water table measurements from boreholes and wells taken across the study area show that groundwater heads varying from -3m to 30m above sea level both in the rainy and dry season (Figure 4.1). There were no large water table variations between the rainy and dry seasons (See Appendix I). The spatial variation map of the water levels is represented in Figure 4.2.

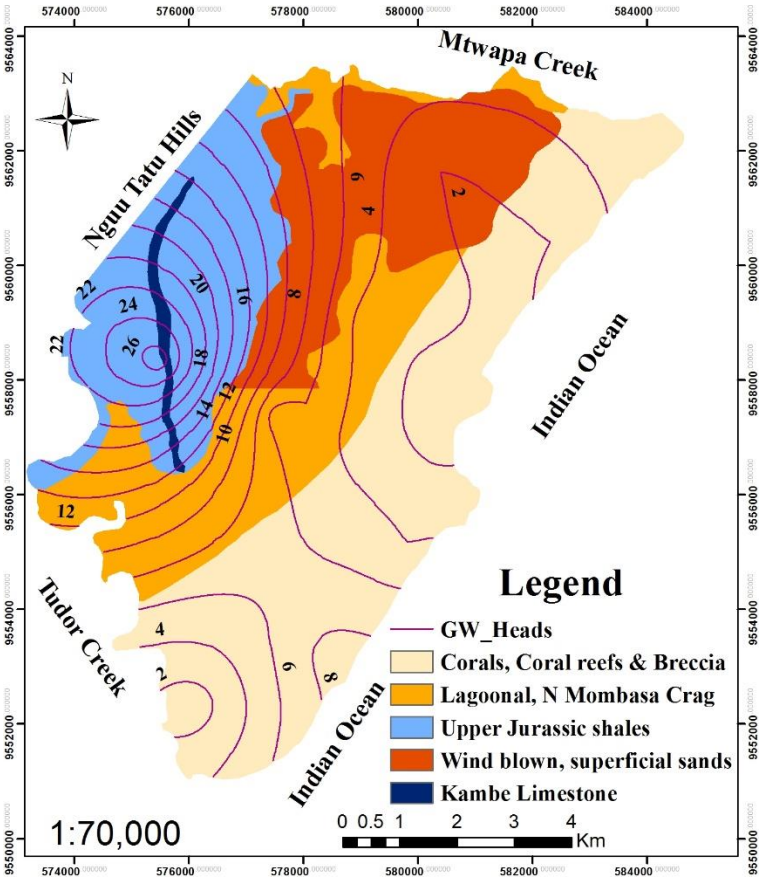

Figure 4. 2: Hydrogeological map of the study area showing the GW heads above MSL (March 2016)

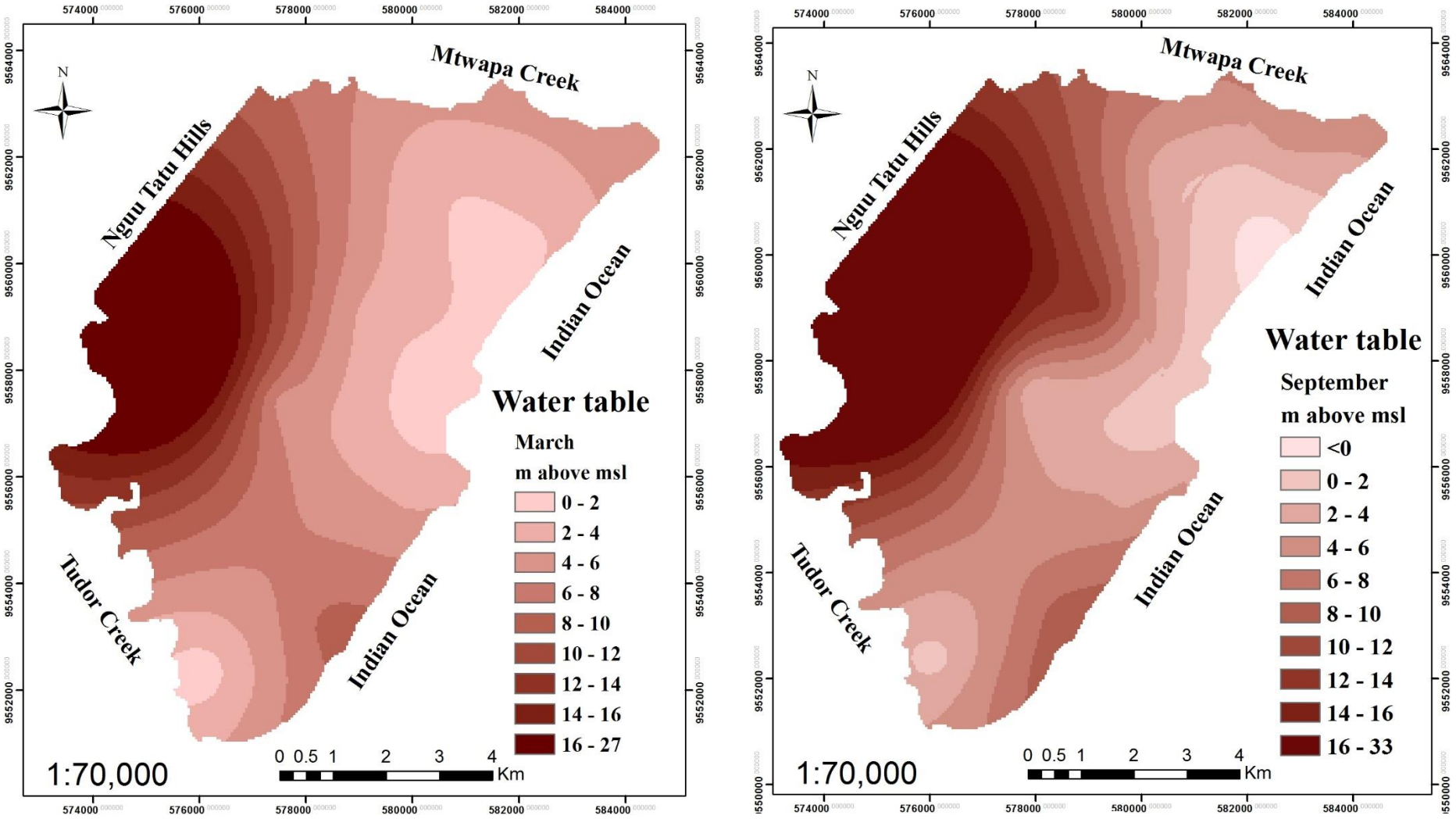

Figure 4.2: Groundwater table in the coastal aquifer at (a.) pre-monsoon and (b.) post-monsoon

It will be observed that the groundwater table was highest in the elevated regions of the Nguu tatu hills on the western part of the study area. The groundwater table is considered shallow. The relatively low elevation topography of the study area implies that the static water levels from boreholes are as shallow as 8m to the surface in some cases. This closeness of the water table to the surface implies an abundance of groundwater. However, it also indicates that the groundwater is more susceptible to surface pollution such as leachates from incinerators and pit latrines.

The analysis of the field and laboratory data taken at the pre-monsoon (March) and in the raining season reveals a substantial insight on the nature of the groundwater. The groundwater pH generally revealed only minor changes across the entire period of observation. The pH values in the groundwater in March, June and September were predominantly slightly alkaline with pH values mostly between 7 and 8. Only very few of the samples had pH values below 7 or above 8 (Table 4.1). Only two mildly acidic values (6.65 & 6.98) were observed in the data, and this was in the rainy month of June (Table 4.1b). These values coincide with the WHO 1984 pH range for rainwater, hence, the mild acidity might be due to the prevalent rainfall in that season. All but three of the samples fall within the range of 6.5 – 8.5 specified for drinking purposes by the Kenya drinking water guidelines (Kenya, 2008) (Table 4.1b, c).

Table 4.1 d: Concentration of the major parameters in the groundwater samples

March 2016 (pre-monsoon)

SN	SAMPLE LOCATION	Source Type	pH	EC (µS/cm)	TDS (mg/L)	NaCl (mg/L)	HCO_3^- (mg/L)	Cl- (mg/L)	Mg^{2+} (mg/L)	Ca^{2+} (mg/L)	Na+ (mg/L)	K+ (mg/L)
W1	**Braeburn**	**B**	7.38	993	556	982.2	143.96	166.5	7.31	32.95	125.93	10.54
W2	**Cinema**	**S/W**	7.52	1566	839	1450	146.40	212.8	3.93	10.73	136.77	7.40
W3	**Krat**	**B**	7.25	2931	1573	2611	119.56	286.4	9.64	26.60	310.73	20.72
W4	**M. Hussein**	**S/W**	7.35	1290	754	1185	95.16	197	6.84	27.36	102.90	6.74
W5	**Milele**	**B**	7.61	10585	4307	10880	102.48	366.4	13.30	20.64	735.55	70.24
W6	**N golf**	**B**	7.52	3128	1934	3003	109.80	277	9.72	19.42	351.45	15.51
W7	**Redeem**	**B**	7.63	761.5	438	659.8	97.60	140.3	0.83	10.13	65.69	2.03
W8	**Ruby**	**B**	7.13	1834	1143	1743	173.24	257.8	6.93	7.39	219.80	6.99
W9	**Sos**	**S/W**	7.41	4427	2295	4406	87.84	348.6	11.47	28.42	412.41	28.49
W10	**Sunsweet**	**B**	7.2	4647	2330	4320	87.84	336.2	10.91	24.44	406.28	18.65
W11	**Utange**	**B**	7.82	1966	1028	1824	129.32	266	7.08	6.93	271.60	14.18
W12	**Vikwatani**	**S/W**	7.64	6711	2915	6832	139.08	379.6	13.10	32.84	482.62	13.19
Drinking water standard (WHO 1984)												
			7.5-8.5	**750**	**500**		**300**	**200**	**30**	**75**	**200**	**100**
Kenya Drinking Water Standards (Kenya, 2008)												
			6.5-8.5					**250**	**100**	**250**	**200**	

B-Boreholes, S/W- Shallow wells, W-Well

Table 4.1 e: Concentration of the major parameters in the groundwater samples

June 2016 (rainy season)

SN	SAMPLE LOCATION	Source Type	pH	EC (µS/cm)	TDS (mg/l)	NaCl (mg/L)	HCO_3^- (mg/L)	Cl- (mg/L)	Mg^{2+} (mg/L)	Ca^{2+} (mg/L)	Na+ (mg/L)	K+ (mg/L)
W1	**Braeburn**	**B**	7.95	1150	596	980	108.82	67.92	1.11	2.49	108.48	4.10
W2	**Cinema**	**S/W**	6.65	1626	846	1573	68.32	81.99	1.14	3.02	180.12	8.64
W3	**Krat**	**B**	7.94	462	240	370	39.04	43.79	1.05	0.81	39.23	8.73
W4	**M. Hussein**	**S/W**	7.53	1260	656	1143	53.68	62.82	1.08	1.86	47.12	3.27
W5	**Milele**	**B**	8.24	9196	4801	10348	73.20	149.85	1.33	2.34	726.46	61.89
W6	**N golf**	**B**	6.98	3804	1974	3825	87.84	25.02	1.23	3.43	323.00	14.10
W7	**Redeem**	**B**	7.97	762	425	642	73.20	10.38	0.97	2.64	49.51	1.37
W8	**Ruby1**	**B**	8.70	550	285	443	48.80	50.51	1.06	0.95	64.25	9.97
W9	**Ruby2**	**B**	8.33	1861	968	1719	126.88	87.71	1.14	1.57	216.94	5.50
W10	**Shimo high**	**S/W**	7.06	4038	2020	4093	97.6	102.64	1.13	5.02	172.39	7.40
W11	**Shimo qtrs**	**B**	7.35	1944	1009	1820	92.72	104.59	1.13	4.04	169.76	6.16
W12	**Sos1**	**S/W**	7.46	4056	2148	4078	91.11	100.92	1.21	2.09	323.48	17.99
W13	**Sos2**	**S/W**	7.41	3122	1624	3109	97.60	123.05	1.20	17.71	285.95	11.70
W14	**Sunsweet**	**B**	7.22	4038	2020	4093	107.36	28.69	1.23	2.95	301.64	9.80
W15	**Utange**	**B**	8.61	1916	996	1793	156.16	92.91	1.14	1.55	224.11	7.82
Drinking water standard (WHO 1984)												
			7.5-8.5	**750**	**500**		**300**	**200**	**30**	**75**	**200**	**100**
Kenya Drinking Water Standards (Kenya, 2008)												
			6.5-8.5					**250**	**100**	**250**	**200**	

B-Boreholes, S/W- Shallow wells, W-Well

Table 4.1 f: Concentration of the major parameters in the groundwater samples

September 2016 (post-monsoon)

SN	SAMPLE LOCATION	NaCl (mg/L)	pH	EC (µS/cm)	TDS (mg/L)	SO4 (mg/L)	HCO_3^- (mg/L)	Cl- (mg/L)	Mg^{2+} (mg/L)	Ca^{2+} (mg/L)	Na+ (mg/L)	K+ (mg/L)
W1	**Braeburn**	1003	7.72	1180	610	95.35	140.54	135.80	1.49	10.89	171.35	6.15
W2	**Cinema**	1451	7.57	1603	835	98.31	154.60	145.50	1.51	14.79	184.70	8.10
W3	**Krat**	376	8.73	480	250	78.91	108.92	132.10	1.08	1.14	47.44	8.87
W4	**M. Hussein**	1140	7.46	1314	687	150.50	125.32	134.50	1.39	13.5	73.70	3.94
W5	**Milele**	10500	7.9	9516	4748	257.19	51.53	279.91	1.74	0.19	729.10	65.77
W6	**N golf**	3725	7.51	3805	1977	221.46	108.92	137.60	1.64	4.32	298.40	8.00
W7	**Redeem**	579	7.68	713	371	89.54	89.01	117.60	0.85	13.19	70.70	1.74
W8	**Ruby2**	1705	7.8	1896	986	134.49	189.15	123.60	1.48	5.71	215.70	3.09
W9	**Shimo high**	1402	7.88	1586	824	100.95	107.75	139.00	1.44	18.44	101.80	2.67
W10	**Shimo qtrs**	1815	7.96	1985	1033	122.95	105.41	140.20	1.52	14.56	157.40	4.37
W11	**Sos1**	4052	8	4188	2140	158.56	73.79	151.30	1.60	2.89	462.70	22.90
W12	**Sos2**	3327	7.98	3490	1812	220.47	106.58	149.30	1.63	4.07	440.60	21.40
W13	**Sunsweet**	4025	7.57	4157	2135	170.46	92.52	137.46	1.66	3.73	179.96	8.7
W14	**Utange**	1726	7.48	1910	992	143.41	156.36	122.46	1.48	2.93	203.60	6.3
W15	**Vikwatani**	6183	7.92	6184	3143	328.92	165.14	134.96	1.74	2.98	375.67	6.58
Drinking water standard (WHO 1984)												
			7.5-8.5	**750**	**500**	**200**	**300**	**200**	**30**	**75**	**200**	**100**
Kenya Drinking Water Standards												
			6.5-8.5			**400**		**250**	**100**	**250**	**200**	

B-Boreholes, S/W- Shallow wells, W-Well

The values and concentrations of the Electrical conductivities and Total dissolved Solids vary vastly in the groundwater across the study area. For instance, the EC values vary from 761.5 to 10585µS/cm at the peak of the dry season just before the rains (pre-monsoon), while TDS values ranged from 438 to 4307mg/l within the same time period (Table 4.2a). This significant variation

in EC and TDS values across the study area is equally observed in June and September. From a seasonal perspective, only slight variations in EC and TDS were observed across the three seasons (Table 4.2a, b). However, the general trend is that EC and TDS values are lower across the study area in the rainy season than during the dry seasons (Tables 4.1 & 4.2). In terms of the allowable standards for drinkable water provided by WHO, the concentration of EC and TDS in over 94% of the water samples taken exceeded the allowable limits (Table 4.1a, b, c).

NaCl field measurement observations were also similar to those of EC and TDS. NaCl values showed a wide range of 659.8 to 10880mg/l across the study area in March 2016 while it was observed that NaCl values were generally lower in the rainy season than the preceding and succeeding dry season (Tables4.1 & 4.2). Increased groundwater flow and heads as a result of higher recharge from rainfall during the rainy season might explain why the EC, TDS and NaCl values tended to be relatively lower in June than in March and September. Of the four cations tested, Na^+ has the highest concentration with values as high as 735.55mg/l in a sample (Table 4.2a).

Table 4.2 d: Statistical analysis of the parameters for March 2016

Parameters	Unit	Min	Max	Mean	Standard Dev
pH	**-**	**7.13**	**7.82**	**7.46**	**0.21**
EC	**(µS/cm)**	**761.5**	**10585**	**3403.21**	**2821.08**
TDS	**(mg/L)**	**438**	**4801**	**1374**	**1120**
NaCl	**(mg/L)**	**659.8**	**10880**	**3324.7**	**2946.4**
HCO_3^-	**(mg/L)**	**87.84**	**173.24**	**119.36**	**26.06**
Cl-	**(mg/L)**	**140.30**	**379.60**	**269.55**	**75.54**
Mg^{2+}	**(mg/L)**	**0.83**	**13.30**	**8.42**	**3.53**
Ca^{2+}	**(mg/L)**	**6.93**	**32.95**	**20.65**	**9.26**
Na+	**(mg/L)**	**65.69**	**735.55**	**301.81**	**184.31**
K+	**(mg/L)**	**2.03**	**70.24**	**17.89**	**17.23**

Table 4.2 e: Statistical analysis of the parameters for June 2016

Parameters	Unit	Min	Max	Mean	Standard Dev
pH	**-**	**6.65**	**8.70**	**7.69**	**0.59**
EC	**(µS/cm)**	**462**	**9196**	**2652**	**2158**
TDS	**(mg/L)**	**240**	**4801**	**1676**	**1097**
NaCl	**(mg/L)**	**370**	**10348**	**2669**	**2445**
HCO_3^-	**(mg/L)**	**39.04**	**156.16**	**88.16**	**29.57**
Cl-	**(mg/L)**	**10.38**	**149.85**	**75.52**	**37.72**
Mg^{2+}	**(mg/L)**	**0.97**	**1.33**	**1.14**	**0.09**
Ca^{2+}	**(mg/L)**	**0.81**	**17.71**	**3.50**	**3.95**
Na+	**(mg/L)**	**39.23**	**726.46**	**215.50**	**167.98**
K+	**(mg/L)**	**1.37**	**61.89**	**11.90**	**13.97**

Table 4.2 f: Statistical analysis of the parameters for September 2016

Parameters	Unit	Min	Max	Mean	Standard Dev
pH	**-**	**7.46**	**8.73**	**7.81**	**0.31**
EC	**(µS/cm)**	**480**	**9516**	**2934**	**2328**
TDS	**(mg/L)**	**250**	**4748**	**1503**	**1164**
NaCl	**(mg/L)**	**376**	**10500**	**2867**	**2566**
HCO_3^-	**(mg/L)**	**51.53**	**189.15**	**118.37**	**35.66**
Cl-	**(mg/L)**	**108.80**	**154.30**	**139.49**	**9.96**
SO_4^{2-}	**(mg/L)**	**78.91**	**328.92**	**158.10**	**68.74**
Mg^{2+}	**(mg/L)**	**0.85**	**1.74**	**1.48**	**0.23**
Ca^{2+}	**(mg/L)**	**0.19**	**18.44**	**7.56**	**5.76**
Na+	**(mg/L)**	**47.44**	**729.10**	**247.52**	**179.38**
K+	**(mg/L)**	**1.74**	**65.77**	**11.91**	**15.58**

WHO and Kenya drinking water standards specify 200mg/l as allowable limits for drinking water. Over 50% of the water samples taken from the three periods exceeded the allowable limit for sodium ion content specified by both regulatory bodies. However Ca^{2+}, K^+ and Mg^{2+} concentrations in all the water samples were within the allowable limits specified by both WHO and Kenya Drinking Water standards, Mg^{2+} and Ca^{2+} exist in comparatively lower concentrations to Na^+ and K^+ in the groundwater (Table 4.1a, b, c). This discrepancy is much more obvious in the samples taken in the rainy season (Table4.2b). Generally, the variations in the maximum and minimum concentrations of Na^+ and K^+ across all the seasons were quite marginal (Tables 4.2a – 4.2c). The anions exhibited varying trends across the study area and over the three periods of data collection. Cl^- ions ranged from 140.30 to 379.60mg/l in March (pre-rains) and dropped to 10.38 to 149.85mg/l in June (rainy season) while HCO_3^- concentrations ranged from 87.84 to 173.24mg/l within the same period. The standard deviation of Cl^- ions drastically plunged from 75.54 to 37.72 in contrast to HCO_3^- whose standard deviation only slightly increased from 26.06 to 29.57. The close values of standard deviation between March and June may imply that the spatial distribution of bicarbonate concentrations in the groundwater do not vary significantly across the seasons.

Graphs showing the variation in concentrations of the groundwater parameters are presented in Appendix II. Both Cl^- and HCO_3^- ions show appreciable changes in June and September with values ranging from 10.38 - 75.72mg/l to 108.80 – 154.30mg/l and 39.04 - 156.16mg/l to 51.53 – 189.15mg/l respectively (see Appendix II). NaCl, EC, TDS, Na and K concentrations were somewhat similar in March and September while Mg and Ca concentrations were much higher in March than the other months (see Appendix II). The SO_4^{2-} ions tested in September varied from 78.91 to 328.92mg/l in the water samples taken from the study area. The chloride concentrations

of 75% of the water samples taken in March exceed WHO's allowable limit for drinking water while over 50% exceeded the Kenya standards for drinking water. In the case of SO_4^{2-}, one-third and one-sixth of the samples had concentrations higher than the WHO (1984) and Kenya drinking water standards respectively (Table 4.1c).

Overall, the relatively high values of EC and TDS and the generally high concentrations of Na, Cl, and NaCl as recorded in the month of March (Fig4.1a), suggests that the groundwater in a large portion of the aquifer is unsuitable for drinking, howbeit useful for other domestic purposes.

4.1.2 **Correlation Matrices and Cross Plots**

Cross plots and correlation matrices are reliable statistical methods for determining the most dominant ions controlling the groundwater chemistry of the study area. All the parameters were analysed for their correlations and the results are represented in Tables 4.3a – 4.3c.

Table 4.3 d: Correlation coefficients for the groundwater parameters in the month of March (Pre-monsoon)

Parameters	pH	EC	TDS	Cl	HCO3	Na	Mg	Ca	K
pH	1								
EC	0.19	1							
TDS	0.13	**0.99**	1						
Cl	0.02	**0.84**	**0.89**	1					
HCO3	-0.09	-0.26	-0.29	-0.18	1				
Na	0.16	**0.97**	**0.99**	**0.91**	-0.25	1			
Mg	-0.08	**0.81**	**0.86**	**0.91**	-0.2	**0.88**	1		
Ca	-0.24	0.31	0.32	0.32	-0.3	0.27	0.60	1	
K	0.16	**0.87**	**0.85**	**0.63**	-0.3	**0.87**	**0.66**	0.18	1

Table 4.3 e: Correlation coefficients for the groundwater parameters in the month of June (Rainy season)

Parameters	pH	EC	TDS	Cl	HCO3	Na	Mg	Ca	K
pH	1								
EC	-0.13	1							
TDS	-0.12	**1**	1						
Cl	0.05	**0.56**	**0.56**	1					
HCO3	0.13	0.13	0.12	0.25	1				
Na	-0.02	**0.96**	**0.96**	**0.58**	0.22	1			
Mg	-0.22	**0.86**	**0.86**	**0.55**	0.30	**0.91**	1		
Ca	-0.32	0.14	0.14	0.36	0.14	0.15	0.23	1	
K	0.16	**0.88**	**0.89**	**0.56**	-0.13	**0.90**	**0.73**	-0.01	1

Table 4.3 f: Correlation coefficients for the groundwater parameters in the month of September (Post-monsoon)

Parameters	pH	EC	TDS	Cl	HCO3	Na	Mg	Ca	K	SO_4^{2-}
pH	1									
EC	-0.07	1								
TDS	-0.08	**1**	1							
Cl	0.06	**0.80**	**0.79**	1						
HCO3	-0.21	-0.39	-0.39	-0.38	1					
Na	-0.02	**0.90**	**0.91**	**0.79**	-0.38	1				
Mg	-0.25	**0.70**	**0.71**	0.42	0.03	**0.67**	1			
Ca	-0.55	**-0.57**	**-0.57**	-0.33	0.14	**-0.59**	-0.34	1		
K	0.18	**0.81**	**0.80**	**0.96**	**-0.60**	**0.87**	0.41	-0.50	1	
SO_4^{2-}	-0.21	**0.84**	**0.84**	0.42	-0.06	**0.78**	**0.71**	-0.56	0.46	1

Interestingly, the correlation matrices for the three time periods all follow the same trend. EC and TDS were observed to be perfectly correlated with values 0.99, 1 and 1 for the months of March, June and September respectively (Table 4.3a, b, c). This implies an absolute direct relationship between the electrical conductivity and the total dissolved solids (solute) in the groundwater across the study area. The EC and TDS are also observed to consistently have a strong correlation with Cl^-, Na, Mg and K over the three periods (Table 4.3a, b, c). It can be inferred that these parameters play significant roles in defining the geochemistry of the study area. Mondal et al, (2010) note that high correlation of parameters in groundwater is suggestive of the parameters/ions controlling the chemistry of the groundwater. Cl^- showed a strong positive relationship with Na and K across the three periods of data collection signifying that these three parameters play significant roles in defining the EC and TDS contents of the groundwater. It is noteworthy that Na had a strong positive relationship with Mg and K across the three periods while Mg had a strong positive relationship with K in both March and June. Conversely, HCO_3^- and Ca^{2+} had no consistent relationship with other parameters/ ions across the three time periods. This lack of consistent relationship was also observed for the pH values. The pH values had no correlation with the other parameters in the groundwater. The water samples taken in September were tested for SO_4^{2-} concentration (Table4.3c). It was observed that SO_4^{2-} strongly correlates with EC, TDS, Na^+ and Mg^{2+} which have been identified to have strong positive correlations amongst themselves. Appendix III shows the cross plot relationships between EC/TDS and the various ions

Hence, the major parameters controlling the groundwater chemistry are EC, TDS, Cl^-, Na^+, Mg^{2+}, K^+, and to some degree SO_4^{2-} while Ca^{2+}, HCO_3 and pH have a paltry impact on the geochemistry of the study area.

4.1.3 **Piper Plots**

The cations and anions concentrations in mg/l were converted into meq/l (See Appendix IV). The values in meq/l were normalised to 100% as shown in Table 4.4. The sum of sodium and potassium (Na+K) were normalised against Mg and Ca for the cations whose summation is 100% and plotted inside the cations triangle for all the water samples. The Cl, SO_4 and HCO_3 were also normalised to 100% and plotted into the anions triangle. All the normalised cation and anion values in the triangles were projected into the diamond to determine the nature of the groundwater based on the quadrant under which the values fall.

Table 4.4: Normalised values for the cations and anions

		Cations (Normalisation)				Anions (Normalisation)			
SN	**Sample location**	**Total Cations**	**Na + K (%)**	**Ca (%)**	**Mg (%)**	**Total Anions**	**HCO_3 (%)**	**Cl (%)**	**SO_4 (%)**
W1	**Braeburn**	**8.28**	91.92	6.58	1.50	**8.12**	28.40	47.13	24.47
W2	**Cinema**	**9.10**	90.50	8.12	1.38	**8.68**	29.20	47.21	23.59
W3	**Krat**	**2.44**	93.97	2.34	3.69	**7.15**	24.98	52.04	22.98
W4	**M. Hussein**	**4.10**	80.69	16.48	2.83	**8.98**	22.89	42.20	34.91
W5	**Milele**	**33.54**	99.54	0.03	0.43	**14.09**	6.00	55.97	38.03
W6	**N golf**	**13.53**	97.39	1.60	1.01	**10.28**	17.38	37.72	44.89
W7	**Redeem**	**3.85**	81.03	17.13	1.84	**6.64**	21.99	49.91	28.10
W9	**Ruby2**	**9.87**	95.86	2.89	1.25	**9.39**	33.05	37.10	29.85
W10	**Shimo high**	**5.54**	81.18	16.65	2.17	**7.79**	22.70	50.29	27.01
W11	**Shimo qtrs**	**7.81**	89.06	9.32	1.62	**8.24**	20.98	47.94	31.08
W12	**Sos1**	**20.98**	98.68	0.69	0.64	**8.77**	13.79	48.57	37.64
W13	**Sos2**	**20.04**	98.31	1.02	0.68	**10.55**	16.57	39.88	43.55
W14	**Sunsweet**	**8.37**	96.12	2.23	1.65	**8.94**	16.97	43.31	39.72
W15	**Utange**	**9.28**	97.10	1.58	1.32	**9.00**	28.49	38.33	33.19
W16	**Vikwatani**	**16.80**	98.25	0.89	0.87	**13.36**	20.27	28.45	51.28

The groundwater samples all fall within the quadrant of Sodium-Chloride waters in the diamond (Figure 4.3). This implies the groundwater is of the marine and deep ancient type (Piper, 1953). The reason is not farfetched- the study area stretches from the seafront to about 7km inland while it is bounded to the north and south by creeks. The prevalent interaction between the aquifer and the saltwater bodies over many thousands of years explains why the water samples all point towards being of marine origin.

The use of piper plots is advantageous in that it is possible to plot the analyses of several water samples on the same diagram and is able to give a broad overview of the groundwater characteristics.

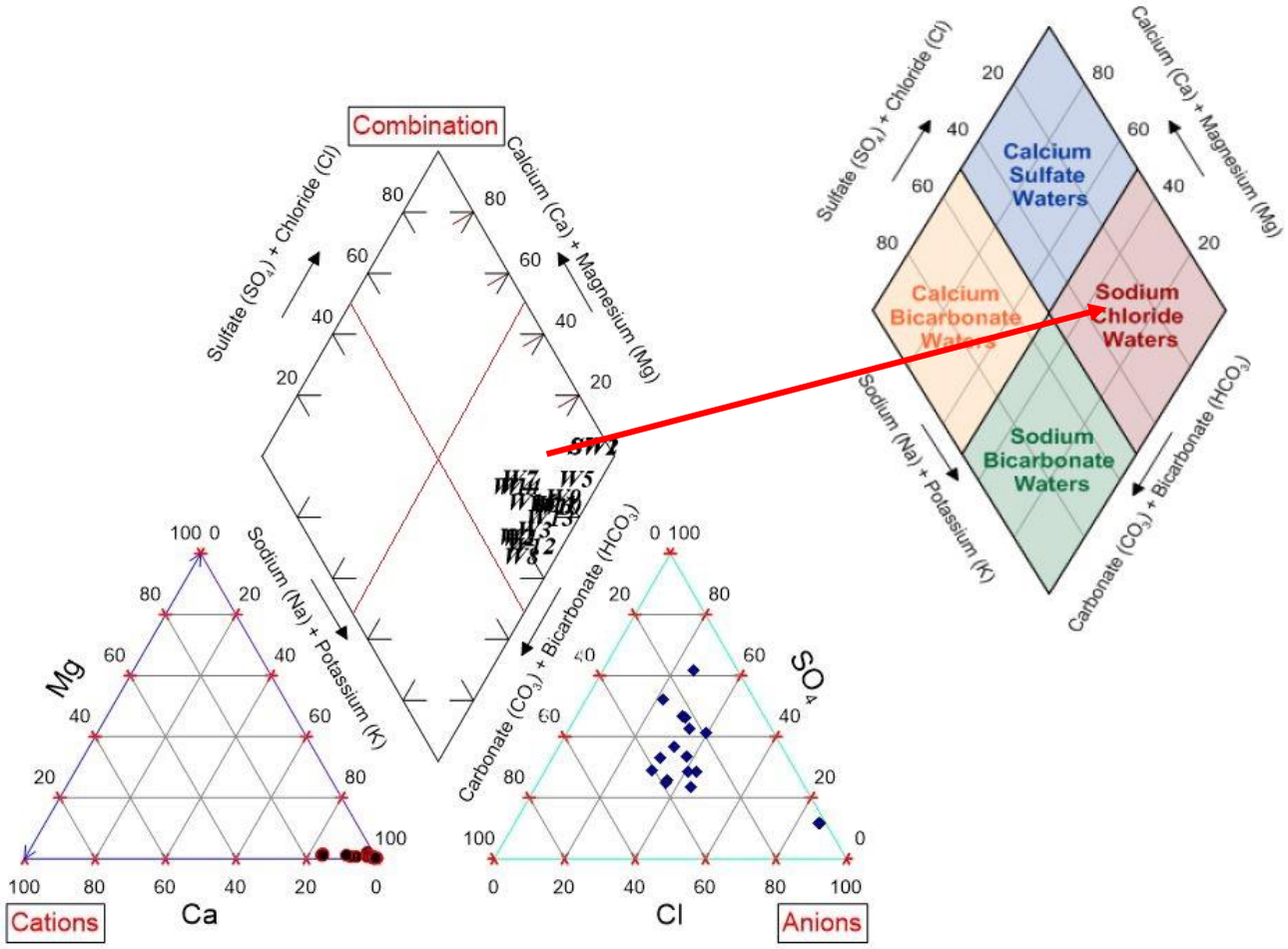

Figure 4. 3: Piper plot for the water samples taken in the study area

4.1.4 Salinity Assessment of the Groundwater in the Study Area

The salinity was assessed based on EC, TDS and NaCl concentration in the groundwater across the study area. The water samples taken were classified based on the EC ranges used by Saxena et al (2003). The classification is based on the rationale that the higher the EC values in a groundwater sample, the higher its value on the salinity range. EC < 1500 µS/cm is considered fresh, 1500 – 3000 µS/cm considered brackish and values over µS/cm taken as saline (Saxena *et al.*, 2003). Point values from boreholes, do not give a visual representation of the spatial distribution of EC across the study area. Hence, using spatial interpolation tools in ArcGIS, the spatial distribution of the EC based on the classification were developed and expressed in Figures 4.4a – 4.4c.

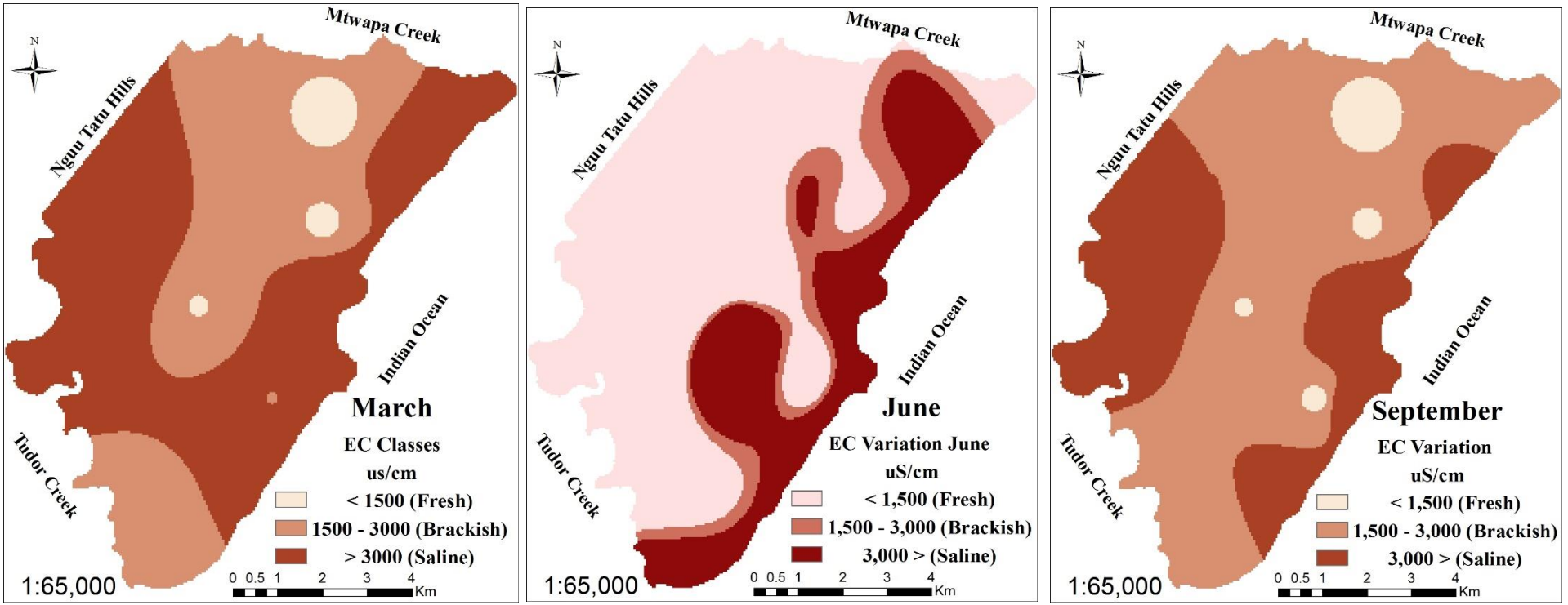

a. **b.** **c.**

Figure 4.4: EC variation across the study area in; (a.) March (b.) June (c.) September

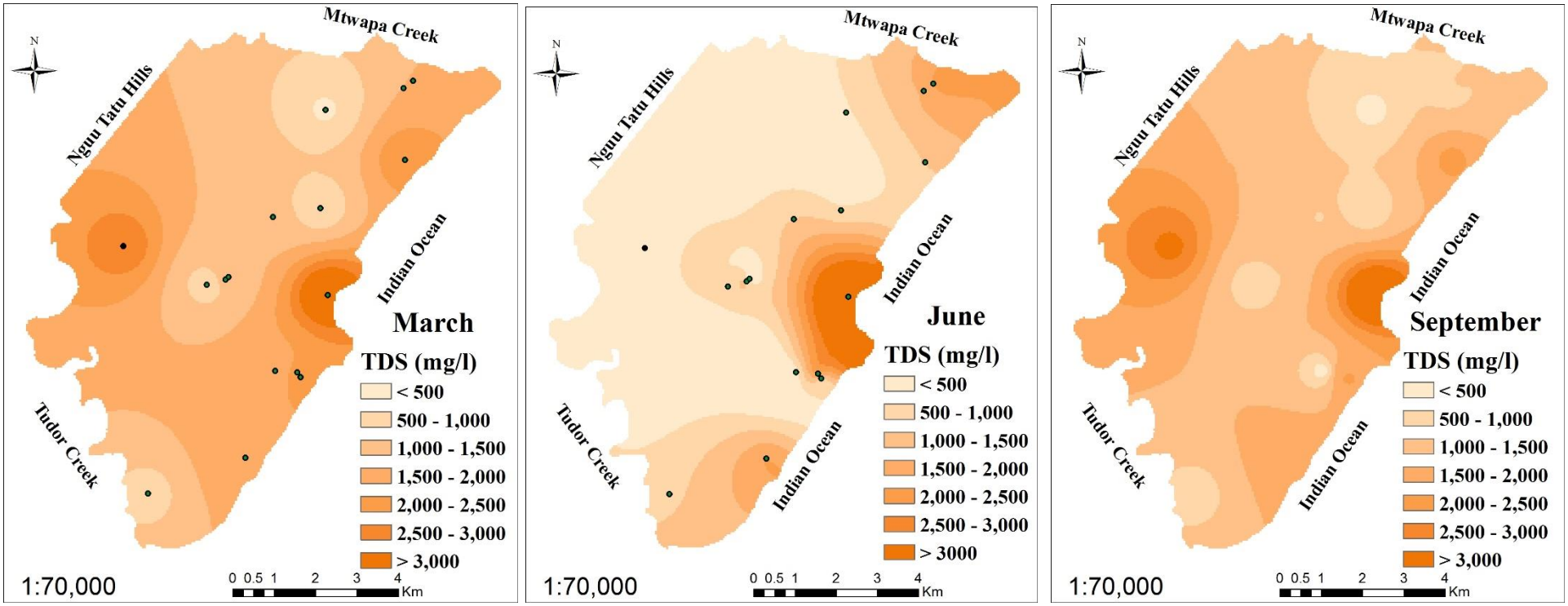

a. **b.** **c.**

Figure 4.5: TDS variation across the study area in; (a.) March (b.) June (c.) September

It is interesting to note that freshwater covers a much larger region of the groundwater in the study area in June (Fig4.4b). This is most likely due to high recharge rates from rainfall which tends to increase the heads and flow of freshwater towards the ocean thereby pushing brackish and saline wedge towards the ocean and creeks. As the dry season approached (June to September), the spatial distribution of the fresh, brackish and saline water categories tended towards taking the pre-monsoon forms in March before the rain started (Figure 4.4a – 4.4c). The implication of this variation is that a large scale artificial groundwater recharge during the dry season might be effective in mitigating groundwater salinity in the absence of adequate natural recharge from rainfall. At pre-monsoon, the spatial coverage of saline water in the aquifer was much wider than that of post-monsoon, owing to the same groundwater recharge from rainfall rationale. The dwellers of the high elevated regions of Nguu tatu hills, mostly depend on freshwater supplies from reservoirs managed by the local water management agencies, however, a shallow well was identified at an elevation of 40m above mean sea level. Water samples taken from this well were observed to have high EC, TDS and NaCl values which are strong indicators of salinity. This explains why the spatial variation maps show high salinity for the groundwater within Nguu tatu hills at both pre-monsoon and post-monsoon (Figure 4.4a,c; Figure 4.5a, c).

The spatial variation of TDS values in the aquifer is represented by Figures 4.5a – 4.5c. TDS spatial distribution in the aquifer also exhibited a similar trend to what was observed in the EC spatial distribution. This is not surprising since the correlation relationship between EC and TDS values were near perfect across the three sets of data (Tables 4.3a – 4.3c).

The percentage coverage of the spatial distribution of the salinity classes was computed from the maps (Tables 4.5).

Table 4.5: Spatial coverage of the EC classification in percentages

Period	Fresh (% coverage)	Brackish (% coverage)	Saline (% coverage)
March (pre-monsoon)	4	42	54
June (rainy season)	6	76	18
Sept (Post-monsoon)	4	62	34

It will be observed that the salinity of the groundwater reduced in the rainy season as evidenced by the reduction of saline percentage coverage from 54% at pre-monsoon to 18% at the peak of

rainy season. Most conversions were from saline to brackish water as over 70% of the groundwater became brackish in the rainy season while just 18% and 6% were covered by saline and fresh water respectively in the same period. The freshwater coverage only showed a meagre increase from pre-monsoon to the rainy season i.e. 4% to 6% but was back to 4% at post-monsoon (Table 4.5). A groundwater study by Sappa *et al.,* (2015) on the coastal aquifer of Dar es salaam, Tanzania, also located along the coast of East Africa also showed a somewhat similar trend. The study reported that groundwater samples taken in November 2012 (post-monsoon) showed higher EC and TDS values than those taken in June 2012 i.e. rainy season (Sappa et al, 2015).

In summary, the salinity distribution in the groundwater varies with seasons while groundwater recharge heavily influences the salinity of the groundwater. The salinity of the groundwater tended to reduce during the rainy season. Field measurements of NaCl concentrations which are direct indicators of salinity were also taken. See Appendix V for the spatial distribution of the NaCl across the three seasons.

4.1.5 **Seawater Intrusion Assessment of the Study Area**

Seawater contains a relatively higher concentration of Cl^-, $Na^+ + K^+$, and Mg^{2+} in excess of Ca^{2+} and $SO_4^{-2} + HCO_3^-$ while, continental fresh groundwater is characterised by high variability of chemical compositions (Moujabber *et al.,* 2006). Hem (1989), also established that the dominant ions found in seawater are Na^+ and Cl^- while the major ions in freshwater are bicarbonates and calcium. These ions formed the basis for the indices used for assessing the extent of seawater intrusion in the study area. The Cl/HCO3, Na/Cl, Ca/Na indices earlier highlighted in the methodology for assessing seawater intrusion were computed and highlighted in Table 4.6.

Observations made for the month of March show that EC has a strong positive correlation with TDS, Cl/HCO_3 ratio, and Na/Cl ratio with values 0.99, 0.74, and 0.93 respectively (Table 4.3a – 4.3c). Cl/HCO_3 and Na/Cl are also strongly positively correlated with a correlation coefficient of 0.74 (Table 4.7). EC and TDS were also observed to have a near perfect correlation with NaCl which in turn has a near perfect relationship with Cl/HCO_3 (Table 4.7). This direct relationship between the NaCl values and Cl/HCO_3 ratio is a pointer that the salinity of the groundwater may be as a result of the influence of seawater intrusion in the coastal aquifer.

Table 4.6: Seawater intrusion indices

SN	Sample location	March			June			September		
		Cl/ HCO_3	Ca/Na	Na/Cl	Cl/ HCO_3	Ca/Na	Na/Cl	Cl/ HCO3	Ca/Na	Na/Cl
W1	Braeburn	1.16	0.262	0.76	1.25	0.023	1.60	0.97	0.06	1.26
W2	Cinema	1.45	0.078	0.64	2.40	0.017	2.20	0.94	0.08	1.27
W3	Krat	2.40	0.086	1.08	2.24	0.021	0.90	1.21	0.02	0.36
W4	M. Hussein	2.07	0.266	0.52	2.34	0.04	0.75	1.07	0.18	0.55
W5	Milele	3.58	0.028	2.01	4.09	0.003	4.85	5.43	0.0003	2.60
W6	N golf	2.52	0.055	1.27	0.57	0.011	12.91	1.26	0.01	2.77
W7	Redeem	1.44	0.154	0.47	0.28	0.053	4.77	1.32	0.19	0.60
W8	Ruby1	1.49	0.034	0.85	2.07	0.015	1.27	-	-	-
W9	Ruby2	-	-	-	1.38	0.007	2.47	0.65	0.03	1.75
W10	Shimo high	-	-	-	2.10	0.029	1.68	1.29	0.18	0.73
W11	Shimo qtrs	-	-	-	2.26	0.024	1.62	1.33	0.09	1.12
W12	Sos1	3.97	0.069	1.18	2.22	0.006	3.21	2.05	0.01	3.06
W13	Sos2	-	-	-	2.52	0.062	2.32	1.40	0.01	2.95
W14	Sunsweet	3.83	0.060	1.21	0.53	0.01	10.52	1.49	0.02	1.31
W15	Utange	2.06	0.025	1.02	1.19	0.007	2.41	0.78	0.01	1.66
W16	Vikwatani	2.73	0.068	1.27	-	-	-	0.82	0.01	2.78

Table 4.7: Correlation for Salinity Indices (March)

Parameters	EC	TDS	Cl/HCO3	Ca/Na	Na/Cl	(NaCl)
EC	1	-	-	-	-	-
TDS	0.99	1	-	-	-	-
Cl/HCO3	0.74	0.80	1	-	-	-
Ca/Na	-0.50	-0.55	-0.45	1	-	-
Na/Cl	0.93	0.95	0.74	-0.61	1	-
(NaCl)	0.999	0.98	0.97	-0.48	0.92	1

The correlation trends observed for the relationship amongst EC, TDS, Cl/HCO_3, Na/Cl and NaCl indices in the month of March(pre-monsoon) was also observed in September (post monsoon). Similar trends were also observed for the relationship amongst EC, TDS and NaCl in June (rainy season) while that of Cl/HCO_3 and Na/Cl were incoherent (Appendix VI).

i. Cl/HCO_3 (Simpson's) Ratio

Cl/HCO_3 ratio is suggested as a proper criterion for assessing the impact of seawater intrusion because the value is 190/1 in seawater (Todd & Mays, 2005). The classification was done based on the categories highlighted by Todd & Mays, (2005) – good quality (<0.5); slightly contaminated (0.5-1.3); moderately contaminated (1.3-2.8); injuriously contaminated (2.8-6.6); and highly contaminated (6.6-15.5). For a better and visual interpretation, the spatial distribution of the Cl/HCO_3 is represented in Figure 4.6. Visually, the aquifer was largely impacted moderately by seawater intrusion at pre-monsoon with some portions experiencing injurious impacts. However, at post monsoon, a sizeable portion of the aquifer experienced slight contamination while a little

portion experienced an injurious impact of seawater intrusion. It will be noticed that the portions under slight impact are the regions tending towards the high elevated Nguu tatu hills where the water table is high. Darcy's law and the Ghyben-Herzberg principle seems to be at work here. Water tends to flow from regions of higher elevation to that of lower elevations (Darcy's law) and in the process, higher hydraulic pressures are built which counterbalances the intrusion of seawater (Ghyben-Herzberg principle).

The statistical representation of the spatial maps according to the classifications was further computed and highlighted in Table 4.8. Ninety percent and 11% of the aquifer coverage experienced moderate and injurious contamination by seawater at pre-monsoon. However, the aquifer did not show any injurious impact in the rainy season. This might be due to the groundwater recharge from rainfall which tends to raise the hydraulic pressure of the fresh groundwater to offset the intrusion of seawater. The impact of seawater intrusion in the aquifer at the time of data collection during the rainy season was largely moderate. Since the impact of seawater intrusion is a dynamic process, the rainy season will most likely experience varying impacts of seawater intrusion within a relatively shorter time due to intermittent rainfall. By post-monsoon, some portions (3%) of the aquifer had started experiencing injurious impacts of seawater as was observed at pre-monsoon. Surprisingly, 55% of the aquifer coverage showed slight contamination by seawater based on the same probable reasons of Darcy's law and Ghyben- Herzberg principle.

On a holistic scale, however, Table 4.8 further confirms that the groundwater in the study area tends to experience moderate to slight impacts of seawater intrusion.

Table 4.8: Spatial coverage of the Cl/HCO_3 index classifications in percentages

Period	Slight (% coverage)	Moderate (% coverage)	Injurious (% coverage)
March (pre-monsoon)	<1	Approx. 90	11
June (rainy season)	0	100	0
Sept (Post-monsoon)	55	42	3

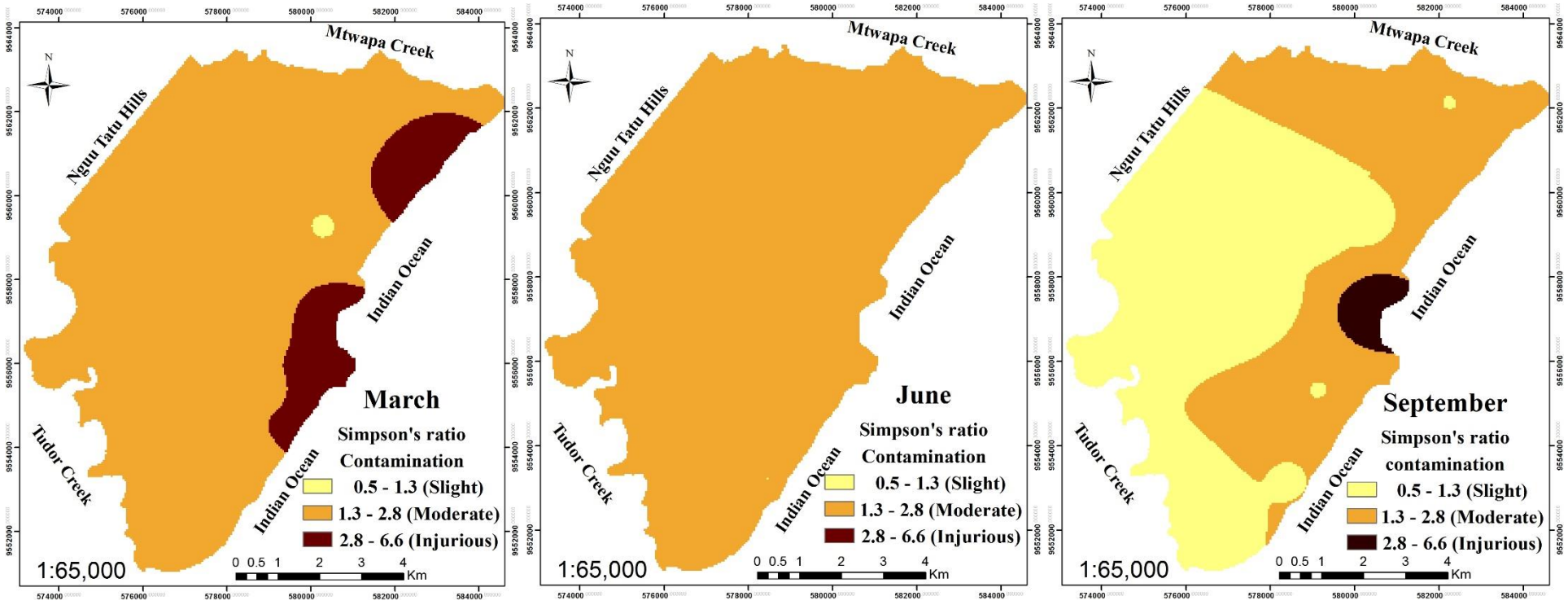

a. **b.** **c.**

Figure 4.6: Spatial representation the Cl/HCO_3 ratios based on Todd & Mays (2005) for the months of (a.) March (b.) June (c.) September

ii Na/Cl Ratio:

Vengosh *et al.* (1997) found that groundwater impacted by seawater intrusion possesses low characteristic values of Na/Cl ratios because marine values of Na/Cl ratio are less than 0.86. Thus, low values of Na/Cl ratios combined with other geological parameters can be indicative of the impact of seawater intrusion. Na/Cl ratios greater than 1 are typical of groundwater contaminated by anthropogenic sources (Jones *et al.*, 1999).

The Na/Cl ratios of groundwater samples taken in March have values ranging from 0.5 to 2.01 while those taken in the months of June and September had ranges of values 0.75 to 12.91 and 0.36 to 3.06 respectively (Table 4.6). However, over 50% of the samples taken in March, 80% in June and 70% in September had values higher than 1 indicating anthropogenic influence. This confirms previous work done in the study area which suggested that the groundwater is being impacted by anthropogenic pollution (Munga *et al.*, 2006).

iii Plots of TDS against HCO^-_3/Cl^- and Ca^{2+}/Na^+ ratios

High concentrations of Na^+ and Cl^- in the coastal groundwater may indicate the impact of seawater mixing while high values of HCO^-_3 and Ca^{2+} are indicators of the impact of water-rock interaction in the aquifer (Park *et al.*, 2005). Hence low values of HCO^-_3/Cl^- and Ca^{2+}/Na^+ ratios are indicative of a high impact of seawater intrusion.

The TDS values were plotted against their HCO^-_3/ Cl^- and Ca^{2+}/ Na^+ ratios. In the month of March, it was observed that the regression line for samples with low TDS values in the study area represented by the continuous trend line had a strongly negative slope with HCO^-_3/ Cl^- ratios while for samples with high TDS values, the regression line represented by the dotted trend lines showed a mildly positive almost horizontal slope (Fig 4.7a). The black trend line is seen to be negatively sloping up to 2000mg/l; beyond that point, a near horizontal slope is observed. As earlier discussed, high TDS values (TDS> 1000mg/l) are indicative of salinity. Hence, the trend observed between TDS and HCO^-_3/ Cl^- may imply that at low TDS concentrations (low salinity), the process of seawater mixing tends to be more active but as the water becomes more saline, an equilibrium is reached between the fresh and salt water which tends to keep the fresh/sea water mixing fairly constant. The inverse relationship between TDS and HCO^-_3/ Cl^- also suggests that the freshwater is being impacted by seawater intrusion until it reaches an equilibrium. The same trend is observed

for TDS vs. Ca^{2+}/ Na^{+} ratios (Fig4.7b). On the contrary, Mondal et.al, (2010) observed positive trends at lower values of TDS and mildly negative trends at high values in the case of Tamilnadu India.

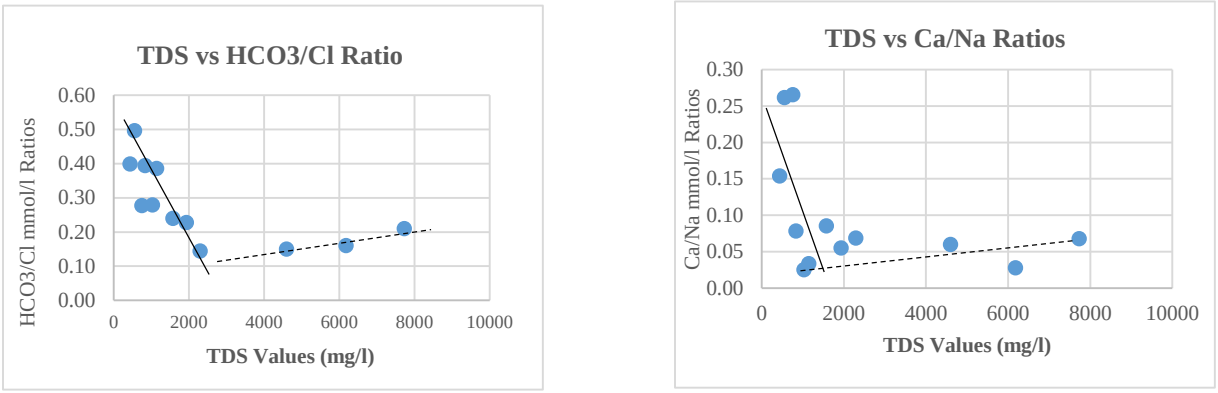

a. **b**

Figure 4.7: TDS Concentration against Molar Ratios of (a. HCO3/Cl; b. Ca/Na)

4.2 Spatial Vulnerability Map to Seawater Intrusion (GALDIT)

As part of the attempts to manage the coastal aquifer against seawater intrusion, the spatial vulnerability map of the aquifer based on the six factors highlighted in GALDIT (Lobo Ferreira et al, 2005) were developed for the dry and rainy seasons with the aid of geospatial tools. Four out of the six GALDIT factors were static factors while the other two were dynamic.

The *static factors* which do not change considerably over a period of time were; Groundwater occurrence, Aquifer hydraulic conductivity, Distance to the shore and Thickness of the aquifer while the *dynamic factors* which experience temporal variation with time are the Level of groundwater above sea level and Impact of existing seawater intrusion. The same static factors were used for the dry and rainy seasons while separate dynamic factors were computed and applied accordingly for either period. The spatial maps developed for each factor are found in Appendix VII. The computed results of equation 8 (see page 38) showed that the total scores (TS) for the final vulnerability map ranged from 55 to 120 while the scores were between 57.5 and 132.5 for the month of June. These TS values were split into three classes- low, moderate and high vulnerability.

The overlay and reclassification of the weighted sum of the thematic raster images gave the final vulnerability maps of the study area to seawater intrusion (Figure 4.8).

The highly vulnerable regions in both cases were the low heads regions with high proximity to the oceans and creeks. This implies that GALDIT factors L and D are the most sensitive factors influencing the vulnerability of the study area to seawater intrusion. GALDIT factor D cannot be altered or improved upon because locations do not change, however, the static levels of groundwater can be managed through recharge and abstraction dynamics of the groundwater. It is, therefore, no surprise that the least vulnerable regions are located close to the high elevated areas of Nguu tatu hills whose groundwater heads are relatively high as shown in Figure 4.2a & 4.2b (see page 47).

The percentage covers of each vulnerability class in each map are represented in Table 4.9. A wider region became less vulnerable to seawater intrusion in the rainy season as observed by the increase in the low vulnerability regions from 13% to 20% (Table 4.9). This is probably because the impact of seawater intrusion is comparatively lower in the rainy season than the dry season as a result of high rate of natural groundwater recharge from rainfall. Groundwater recharge increases pressure heads of freshwater, thereby pushing freshwater/saltwater equilibrium zones towards the sea (Roger, 1998).

Table 4.9: Percentage changes in vulnerability classes between pre-monsoon and rainy season

Vulnerability class	March 2016 (%)	June 2016 (%)
Low	13	20
Moderate	64	55
High	23	25

Generally, a large percentage of the study area falls within the moderate vulnerability class. Invariably, the vulnerability of the study area to seawater intrusion is largely moderate. This implies that the current groundwater abstraction rates still seems low with respect to the study area's high rainfall which is usually above 1000mm per year (Climatemps, 2015).

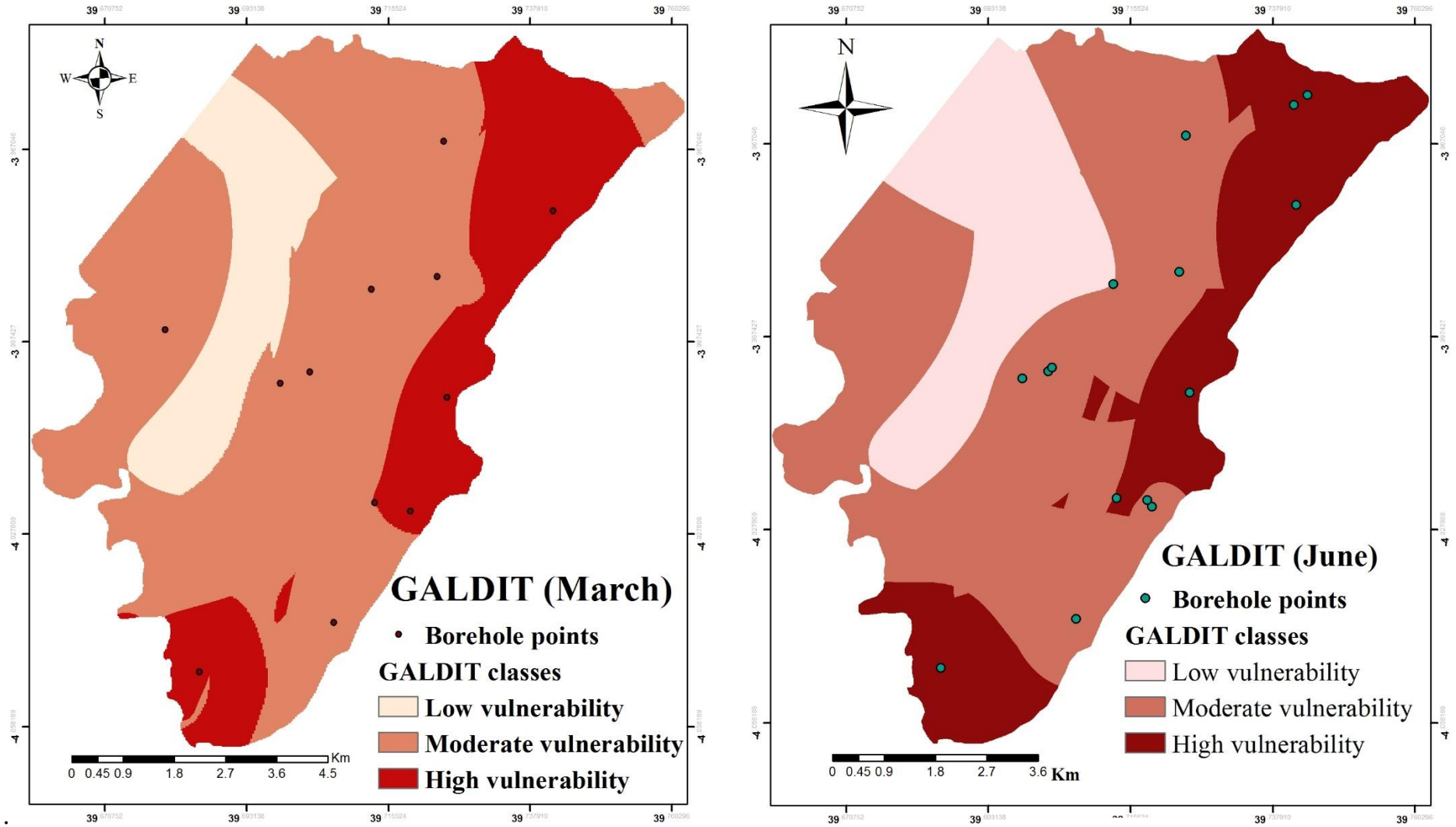

Figure 4.8: Vulnerability maps of the study area to seawater intrusion a. (pre-rains) b. (rainy season)

4.3 Groundwater Simulation and Solute Transport Model of the Study Area

A simple 3D model was developed to simulate the groundwater flow and solute (NaCl) transport in the study area using MODFLOW, MT3DMS and SEAWAT in a robust software package called GMS.

4.3.1 Steady State Flow Simulation

The outcomes of the steady state flow simulation gave the direction of groundwater flow in the study area. Figure 4.9. The direction of groundwater flow is generally towards the northeast and southern directions. The groundwater heads were similarly observed to be highest in the high elevation areas of Nguu Tatu hills on the western part of the study area. The groundwater flows generally towards the Indian Ocean, to Mtwapa creek in the Shanzu region on the north-eastern part of the study area and the Tudor creek close to the Nyali/Kongowea region on the southern region. The groundwater flow direction tends to obey Darcy's basic law which simply put, stipulates that the fluid flow through a porous media (aquifer) is proportional to the elevation drop between two points in the medium and inversely proportional to the distance between them (Kiplangat, 2014).

The steady-state simulated flow direction is in agreement with a previous study by Munga et al, (2006) where the outcome of their steady state simulation studies showed that the prevailing groundwater flow direction is towards the "Mtwapa creek along the northern boundary and Tudor creek along the southern boundary of the study area and relatively less intense flow towards the Indian Ocean. The southern end of the study area bordering the Indian Ocean but experiencing a flow towards Creek rather than the Ocean is a region of high groundwater head. The most probable reason is that, since water moves by gravity in obeying Darcy's law, the groundwater's movement from that high head region could only move to lower head regions- in this case, the creek.

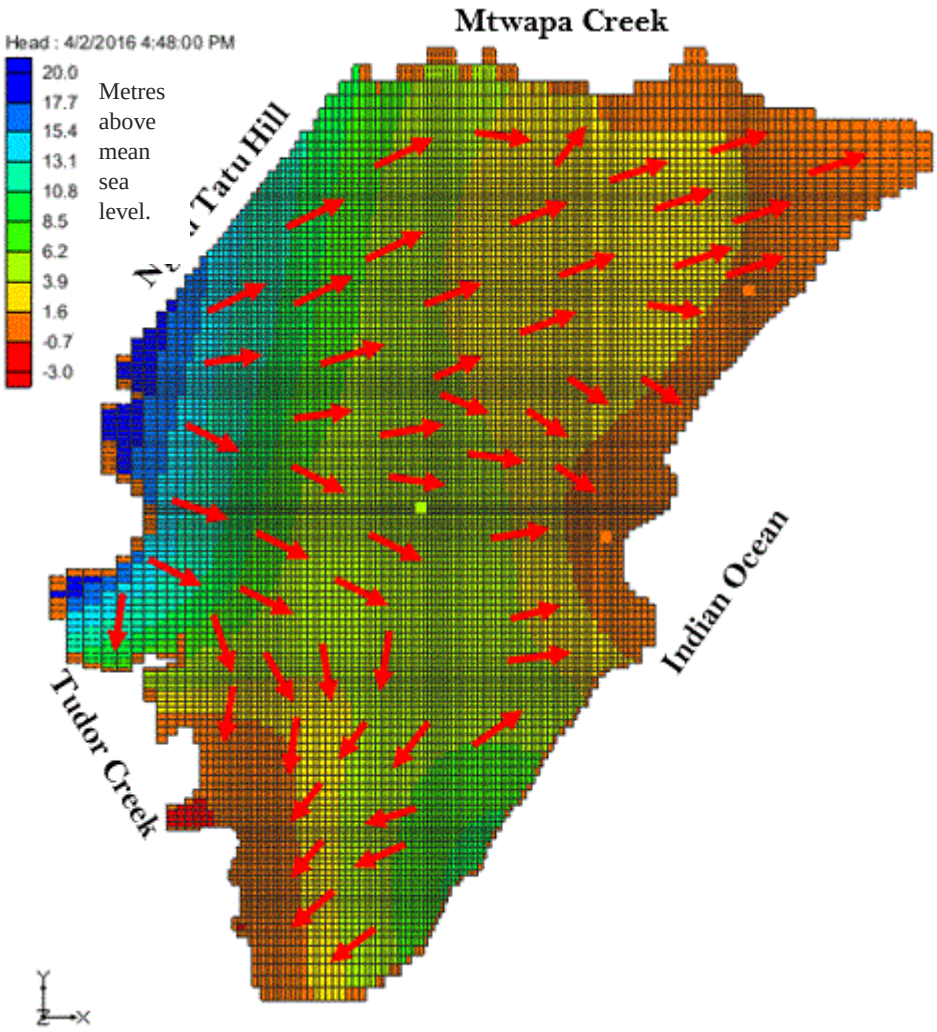

Figure 4.9: Steady-state simulated groundwater heads (m) and flow direction in the North Coast of Mombasa

4.3.2 **Transient State Flow Simulation and Calibration**

The solution from the transient state simulation was used as the first stress period for the transient state simulation. The transient state solution over the three stress periods showed very little variation in groundwater heads. The observed field data was used to calibrate the transient state solution until the error margin was within the allowable interval. Calibration was done by varying the recharge and hydraulic conductivity values. The difference between the observed and computed heads are highlighted in Figures 4.10 and 4.11.

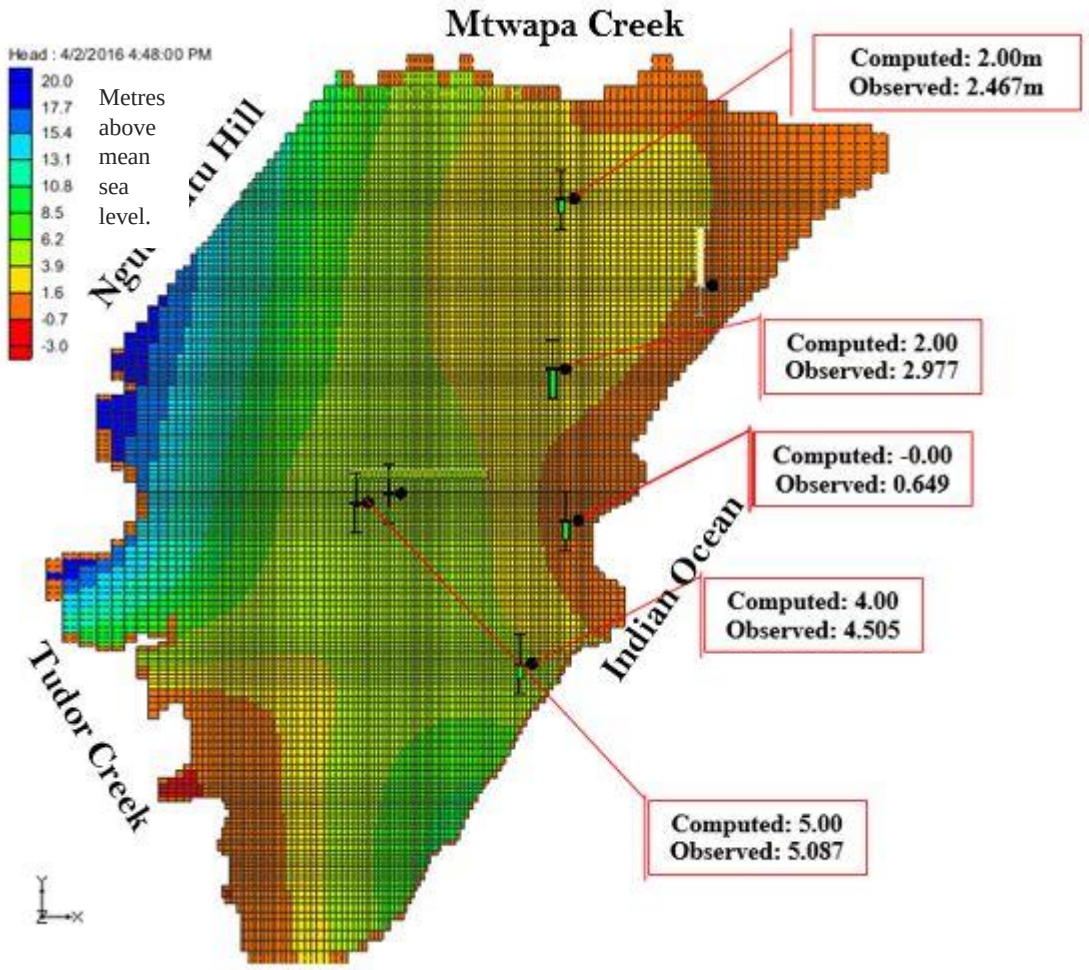

Figure 4.10: Differences between the Observed and Computed heads after calibration

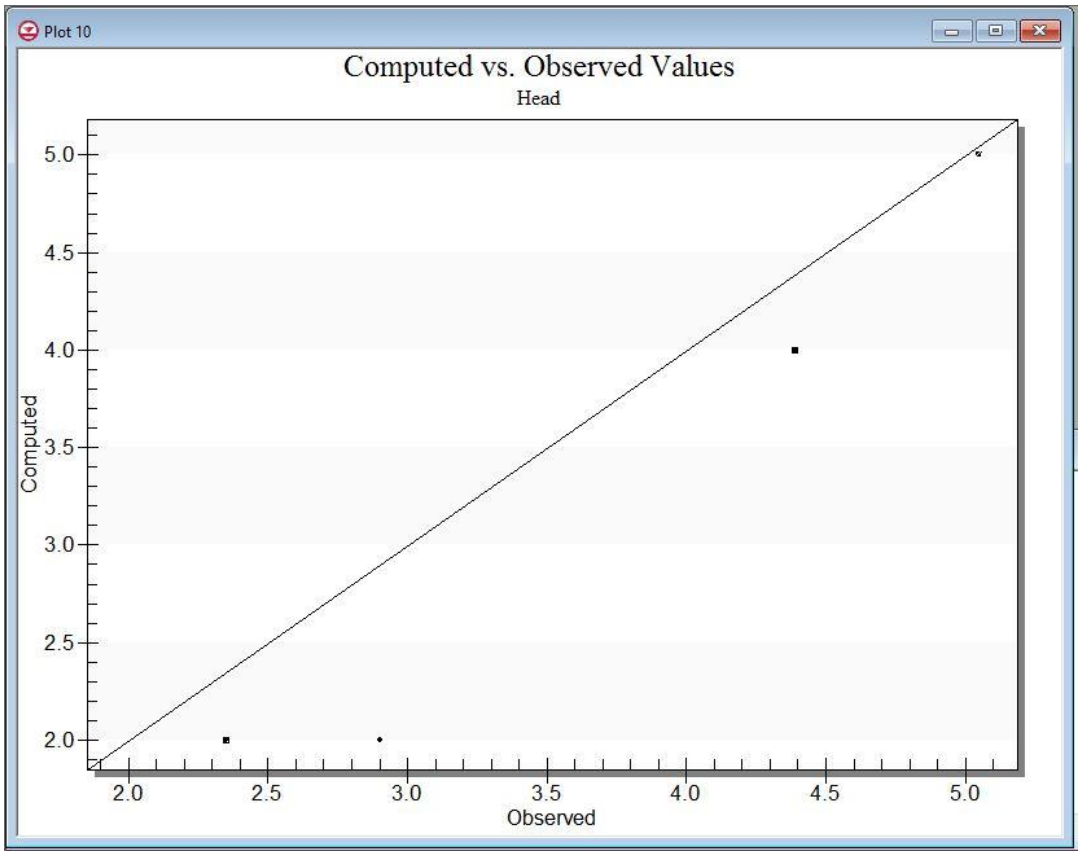

Figure 4.11: Cross plot for Observed heads vs. computed heads

4.3.3 **Solute Transport Simulation**

The solution from the transient state model was used for running the NaCl solute transport with the aid of MT3D and SEAWAT. The solute transport solutions for three stress periods are represented in Figures 4.12a – d. The red zones in each figure are the regions unaffected by the transport of NaCl solute from the Ocean and creeks. It will be observed that the red zones showed a minute progressive increase from June to September. This implies that as the season progressed from rainy to dry the concentrations of NaCl in the groundwater reduced gradually from the centre of the study area outwards.

However, the model needs to be improved upon by incorporating a longer time frame in order to make it more robust for long-term predictive studies.

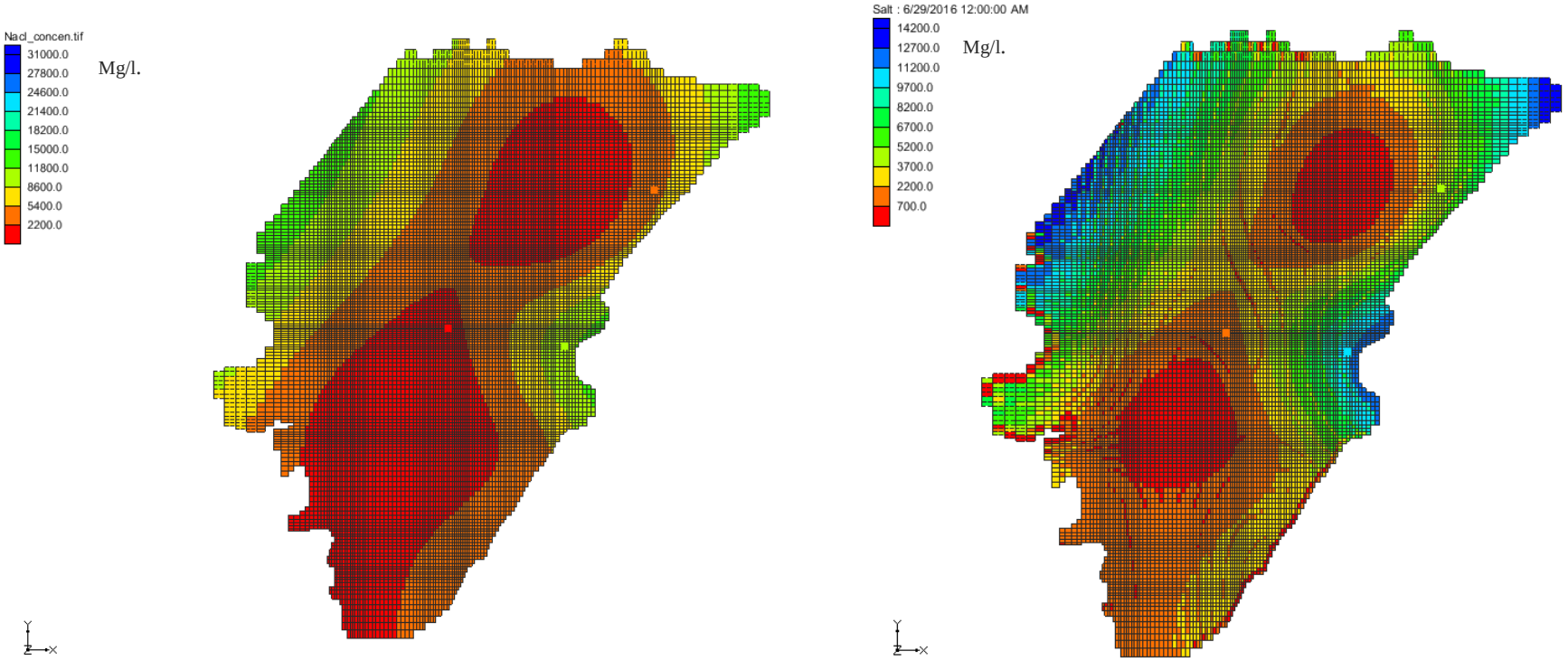

a. **b.**

Figure 4.12a, b: NaCl solute concentrations in mg/l for (a.) 25th March (Initial concentration) and (b.) 29th June 2016

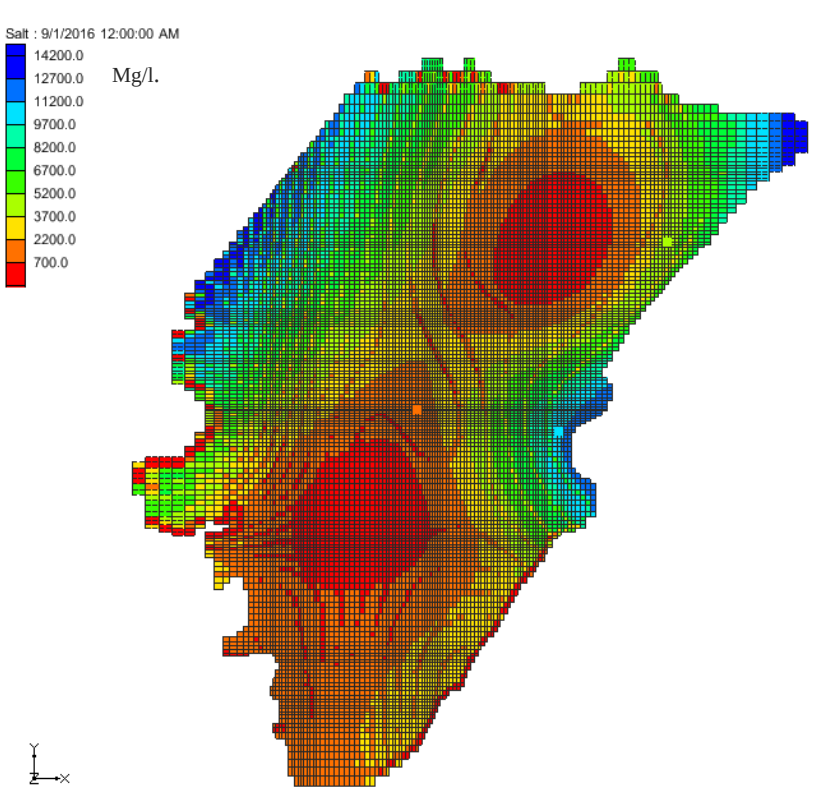

c.

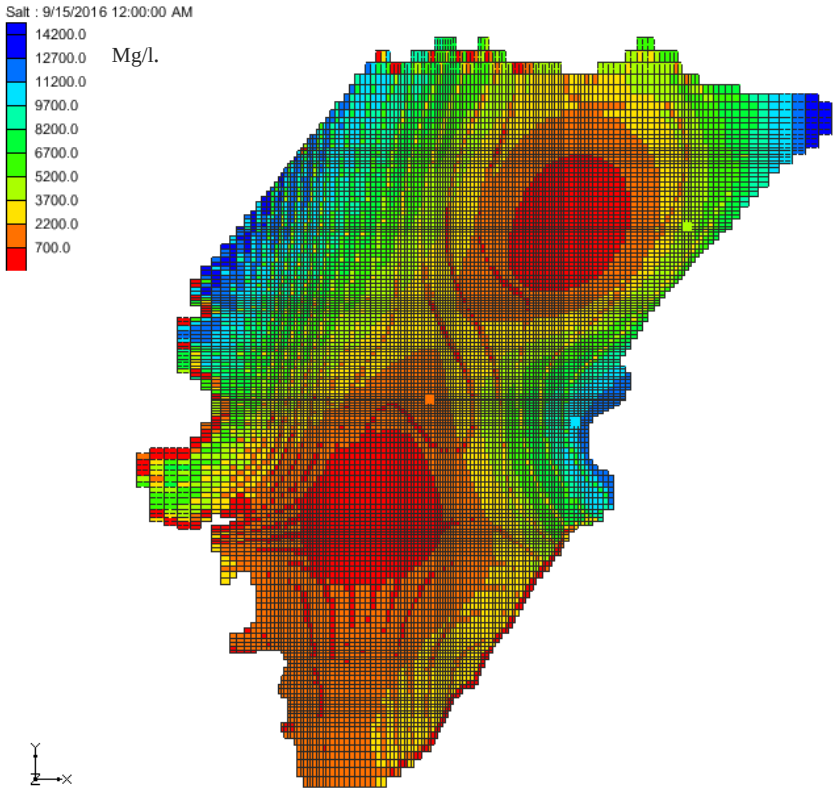

d.

Figure 4.12c, d: NaCl solute concentrations in mg/l for (c.) 1st September and (d.) 15th September 2016

CHAPTER FIVE- CONCLUSION AND RECOMMENDATION

5.1 Conclusion

This study extensively covered the hydrogeology, vulnerability to seawater intrusion, and flow of the groundwater in the North Coast of Mombasa area before, during and after the long rains in 2016. The conclusions in relation to the objectives are highlighted below;

a. The hydrogeology of the study area is that of an unconfined aquifer, with water heads varying from -1m to 33m above mean sea level. The groundwater heads did not vary significantly across seasons.
b. The EC and TDS values were observed to have near perfect correlations and generally high as over 94% of the water samples exceeded WHO drinking water limit.
c. The pH of the groundwater was slightly alkaline as over 90% of the water samples had pH values within 6.5 and 8.5 the acceptable limit of WHO guidelines, however, the pH could be slightly acidic in the rainy season.
d. The parameters with high impacts on the groundwater chemistry are EC, TDS, Cl^-, Na^+, Mg^{2+}, K^+, and to some degree SO_4^{2-} while Ca^{2+}, HCO_3 and pH have paltry impacts on the geochemistry of the aquifer.
e. The groundwater in the coastal aquifer is generally of marine and deep ancient type.
f. The salinity distribution in the groundwater varies with seasons while groundwater recharge heavily influences the salinity of the groundwater.
g. About 90% of the aquifer coverage experienced a moderate impact of seawater intrusion at pre-monsoon; 100% experienced a moderate impact in June (rainy season); 55% and 42% experienced slight and moderate impacts respectively in September (post-monsoon). There are mild evidence of anthropogenic-driven groundwater pollution.
h. The vulnerability of the study area to seawater intrusion is largely moderate irrespective of seasons. However, lower vulnerability is experienced in the rainy season than at pre-monsoon.
i. The groundwater flow and direction in the coastal aquifer is generally towards the northeast and southern part of the study area.
j. The concentrations of NaCl in the groundwater slightly reduced from the centre of the study area outwards from June (peak of rainy season) to September (post-monsoon).

5.2 Recommendation

Several methods have been devised all over the world for preventing or controlling the impact of seawater intrusion into coastal aquifers. Some of the direct preventive methods are; extraction barriers, injection barriers, artificial recharge (Todd & Mays 2005; Pliakas *et al.,* 2005). However, these direct methods are usually financially costly and technically demanding (Kallioras *et al.,* 2013), hence, may prove unfeasible in the study area. Based on the conclusions drawn from the study, more realistic indirect methods revolving around management may be recommended as follows;

a. The wells used for these studies may be revised for creating a network of monitoring wells to observe the long term hydrogeologic regime of the aquifer for effective aquifer system management
b. Management of the pumping scheme- By working closely with the local Water Resources Management Authority, recommendations could be written to borehole owners based on the GALDIT vulnerability map. Boreholes/shallow wells located in the regions of low vulnerability may be advised to stay in full operation while those located within the injurious vulnerability regions are advised to ration pumping rates i.e. operate mainly in the wet season when the water table levels are high but in shifts during the dry season.
c. Modification of the pumping Scheme: Records on all existing and future groundwater wells should be created. It is advised that future boreholes/wells should be made as shallow as possible especially in regions close to the ocean and creeks and regions identified as under injurious vulnerability

Recommended areas of further research identified from this study are as follows;

a. Empirical studies on the horizontal and vertical hydraulic conductivities under isotropic, and anisotropic conditions
b. Long term regular and periodic groundwater data collection and monitoring for a richer and more comprehensive understanding of the long-term groundwater dynamics of the study area
c. Detailed long term and predictive studies on the effects of pumping regimes on the intrusion of seawater.

REFERENCES

Adepelumi, A. A., Ako, B. D., Ajayi, T. R., Afolabi, O., & Omotoso, E. J. (2009). Delineation of saltwater intrusion into the freshwater aquifer of Lekki Peninsula, Lagos, Nigeria. *Environmental Geology, 56*, 927–933.

Albinet M, Margat J (1970) Cartographie de la vulnérabilité à la pollution des nappes d'eau souterraine Orleans, France. Bull BRGM 2ème série, 4 : 13–22.

Aller L, Bennet T, Lehr J.H, Petty R.J (1987) DRASTIC: a standardised system for evaluating groundwater pollution potential using hydrologic settings. US EPA Report, 600/2–87/ 035, Robert S. Kerr Environmental Research Laboratory, Ada, OK.

Aquaveo. (2016). *Introduction*. Retrieved September 5, 2016, from http://www.aquaveo.com/In.

Ashton, P.J., 2002: Avoiding conflicts over Africa's water resources. *Ambio*, 31,236-242.

Ayolabi, E. A., Folorunso, A. F., Odukoya, A. M., & Adeniran, A. E. (2013). Mapping saline water intrusion into the coastal aquifer with geophysical and geochemical techniques: The university of Lagos campus case (Nigeria). *SpringerPlus*, *2*(1), 433. doi:10.1186/2193-1801-2-433.

Balathandayutham, K., Mayilswami, C. and Tamilmani, D. (2015). 'Assessment of groundwater quality using GIS: A case study of Walayar watershed, Parambikulam-Aliyar-Palar basin, Tamilnadu, India', *Current World Environment*, 10(2), pp. 602–609. doi: 10.12944/cwe.10.2.25.

Barlow, P. M. (2003). *Ground water in freshwater-saltwater environments of the Atlantic Coast*. Reston, VA: U.S. Dept. of the Interior, U.S. Geological Survey.

Benoit J, Hardaway CS, Hernandez D, Holman R, Koch E, McLellan N, Peterson S, Reed D, Suman D (2007) Mitigating shore erosion along sheltered coasts. The National Academies Press, Washington, DC.

Bhatt, G., Kumar, M., & Duffy, C. J. (2014). A tightly coupled GIS and distributed hydrologic modelling framework. *Environmental Modelling & Software*, *62*, 70–84.

doi:10.1016/j.envsoft.2014.08.003.

Boko, M., I. Niang, A. Nyong, C. Vogel, A. Githeko, M. Medany, B. Osman-Elasha, R. Tabo and P. Yanda, 2007: Africa. Climate Change 2007: Impacts, Adaptation and Vulnerability. Contribution of Working Group II to the Fourth Assessment Report of the Intergovernmental Panel on Climate Change, M.L. Parry, O.F. Canziani, J.P. Palutikof, P.J. van der Linden and C.E. Hanson, Eds., Cambridge University Press, Cambridge UK, 433-467.

Boon, J. D., Brubaker, J. M., & Forrest, D. R. (2010). *Chesapeake Bay Land Subsidence and Sea Level Change: An Evaluation of Past And Present Trends And Future Outlook*. Virginia Institute of Marine Science Special Report No. 425 in Applied Marine Science and Ocean Engineering Retrieved from http://www.vims.edu/GreyLit/VIMS/sramsoe425.pdf.

Boswinkel J. A., Information Note, 2000. *International Groundwater Resources Assessment Centre (IGRAC), Netherlands Institute of Applied Geoscience*, Netherlands.

Bouderbala, A., & Remini, B. (2014). Geophysical approach for assessment of seawater intrusion in the coastal aquifer of Wadi Nador (Tipaza, Algeria). *Acta Geophysica*, *62*(6), . doi:10.2478/s11600-014-0220-y.

Brown, C. H. (1998). *Applied multivariate statistics in geohydrology and related sciences*. Berlin: Springer.

Brown, E., Skougstad, M. W., & Fishmen, M. J. (1983). *Method for collection and analyzing of water samples for dissolved minerals and gases*. Washington DC, USA: U.S. Govt. Printing Office.

Buddemeier, R.W., S.V. Smith, D.P. Swaaney and C.J. Crossland, (2002). *The Role of the Coastal Ocean in theDisturbed andUndisturbed Nutrient and Carbon Cycles.* LOICZ Reports and Studies Series No. 24. 84 pp.

Caswell, P. V. (1954a). *Geology of the Kilifi-Mazeras area degree sheet 66 SE quarter* [Map]. Nairobi: Survey, Min., Colony and Protectorate of Kenya.

Caswell, P. V. (1954b). *Geology of the Mombasa-Kwale area degree sheet 69 ; with coloured map* [Map]. Nairobi: Survey, Min., Colony and Protectorate of Kenya.

Caswell, P. V. (2007). *Geology of the kilifi-mazeras area* (Report No 34, pp. 1-54) ,Reprinted 2007

Kenya, Ministry of Mining, Geology Department. NAIROBI, Nairobi Area.

Chachadi A.G. & Lobo-Ferreira, J.P (2001), Sea water intrusion vulnerability mapping of aquifers using GALDIT method. Proc. Workshop on modelling in hydrogeology, Anna University, Chennai, pp.143-156, and in COASTIN A Coastal Policy Research Newsletter, Number 4, March 2001. New Delhi, TERI, pp.7-9, (cf*http://www.teriin.org/teriwr/coastin/newslett/coastin4.pdf*).

Chachadi A.G. & Lobo-Ferreira, J.P (2001), Sea water intrusion vulnerability mapping of aquifers using GALDIT method. Proc. Workshop on modelling in hydrogeology, Anna University, Chennai, pp.143-156, and in COASTIN A Coastal Policy Research Newsletter, Number 4, March 2001. New Delhi, TERI, pp. 7-9, (cf *http://www.teriin.org/teri-wr/coastin/newslett/coastin4.pdf*).

Chachadi AG, Lobo-Ferreira JP (2005) Assessing aquifer vulnerability to sea-water intrusion using GALDIT method: Part 2— GALDIT Indicators Description, Fourth Inter-Celtic Colloquium on Hydrogeology and Management of Water Resources, Portugal, 11–14, July 2005, CD of Proceeding.

Chachadi AG, Lobo-Ferreira JP (2005) Assessing aquifer vulnerability to sea-water intrusion using GALDIT method: Part 2— GALDIT Indicators Description, Fourth Inter-Celtic Colloquium on Hydrogeology and Management of Water Resources, Portugal, 11–14, July 2005, CD Of Proceeding.

Cimino, A., Cosentino, C., Oieni, A., & Tranchina, L. (2007). A geophysical and geochemical approach for seawater intrusion assessment in the Acquedolci coastal aquifer (northern Sicily). *Environmental Geology*, *55*(7), 1473–1482. doi:10.1007/s00254-007-1097-8.

Civita M (1994) Le carte della vulnerabilità degli acquiferi all'inquinamento. Teoria and practica (Aquifer vulnerability maps to pollution) Pitagora, Bologna.

Civita M, De Regibus C (1995) Sperimentazione di alcune metodologie per la valutazione della vulnerabilità degli aquiferi. Q Geol Appl Pitagora, Bologna, 3: 63–71.

Climatemps, (2015). *Mombasa climate Mombasa temperatures Mombasa weather averages*.

Retrieved July 24, 2016, from http://www.mombasa.climatemps.com/.

Corniello A, Ducci D, Napolitano P (1997). Comparison between parametric methods to evaluate aquifer pollution vulnerability using GIS: an example in the ”Piana Campana“, southern Italy. In: Marinos PG, Koukis GC, Tsiambaos GC, and Stournaras GC (eds) Engineering geology and the environment. Balkema, Rotterdam, pp 1721–1726.

Darcy, H. (1856). Les Fontaines Publiques de la Ville de Dijon, Dalmont, Paris.

Darnault C.J.G & Godinez I.G (2008). Coastal Aquifers and Seawater intrusion. In Christophe J.G Darnault (Editor), *Overexploitation and contamination of shared groundwater resources* (pp. 185 - 201), New York, NY, United States: Springer science+Business Media B. V.

Deb, P. K. (2014). Pumping tests and Aquifer parameters. In P. Kumar Deb, *An Introduction to Mine Hydrogeology, SpringerBriefs in Water Science and Technology (pp. 13–21)* DOI: 10.1007/978-3-319-02988-7_3.

Doerfliger N, Zwahlen F (1997). EPIK: a new method for outlining of protection areas in karstic environment. In: Gü- nay G, Jonshon AI (eds) International symposium and field seminar on “karst waters and environmental impacts”. Antalya, Turkey. Balkema, Rotterdam, pp 117–123.

Draoui, M., Vias, J., Andreo, B., Targuisti, K., & Stitou El Messari, J. (2007). A comparative study of four vulnerability mapping methods in a detritic aquifer under mediterranean climatic conditions. *Environmental Geology*, *54*(3), 455–463. doi:10.1007/s00254-007-0850-3.

Fadili, A., Mehdi, K., Riss, J., Najib, S., Makan, A., & Boutayab, K. (2015). Evaluation of groundwater mineralization processes and seawater intrusion extension in the coastal aquifer of Oualidia, Morocco: Hydrochemical and geophysical approach. *Arabian Journal of Geosciences*, *8*(10), 8567–8582. doi:10.1007/s12517-015-1808-5.

Foster SSD (1987). Fundamental concepts in aquifer vulnerability, pollution risk and protection strategy. In: Duijvenbooden W van, Waegeningh HG van (eds) TNO Committee on Hydrological Research, The Hague. Vulnerability of soil and groundwater to pollutants, Proceedings and Information. 38 : 69–86.

Freeze A. and Cherry J.A. (1979), Groundwater, Prentice Hall, Englewood Cliffs.

Gaaloul, N. (2012). Simulation of seawater intrusion in coastal aquifers: Forty Five-Years exploitation in an eastern coast aquifer in NE Tunisia. *The Open Hydrology Journal*, *6*(1), 31–44. doi:10.2174/1874378101206010031.

Gogu, R. C., & Dassargues, A. (2000). Current trends and future challenges in groundwater vulnerability assessment using overlay and index methods. *Environmental Geology*, *39*(6), 549–559. doi:10.1007/s002540050466.

Gogu, R., Carabin, G., Hallet, V., Peters, V., & Dassargues, A. (2001). GIS-based hydrogeological databases and groundwater modelling. *Hydrogeology Journal*, *9*(6), 555–569. doi:10.1007/s10040-001-0167-3.

GOK 1979. National population and housing census. Vol 1. Ministry of Planning and National Development, Central Bureau of Statistics.

GOK 1989. National population and housing census. Vol 1. Ministry of Planning and National Development, Central Bureau of Statistics.

GOK 1999. National population and housing census. Vol 1. Ministry of Planning and National Development, Central Bureau of Statistics.

Goldman, M., Gilad, D., Ronen, A., & Melloul, A. (1991). Mapping of seawater intrusion into the coastal aquifer of Israel by the time domain electromagnetic method. *Geoexploration*, *28*(2), 153–174. doi:10.1016/0016-7142(91)90046-f.

Goldscheider N, Klute M, Sturm S, Ho¨tzl H (2000). The PI method—a GIS-based approach to mapping groundwater vulnerability with special consideration on karst aquifers. Z Angew Geol 46(3):157–166.

Gontara, M., Allouche, N., Jmal, I., & Bouri, S. (2016). Sensitivity analysis for the GALDIT method based on the assessment of vulnerability to pollution in the northern Sfax coastal aquifer, Tunisia. *Arabian Journal of Geosciences*, *9*(5),. doi:10.1007/s12517-016-2437-3.

Goodchild M.F. & Kemp K.K (1990) NCGIA Core curriculum in GIS, Santa Barbara, CA: National Centre for Geographic Information and Analysis.

Gueye, L., M. Bzioul & O. Johnson (2005). Water and sustainable development in the countries of Northern Africa: coping with the challenges and scarcity. *Assessing sustainable development in Africa*. Africa's sustainable development Bulletin, Economic Commission for Africa, Addis Ababa, 24-28.

Guo, W., and C.D. Langevin. (2002). User's guide to SEAWAT: A computer program for the simulation of three-dimensional variable-density ground-water flow. USGS Techniques of Water Resources Investigations Book 6, Chapter A7. USGS.

Harbaugh, A.W., Banta, E.R., Hill, M.C., and McDonald, M.G. (2000). *MODFLOW-2000, the U.S. Geological Survey modular ground-water model — User guide to modularization concepts and the Ground-Water Flow Process* (PDF). Open-File Report 00-92. U.S. Geological Survey.

Herzberg, A., (1901), Die Wasserversorgung einiger Nordseebder (The water supply of parts of the North Sea coast in Germany), *Z. Gasbeleucht. Wasserversorg* 44:815–819 and 45:842–844.

Huang, B., & Jiang, B. (2002). AVTOP: A full integration of TOPMODEL into GIS. *Environmental Modelling & Software*, *17*(3), 261–268.doi:10.1016/s1364-8152(01)00073-1.

Hwang, S., Shin, J., Park, I., & Lee, S. (2004). Assessment of seawater intrusion using geophysical well logging and electrical soundings in a coastal aquifer, Youngkwang-gun, Korea. *Exploration Geophysics*, *35*(1), 99. doi:10.1071/eg04099.

Idowu, T. E., Nyadawa, M., & K'Orowe, M. O. (2016). Seawater Intrusion Vulnerability Assessment of a Coastal Aquifer: North Coast Of Mombasa, Kenya as a Case Study. *Int. Journal of Engineering Research and Application*, *6*(8, (Part -3)), 37–45. ISSN : 2248-9622.

Ingebritsen, S. E., & Galloway, D. L. (2014). Coastal subsidence and relative sea level rise. Environmental Research Letters, 9(9), 091002. doi:10.1088/1748-9326/9/9/.

IPCC, (1997) - R.T.Watson, M.C.Zinyowera, R.H.Moss (Eds) Cambridge University Press, UK. Available from Cambridge University Press, The Edinburgh Building Shaftesbury Road,

Cambridge CB2 2RU ENGLAND. Accessible online from: http://www.ipcc.ch/ipccreports/sres/regional/index.php?idp=30.

Jackson, J. (2007). *Hydrogeology and Groundwater Flow Model, Central Catchment of Bribie Island, SouthEast Queensland* (Unpublished master's thesis). School of Natural Resource Sciences, Queensland University of Technology, Queensland Australia.

Javadi, A. A., Abd-Elhamid, H. F., & Farmani, R. (2011). A simulation-optimization model to control seawater intrusion in coastal aquifers using abstraction/recharge wells. *International Journal for Numerical and Analytical Methods in Geomechanics*, *36*(16), 1757–1779. doi:10.1002/nag.1068.

Kallioras A, Pliakas F, Skias S, Gkiougkis I (2011) Groundwater vulnerability assessment at SW Rhodope aquifer system in NE Greece. In: Lambrakis N, Stournaras G, Katsanou (eds) Advances in the research of aquatic environment. Environ Earth Sci. Springer 2:351–358. doi:10.1007/978-3-642-24076-8_41.

Kallioras Andreas, Pliakas Fotios-Konstantinos, Schuth Christoph & Rausch Randolf (2013). Methods to Countermeasure the Intrusion of Seawater into Coastal Aquifer Systems. In , Sharma, S. K., & Sanghi, R. (Eds). Wastewater Reuse and Management, Springer Science+Business Media Dordrecht: (pp 479 - 490) DOI 10.1007/978-94-007-4942-9_17.

Karmegam, U., Chidambaram, S., Prasanna, M. V., Sasidhar, P., Manikandan, S., Johnsonbabu, G., … Anandhan, P. (2011). A study on the mixing proportion in groundwater samples by using piper diagram and Phreeqc model. *Chinese Journal of Geochemistry*, *30*(4), 490–495. doi:10.1007/s11631-011-0533-3.

Kenya, Water Services Regulatory Board (WASREB). (2008). *Drinking Water Quality and Effluent Monitoring Guideline*.

Kim, K.Y., Chon, C.M. & Park, K.H. (2007) 'A simple method for locating the fresh Water–Salt water interface using pressure data', *Ground Water*, 45(6), pp. 723–728. doi: 10.1111/j.1745-6584.2007.00349.x.

Kim, O.B. & Park, H.Y. (1998) 'Variation of Hydrochemical characteristics of major elements in

groundwater by the seawater intrusion in the Byeonsan Peninsular, Korea', *Geosystem Engineering*, 1(2), pp. 106–110. doi: 10.1080/12269328.1998.10541131.

King, A.C., Raiber, M. & Cox, M.E. (2013) 'Multivariate statistical analysis of hydrochemical data to assess alluvial aquifer–stream connectivity during drought and flood: Cressbrook creek, southeast Queensland, Australia', *Hydrogeology Journal*, 22(2), pp. 481–500. doi: 10.1007/s10040-013-1057-1.

Kiplangat Vincent, K., Nicholas Muthama, M., & Nicodemus Muoki, S. (2014). Darcy's law equation with application to underground seepage in earth dams in calculation of the amount of seepage. *American Journal of Applied Mathematics and Statistics*, *2*(3), 143–149. doi:10.12691/ajams-2-3-8

Klassen, J., Allen, D. M., & Kirste, D. (2014). *Chemical Indicators of Saltwater Intrusion for the Gulf Islands, British Columbia* (Rep. No. T). Submitted to BC Ministry of Forests, Lands and Natural Resource Operations and BC Ministry of Environment.

KNBS (2010). 2009 Kenya Population and Housing Census, Population Distribution by Political Units, Vol.1B, KNBS.

Kouzana, L., Benassi, R., Ben mammou, A., & Sfar felfoul, M. (2010). Geophysical and hydrochemical study of the seawater intrusion in Mediterranean semi arid zones. Case of the Korba coastal aquifer (cap-bon, Tunisia). *Journal of African Earth Sciences*, *58*(2), 242–254. doi:10.1016/j.jafrearsci.2010.03.005.

Kumar, C. P. (2006). Management of Groundwater in Salt Water Ingress Coastal Aquifers. In: Groundwater Modelling and Management (Eds. N. C. Ghosh and K. D. Sharma), Capital Publishing Company, New Delhi, pp. 540-560. http://www.angelfire.com/nh/cpkumar/publication/gwman.pdf.

Kundzewicz, Z.W., L.J. Mata, N.W. Arnell, P. Döll, P. Kabat, B. Jiménez, K.A. Miller, T. Oki, Z. Sen & I.A. Shiklomanov, (2007). Freshwater resources and their management. *Climate Change 2007: Impacts, Adaptation and Vulnerability. Contribution of Working Group II to the Fourth Assessment Report of the Intergovernmental Panel on Climate Change*, M.L. Parry, O.F. Canziani, J.P. Palutikof, P.J. van der Linden and C.E. Hanson, Eds., Cambridge

University Press, Cambridge, UK, 173-210.

Kura NU, Ramli MF, Ibrahim S, Sulaiman WNA, Aris AZ (2014) An integrated assessment of seawater intrusion in a small island using geophysical, geochemical and geostatistical techniques. Environ Sci Pollut Res 21:7047–7064.

Langevin, C. D.; Guo, W. X (2006). MODFLOW/MT3DMS-based simulation of variable-density ground water flow and transport. Ground Water, 44, 339–351.

Langevin, C.D., Shoemaker, W.B., and Guo, W. (2003). MODFLOW-2000, the U.S. Geological Survey Modular Ground-Water Model–Documentation of the SEAWAT- 2000 Version with the Variable-Density Flow Process (VDF) and the Integrated MT3DMS Transport Process (IMT): U.S. Geological Survey Open-File Report 03-426, 43 p.

Lin, H., Ke, K., Tan, Y., Wu, S., Hsu, G., Chen, P., & Fang, S. (2013). Estimating Pumping Rates and Identifying Potential Recharge Zones for Groundwater Management in Multi-Aquifers System. *Water Resour Manage Water Resources Management, 27*(9), 3293-3306.

Lobo Ferreira JP, Chachadi AG, Diamantino C, Henriques MJ (2005) Assessing aquifer vulnerability to seawater intrusion using GALDIT method: Part 1 Application to the Portuguese Aquifer of Monte Gordo. Fourth Inter-Celtic Colloquium on Hydrogeology and Management of Water Resources, Portugal, 11–14, July 2005, CD of Proceedings.

Lobo-Ferreira JP, Cabral M (1991) Proposal for an operational definition of vulnerability for the European community's Atlas of groundwater resources, in meeting of the European Institute for Water, Groundwater Work Group Brussels.

Lusczynski, N.J. 1961. Head and flow of ground water of variable density. Journal ofGeophysical Research 66, no. 12: 4247–4256.

Markusen, A. R. (1996). The economics of postwar regional disparity. In S. S. Fainstein & S. Campbell (Eds.), *Readings in urban theory* (pp. 102–131). Cambridge, MA: Blackwell.

Mercer, J. W., & Faust, C. R. (1980). Ground-Water Modeling: An Overview. *GROUND WATER, 18*(2), 108-116.

MODFLOW: USGS. (2013). Retrieved September 5, 2016, from USGS- Science for a changing

world, http://water.usgs.gov/ogw/modflow/MODFLOW.html.

Mondal, N. C., Singh, V. S., Saxena, V. K., & Singh, V. P. (2010). Assessment of seawater impact using major hydrochemical ions: A case study from Sadras, Tamilnadu, India. *Environmental Monitoring and Assessment Environ Monit Assess, 177*(1-4), 315-335. doi:10.1007/s10661-010-1636-8.

MT3D (2000). Retrieved September 5, 2016, from http://hydro.geo.ua.edu/mt3d/.

Mtoni, Y., Mjemah, I. C., Bakundukize, C., Camp, M. V., Martens, K., & Walraevens, K. (2013). Saltwater intrusion and nitrate pollution in the coastal aquifer of Dar es Salaam, Tanzania. *Environ Earth Sci Environmental Earth Sciences, 70*(3), 1091-1111. doi:10.1007/s12665-012-2197-7.

Moujabber, M. E., Samra, B. B., Darwish, T., & Atallah, T. (2006). Comparison of different indicators for groundwater contamination by seawater intrusion on the Lebanese coast. *Water Resources Management, 20*(2), 161–180. doi:10.1007/s11269-006-7376-4.

Munga, D., Mwangi, S., Ong'anda, H., Kitheka, J. U., Mwaguni, S. M., Mdoe, F., & Opello, G. (2006). Vulnerability and pollution of groundwater in Kisauni, Mombasa, Kenya. *Groundwater pollution in Africa. Taylor and Francis (Balkema), The Netherlands*, 213-228.

Musa, O. K., Kudamnya, E. A., Omali, A. O., & Akuh, T. I. (2014). Physico-chemical characteristics of surface and groundwater in Obajana and its environs in Kogi state, central Nigeria. *African Journal of Environmental Science and Technology*, *8*(9), 521–531. doi:10.5897/ajest2014.1708.

Najib S, Grozavu A, Mehd K, Breaban IG, Guessir H, Boutayeb K (2012) Application of the method GALDIT for the cartography of groundwaters vulnerability: aquifer of Chaouia coast (Morocco). Sci Ann Alexandru Ioan Cuza 63(3):77.

Nicholls, R.J., P.P. Wong, V.R. Burkett, J.O. Codignotto, J.E. Hay, R.F. McLean, S. Ragoonaden & C.D. Woodroffe, (2007). Coastal systems and low-lying areas. *Climate Change 2007: Impacts, Adaptation and Vulnerability. Contribution of Working Group II to the Fourth*

Assessment Report of the Intergovernmental Panel on Climate Change, M.L. Parry, O.F. Canziani, J.P. Palutikof, P.J. van der Linden and C.E. Hanson, Eds., Cambridge University Press, Cambridge, UK, 315-356.

Oladapo, M. I., Ilori, O. B., & Adeoye-Oladapo, O. O. (2014). English. *African Journal of Environmental Science and Technology*, *8*(1), 16–30. doi:10.5897/ajest2013.1554.

Olivera, F., Valenzuela, M., Srinivasan, R., Choi, J., Cho, H., Koka, S., & Agrawal, A. (2006). ARCGIS-SWAT: A GEODATA MODEL AND GIS INTERFACE FOR SWAT. *Journal of the American Water Resources Association*, *42*(2), 295–309. doi:10.1111/j.17521688.2006.tb03839.x.

Park, S. C., Yun, S. T., Chae, G. T., Yoo, I. S., Shin, K. S., Heo, C. H., et al. (2005). Regional hydrochemical study on salinization of coastal aquifers, western coastal area of South Korea. *Journal of Hydrology*, *313*, 182–194.

Piper, A.M. (1953). *A Graphic Procedure in the Geochemical Interpretation of Water Analysis*. Washington D.C USGS. OCLC 37707555. ASIN B0007HRZ36.

Pliakas F, Petalas C, Diamantis I, Kallioras A (2005) Modeling of groundwater artificial recharge by reactivating an old stream bed. Water Res Manag 19:279–294.

Recinos, N., Kallioras, A., Pliakas, F., & Schuth, C. (2014). Application of GALDIT index to assess the intrinsic vulnerability to seawater intrusion of coastal granular aquifers. *Environ Earth Sci Environmental Earth Sciences*, *73*(3), 1017-1032. doi:10.1007/s12665-014-3452-x.

Rientjes T. (2006). Modelling in hydrology, Department of water resources, *Institute for Geo-information Science and Earth Observation,* The Netherlands.

Rabinove, C. L., Longford, R. H., & Brookhart, J. W. (1958). *Saline water resources of North Dakota* (p. 364). US Geographical Survey Water Supply, Paper 1418.

Roger J.M. De Weist (1998). Ghyben-Herzberg theory. In Reginald W.H, Rhodes W.F (Eds). Encyclopedia of Hydrology and Water Resources. Encyclopedia of Earth Sciences,

Springer Netherlands. Springer Science+business Media B.V pp 340 – 341. Doi 10.1007/1-4020-4497-6_104.

Rolf A. de (2001). *Principles of geographic information systems: An introductory textbook* (2nd ed.). Enschede: ITC, International Institute for Aerospace Survey and Earth Sciences. Retrieved from https://www.itc.nl/library/papers_2009/general/principlesgis.pdf.

Saidi, S., Bouri, S., & Dhia, H. B. (2013). Erratum to: Groundwater management based on GIS techniques, chemical indicators and vulnerability to seawater intrusion modelling: Application to the Mahdia–Ksour Essaf aquifer, Tunisia. *Environmental Earth Sciences*, *70*(4), 1569–1570. doi:10.1007/s12665-013-2444-6.

Santha Sophiya, M. and Syed, T.H. (2013) 'Assessment of vulnerability to seawater intrusion and potential remediation measures for coastal aquifers: A case study from eastern India', *Environmental Earth Sciences*, 70(3), pp. 1197–1209. doi: 10.1007/s12665-012-2206-x.

Sappa, G., Ergul, S., Ferranti, F., Sweya, L. N., & Luciani, G. (2015). Effects of seasonal change and seawater intrusion on water quality for drinking and irrigation purposes, in coastal aquifers of Dar es Salaam, Tanzania. *Journal of African Earth Sciences, 105*, 64-84. doi:10.1016/j.jafrearsci.2015.02.007.

Saxena, V. K., Singh, V. S., Mondal, N. C., & Jain, S. C. (2003). Use of chemical parameters to delineation fresh ground water resources in Potharlanka Island,India. *Environmental Geology, 44*(5), 516–521.

Shiklomanov I.A (1993). World fresh water resources. In P.H Gleick (Editor), *Water in Crisis: A guide to the World's Fresh Water resources* (pp. 13 – 23), New york 10016, Oxford University Press, Inc.

Small, C., and Nicholls R.J (2003). A global analysis of Human Settlement in Coastal Zones. *J. Coastal Res*, 19, 584-599.

Sophiya MS, Syed TH (2013) Assessment of vulnerability to seawater intrusion and potential remediation measures for coastal aquifers: a case study from eastern India. Environ Earth Sci 70(3):1197–1209. doi:10.1007/s12665-012-2206-x.

Steyl, G., & Dennis, I. (2009). Review of coastal-area aquifers in Africa. *Hydrogeology Journal, 18*(1), 217–225. doi:10.1007/s10040-009-0545-9.

Todd D K, Mays LW (2005) Groundwater hydrology, 3rd edn. Wiley, New York, 636 p.

Trabelsi, N., Triki, I., Hentati, I. & Zairi, M. (2016) 'Aquifer vulnerability and seawater intrusion risk using GALDIT, GQISWI and GIS: Case of a coastal aquifer in Tunisia', *Environmental Earth Sciences,* 75(8). doi: 10.1007/s12665-016-5459-y.

UN Habitat (2008). United Nations Human Settlements Programme *The state of African cities*. Nairobi:UN Habitat.

UNEP (2008), Vital Water Graphics - An Overview of the State of the World's Fresh and Marine Waters. 2nd Edition. UNEP, Nairobi, Kenya. ISBN: 92-807-2236-0.

Van Stempvoort D, Evert L, Wassenaar L (1993) Aquifer vulnerability index: a GIS compatible method for groundwater vulnerability mapping. Can Wat Res J 18 : 25–37.

Vengosh, A., Gill, J., Reyes, A., and Thoresberg, K., (1997). A multi-isotope investigation of the origin of groundwater salinity in Salinas valley, California. *American Geophysical Union,* San Francisco, California.

Verruijt, A. (1968). A note on GHyben-Herzberg Formula. *Bulletin of the International Association of Scientific Hydrology, XIII*, 4-12.

World Bank, (1995). A Framework for Integrated Coastal Zone Management in Sub-Saharan Africa: Building Blocks for Environmentally Sustainable Development in Africa. *Paper No. 4, Africa. Technical Department. The World Bank*, Washington, DC, USA.

World Health Organization (WHO) (1984). *Guideline of drinking quality* (pp. 333–335). Washington, DC, USA: World Health Organization.

WUP- World Urbanization Prospects (2014). *The 2014 Revision, Highlights.* United Nations, Department of Economic and Social Affairs, Population Division.

Yang, Q., Zhang, J., Wang, Y., Fang, Y. & Martin, J. (2015) 'Multivariate statistical analysis of

Hydrochemical data for shallow ground water quality factor identification in a coastal aquifer', *Polish Journal of Environmental Studies*, 24. doi: 10.15244/pjoes/30263.

Zheng, Chunmiao, (1990). *MT3D, A modular three-dimensional transport model for simulation of advection, dispersion and chemical reactions of contaminants in groundwater systems*, Report to the U.S. Environmental Protection Agency, 170 p.

Zheng, Chunmiao, and P. Patrick Wang, 1999, *MT3DMS, A modular three-dimensional multi-species transport model for simulation of advection, dispersion and chemical reactions of contaminants in groundwater systems; documentation and user¡¯s guide*, U.S. Army Engineer Research and Development Center Contract Report SERDP-99-1, Vicksburg, MS, 202 p.

Zhou, X., Chen, M., Ju, X., Ning, X., & Wang, J. (2000). Numerical simulation of sea water intrusion near Beihai, china. *Environmental Geology*, *40*(1-2), 223–233. doi:10.1007/s002540000113.

APPENDICES

APPENDIX I

Groundwater Heads above mean sea level

SN	Sample location	Longitude	Latitude	March	June	Sept
W1	Braeburn	580281.0326	9559250.6848	2.9	3.83	3.77
W2	Cinema	576106.3909	9552365.9589	0.9	1.06	1.2
W3	Krat	579181.2187	9555320.1432	5	4.50	4.48
W4	M. Hussein	577531.7055	9557403.1077	5.05	5.49	5.39
W5	Milele	580455.1451	9557154.2796	0.64	1.06	0.81
W6	N golf	578466.5947	9553221.3129	8.9	9.04	9.1
W7	Redeem	580398.9022	9561622.8615	2.35	3.76	2.93
W8	Ruby1	578051.0775	9557591.8047	5.5	1.30	-
W9	Ruby2	577986.0766	9557524.2075	-	3.06	2.86
W10	Shimo high	582518.5623	9562327.3646	-	4.45	5.84
W11	Shimo qtrs	582283.2633	9562151.0353	-	2.05	2.85
W12	Sos1	579799.9737	9555168.7077	4.39	5.6	4.63
W13	Sos2	579715.5969	9555285.5167	-	3.5	3.54
W14	Sunsweet	582320.1225	9560416.5563	1.54	-0.95	-0.84
W15	Utange	579126.6152	9559040.4411	3.35	10.46	12.6
W16	Vikwatani	575516.7016	9558338.7809	-	26.89	33.08

Geographic coordinate system: GCS_WGS_1984

Datum: D_WGS_1984

Projected Coordinate System:WGS_1984_UTM_Zone_37S

Projection: Transverse_Mercator

APPENDIX II

Graphs showing the variations in the groundwater parameters in across the season

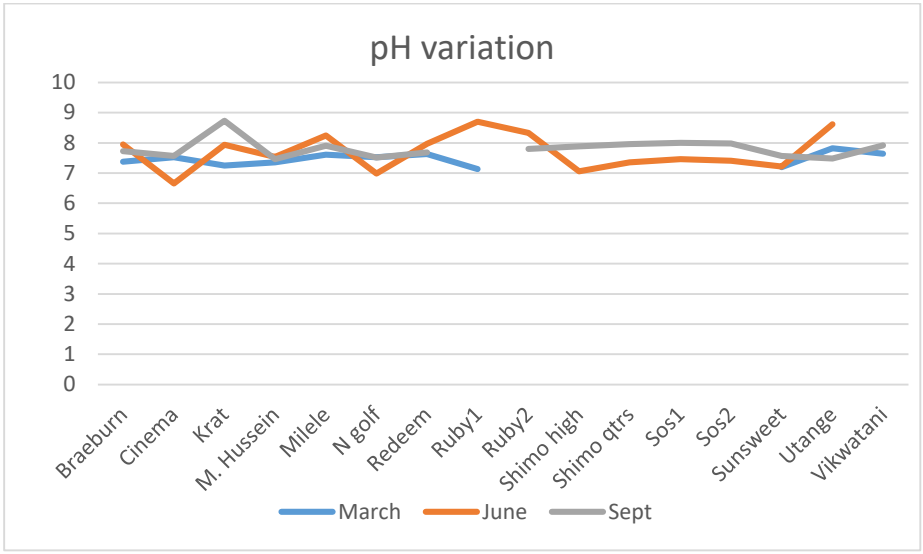

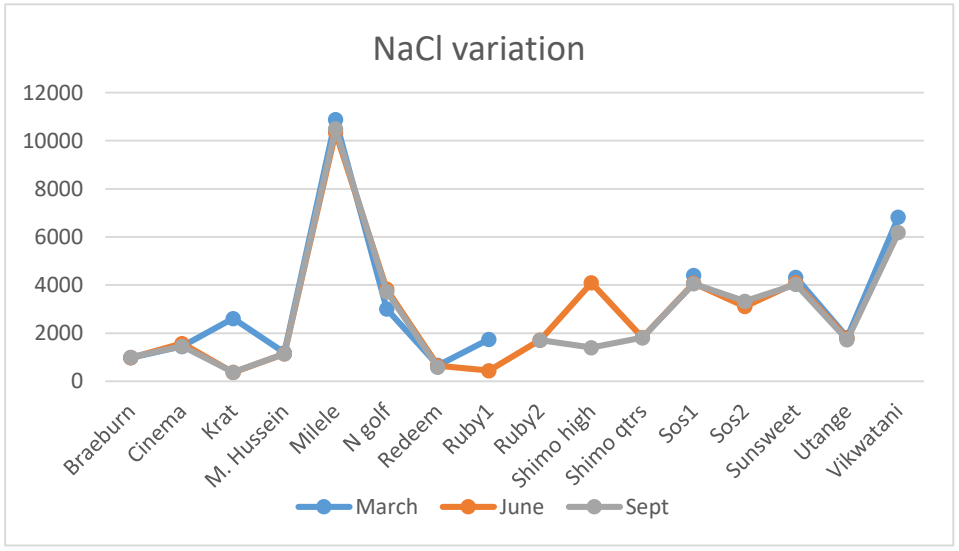

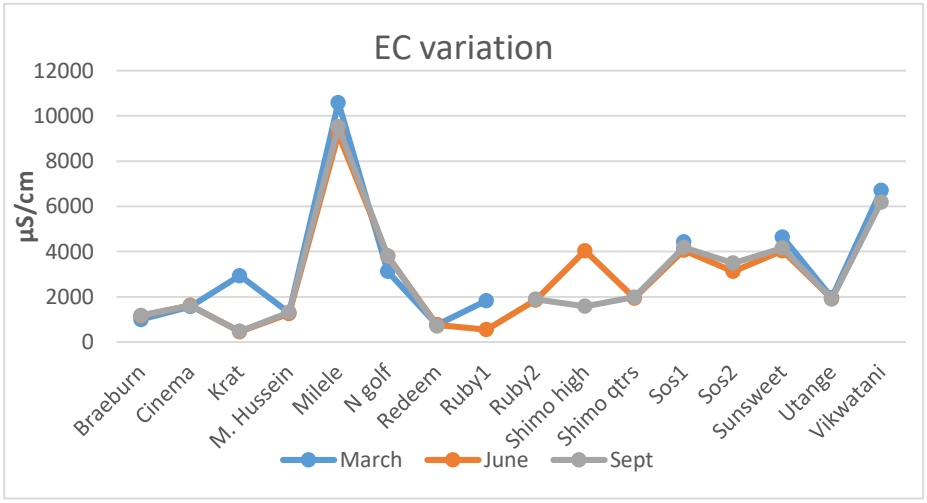

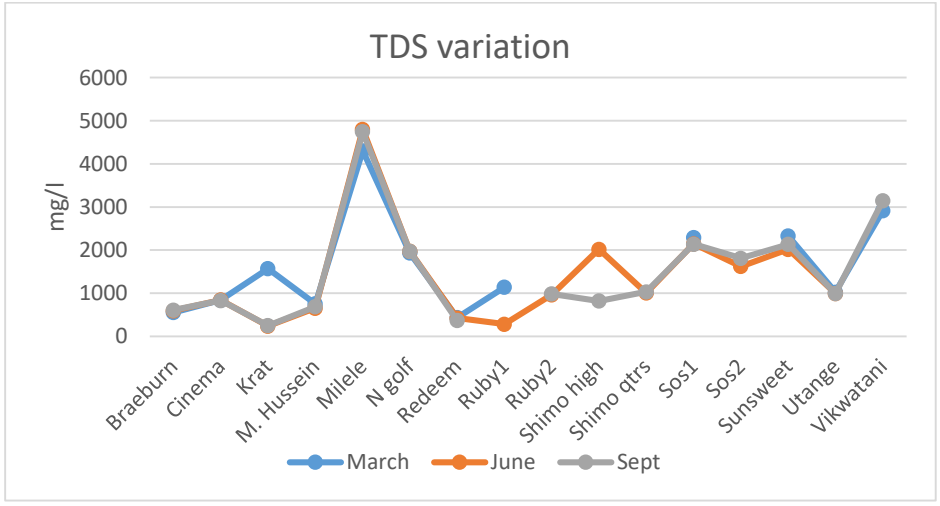

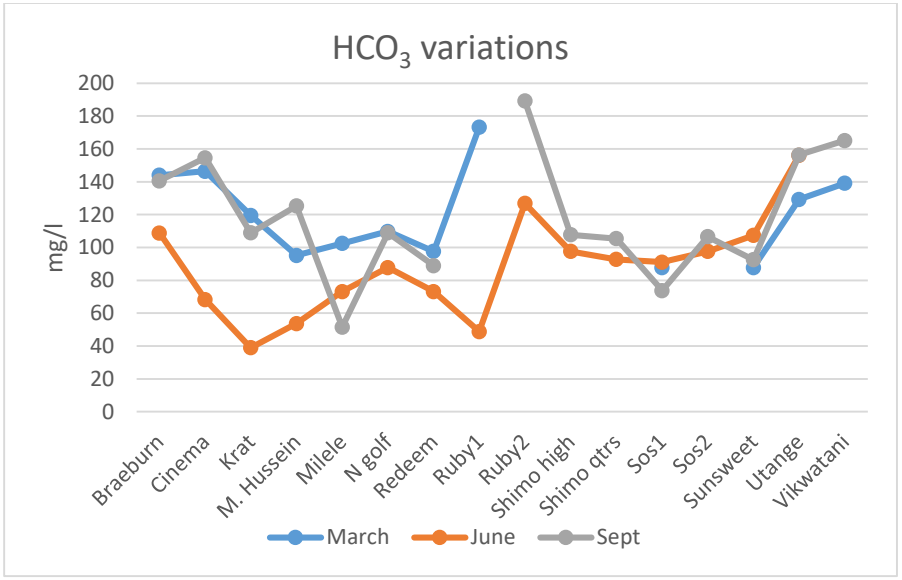
HCO3 variations
mg/l
200
180
160
140
120
100
80
60
40
20
0
Braeburn
Cinema
Krat
M. Hussein
Milele
N golf
Redeem
Ruby1
Ruby2
Shimo high
Shimo qtrs
Sos1
Sos2
Sunsweet
Utange
Vikwatani
March
June
Sept

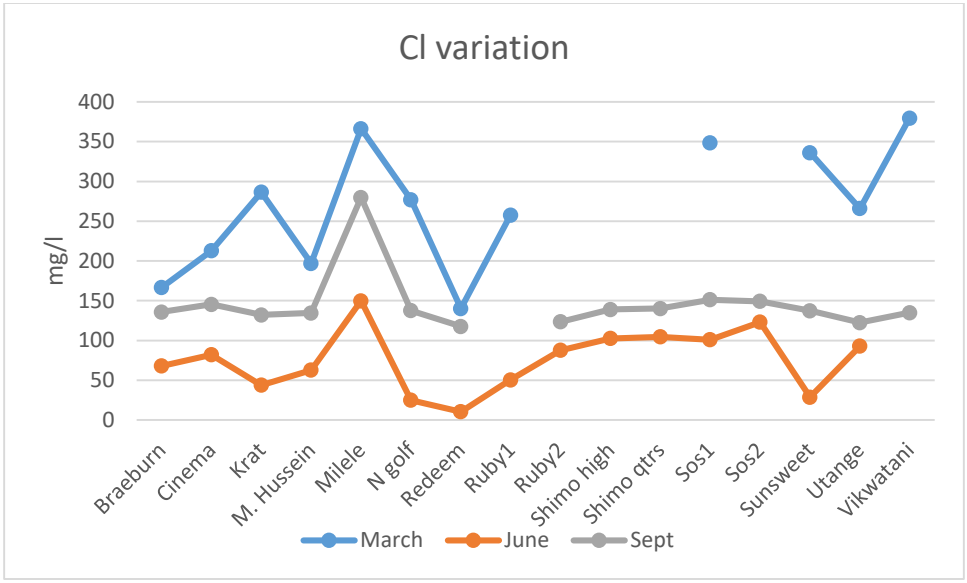
Cl variation
mg/l
400
350
300
250
200
150
100
50
0
Braeburn
Cinema
Krat
M. Hussein
Milele
N golf
Redeem
Ruby1
Ruby2
Shimo high
Shimo qtrs
Sos1
Sos2
Sunsweet
Utange
Vikwatani
March
June
Sept

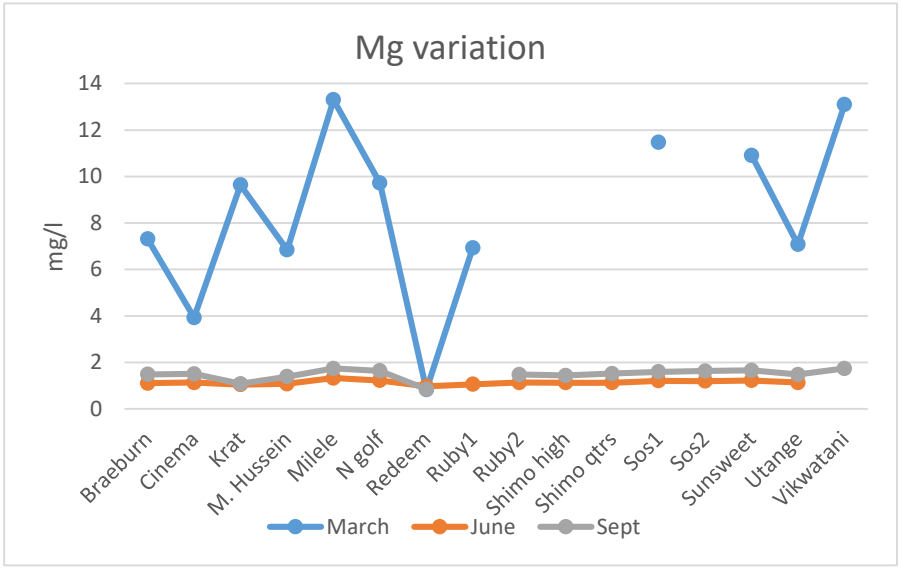
Mg variation
mg/l
14
12
10
8
6
4
2
0
Braeburn
Cinema
Krat
M. Hussein
Milele
N golf
Redeem
Ruby1
Ruby2
Shimo high
Shimo qtrs
Sos1
Sos2
Sunsweet
Utange
Vikwatani
March
June
Sept

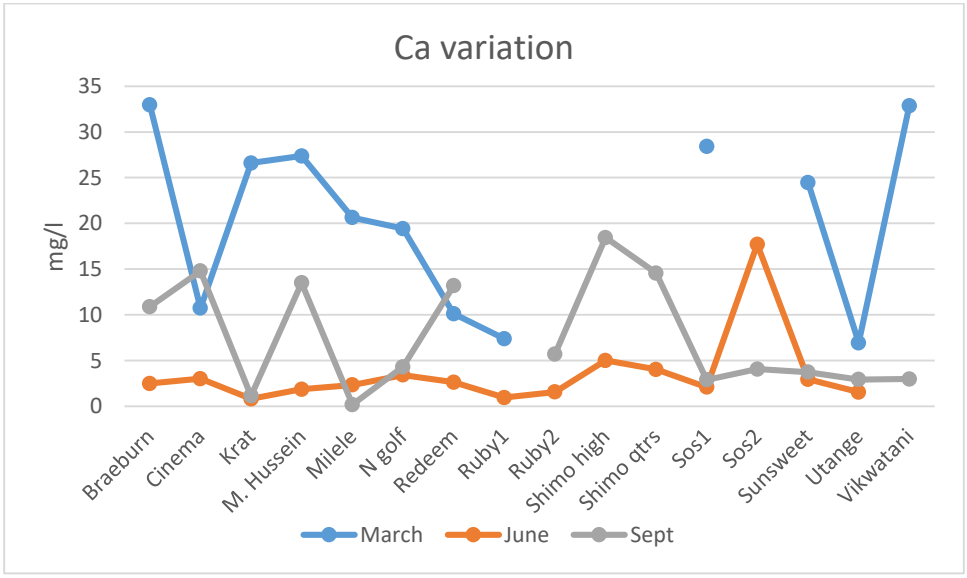
Ca variation
mg/l
35
30
25
20
15
10
5
0
Braeburn
Cinema
Krat
M. Hussein
Milele
N golf
Redeem
Ruby1
Ruby2
Shimo high
Shimo qtrs
Sos1
Sos2
Sunsweet
Utange
Vikwatani
March
June
Sept

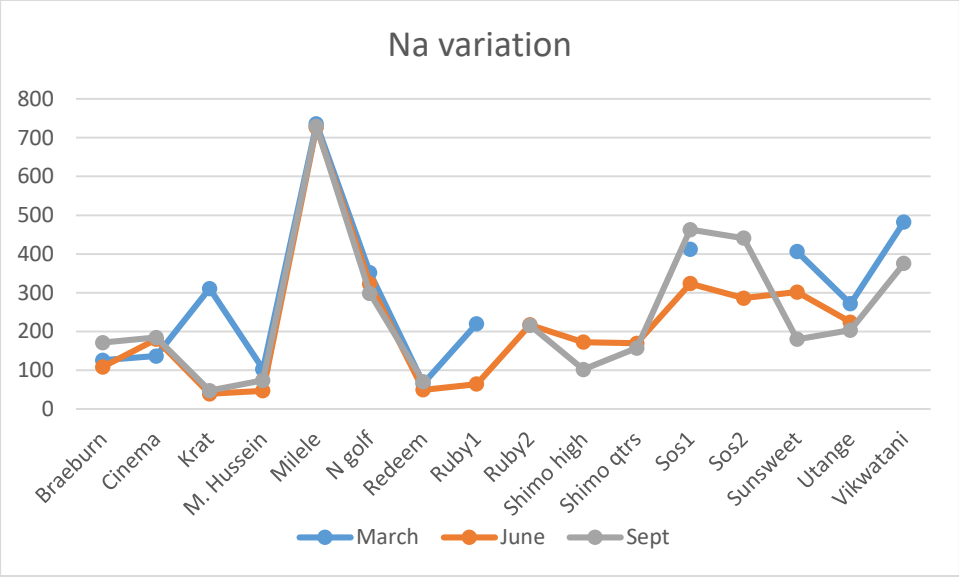
Na variation
800
700
600
500
400
300
200
100
0
Braeburn
Cinema
Krat
M. Hussein
Milele
N golf
Redeem
Ruby1
Ruby2
Shimo high
Shimo qtrs
Sos1
Sos2
Sunsweet
Utange
Vikwatani
March
June
Sept

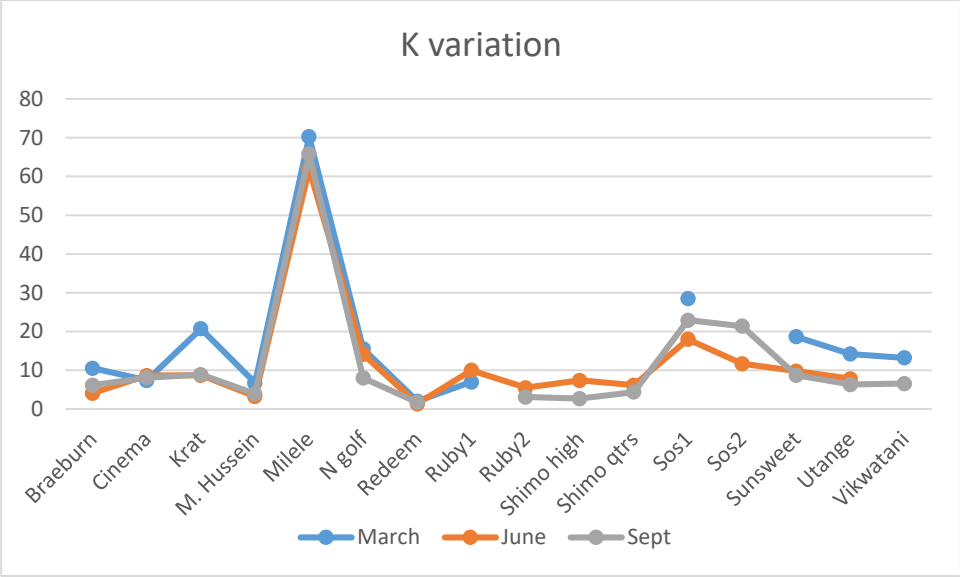
K variation
80
70
60
50
40
30
20
10
0
Braeburn
Cinema
Krat
M. Hussein
Milele
N golf
Redeem
Ruby1
Ruby2
Shimo high
Shimo qtrs
Sos1
Sos2
Sunsweet
Utange
Vikwatani
March
June
Sept

APPENDIX III

Cross plots showing the relationships between EC/TDS and the cations & anions (pre-monsoon)

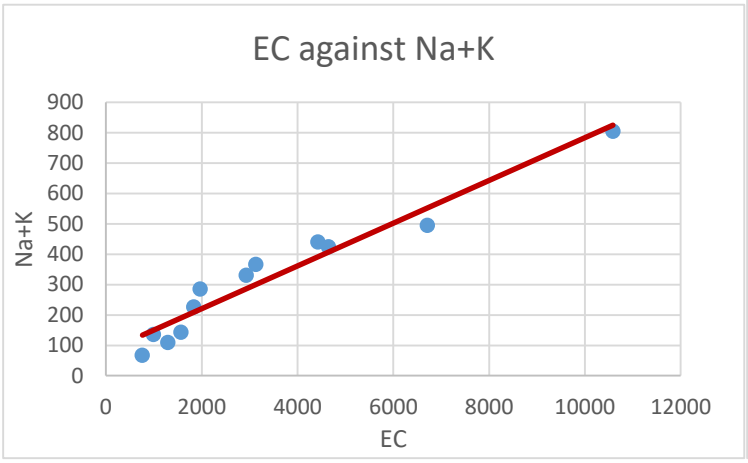

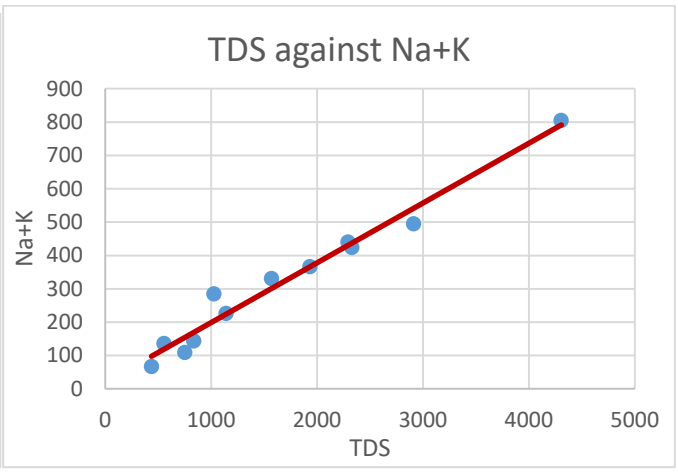

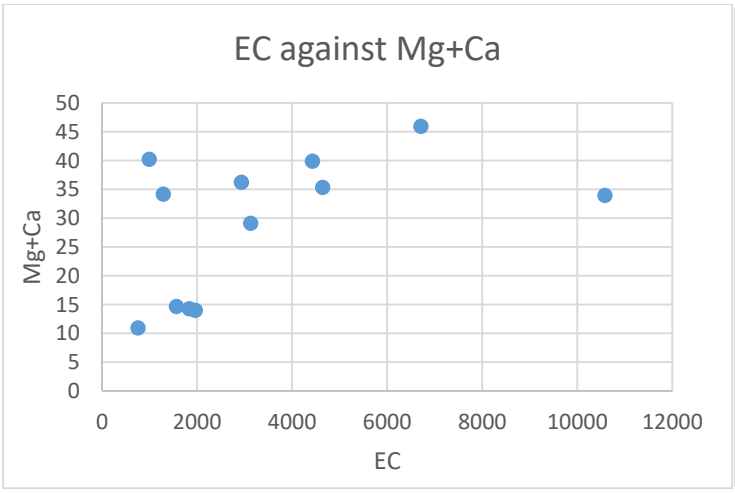

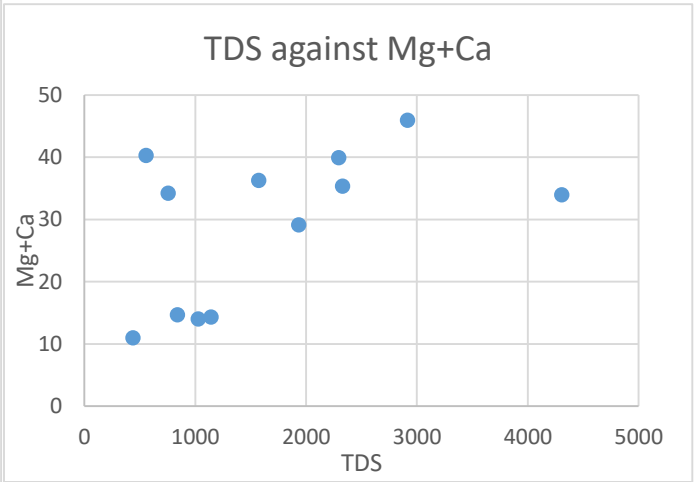

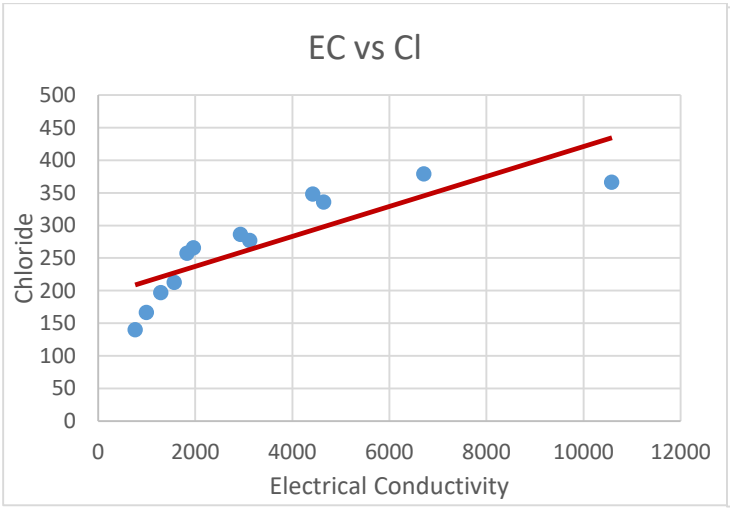

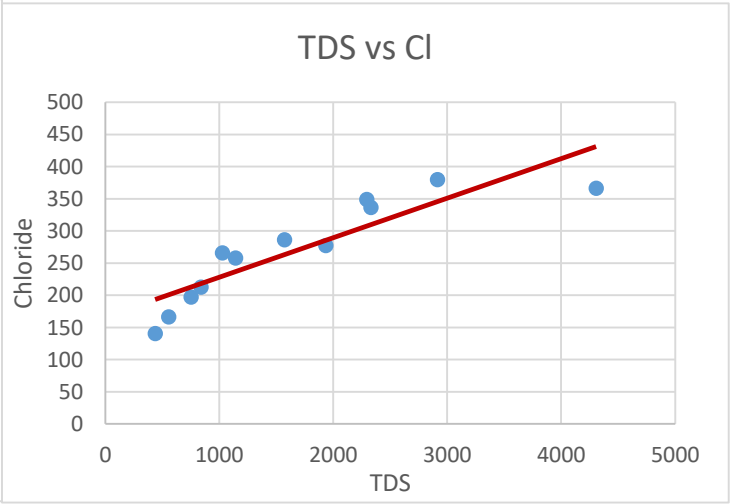

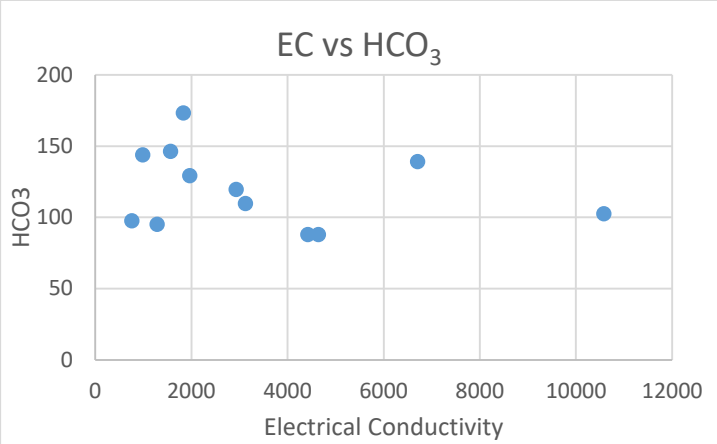
EC vs HCO3
HCO3
Electrical Conductivity
0
50
100
150
200
0
2000
4000
6000
8000
10000
12000

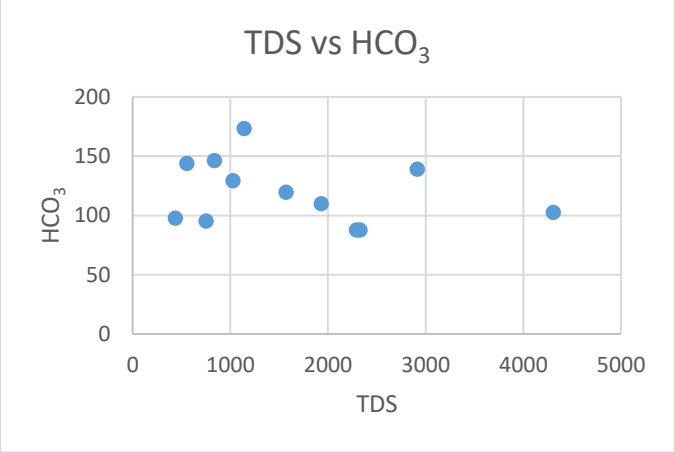
TDS vs HCO3
HCO3
TDS
0
50
100
150
200
0
1000
2000
3000
4000
5000

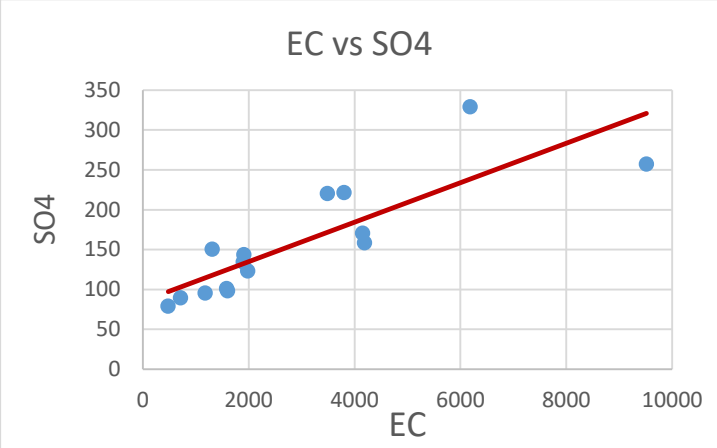
EC vs SO4
SO4
EC
0
50
100
150
200
250
300
350
0
2000
4000
6000
8000
10000

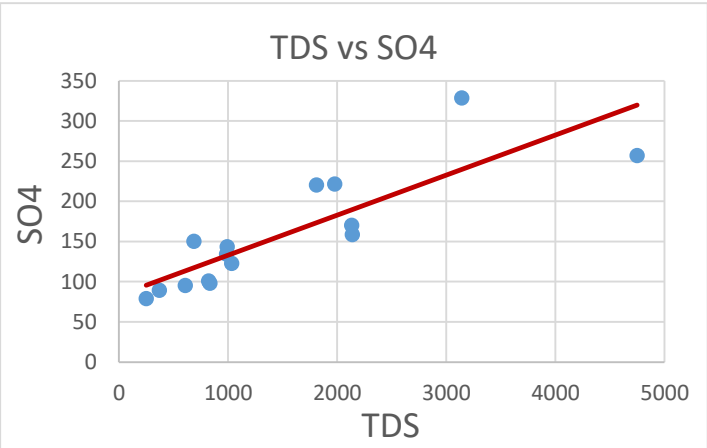
TDS vs SO4
SO4
TDS
0
50
100
150
200
250
300
350
0
1000
2000
3000
4000
5000

APPENDIX IV

Table of conversion from mg/l to meq/l

		Cations				Anions		
SN	**Sample location**	**Na (meq/l)**	**K (meq/l)**	**Ca (meq/l)**	**Mg (meq/l)**	**HCO3 (meq/l)**	**Cl (meq/l)**	**SO4 (meq/l)**
W1	**Braeburn**	7.450298	0.15744	0.5445	0.124117	2.304922	3.825486	1.986147
W2	**Cinema**	8.030756	0.20736	0.7395	0.125641	2.535414	4.098735	2.047854
W3	**Krat**	2.062691	0.227072	0.057	0.089956	1.786314	3.721257	1.643624
W4	**M. Hussein**	3.204476	0.100864	0.675	0.115954	2.055222	3.788865	3.134886
W5	**Milele**	31.70127	1.683712	0.0095	0.144692	0.845138	7.885155	5.357178
W6	**N golf**	12.97443	0.2048	0.216	0.136779	1.786314	3.876192	4.612928
W7	**Redeem**	3.074036	0.044544	0.6595	0.070822	1.459784	3.312792	1.86506
W9	**Ruby2**	9.378636	0.079104	0.2855	0.122909	3.10204	3.481812	2.801335
W10	**Shimo high**	4.426264	0.068352	0.922	0.12021	1.767107	3.91563	2.102739
W11	**Shimo qtrs**	6.843752	0.111872	0.728	0.126299	1.728691	3.949434	2.561015
W12	**Sos1**	20.1182	0.58624	0.1445	0.133322	1.210084	4.262121	3.30273
W13	**Sos2**	19.15729	0.54784	0.2035	0.136171	1.747899	4.205781	4.592419
W14	**Sunsweet**	7.824661	0.22272	0.1865	0.13832	1.517407	3.872174	3.550638
W15	**Utange**	8.852528	0.16128	0.1465	0.122934	2.564225	3.449755	2.987239
W16	**Vikwatani**	16.33413	0.168448	0.149	0.145317	2.708283	3.801771	6.851499
	Conversion rates from mg/l to meq/l	**0.04348**	**0.0256**	**0.05**	**0.0833**	**0.0164**	**0.02817**	**0.02083**

APPENDIX V

NaCl variation in the groundwater across the study area for pre-monsoon, rainy season and post-monsoon

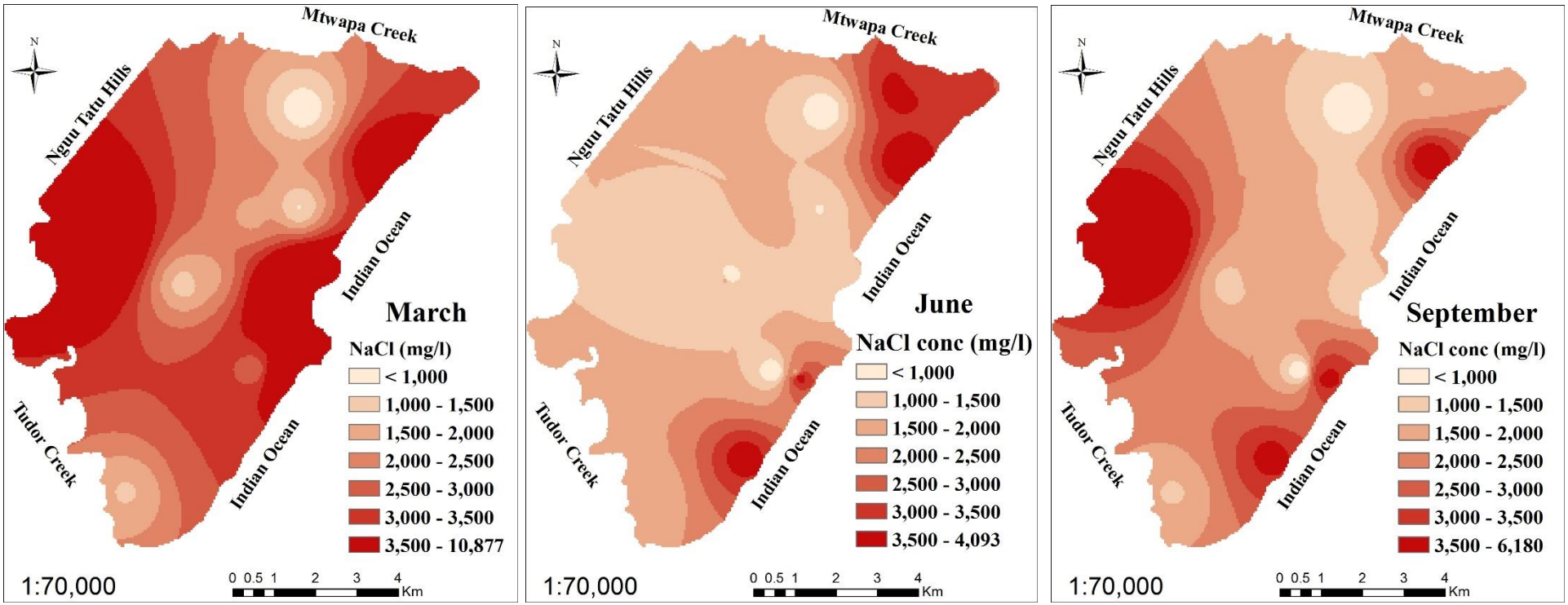

a. **b.** **c.**

NaCl variation in the groundwater across the study area in; (a.) March (b.) June (c.) September

APPENDIX VI

Correlation coefficients for salinity induces for the rainy season and post-monsoon

Table 4.8: Correlation for Salinity Indices (June)

Parameters	EC	TDS	Cl/HCO3	Ca/Na	Na/Cl	(NaCl)
EC	1	-	-	-	-	-
TDS	**1**	1	-	-	-	-
Cl/HCO3	**0.47**	**0.48**	1	-	-	-
Ca/Na	-0.34	-0.34	-0.07	1	-	-
Na/Cl	**0.40**	**0.40**	**-0.48**	-0.26	1	-
(NaCl)	**0.999**	**0.999**	**0.49**	-0.34	0.39	1

Table 4.8: Correlation for Salinity Indices (September)

Parameters	EC	TDS	Cl/HCO3	Ca/Na	Na/Cl	(NaCl)
EC	1	-	-	-	-	-
TDS	**1**	1	-	-	-	-
Cl/HCO3	**0.76**	**0.75**	1	-	-	-
Ca/Na	-0.55	-0.55	-0.23	1	-	-
Na/Cl	**0.74**	**0.74**	**0.35**	-0.71	1	-
(NaCl)	**0.998**	**0.998**	**0.80**	-0.53	0.71	1

APPENDIX VII

The GALDIT factors

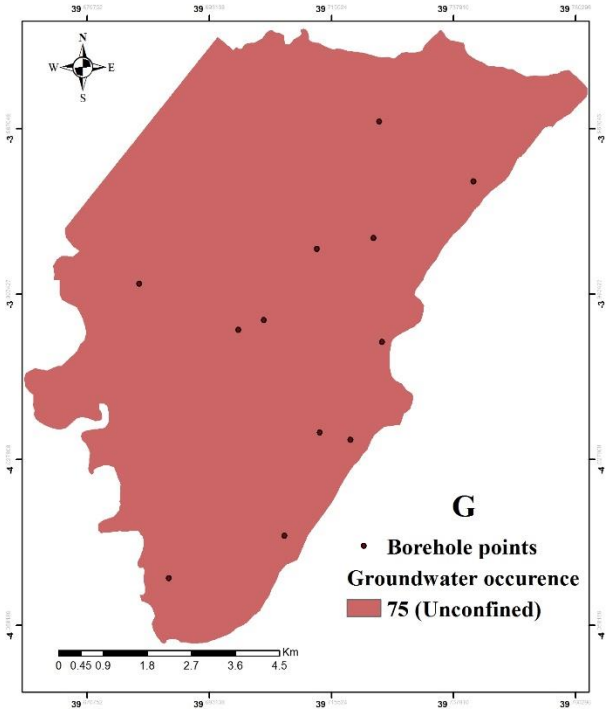

Parameter G (Groundwater occurrence)

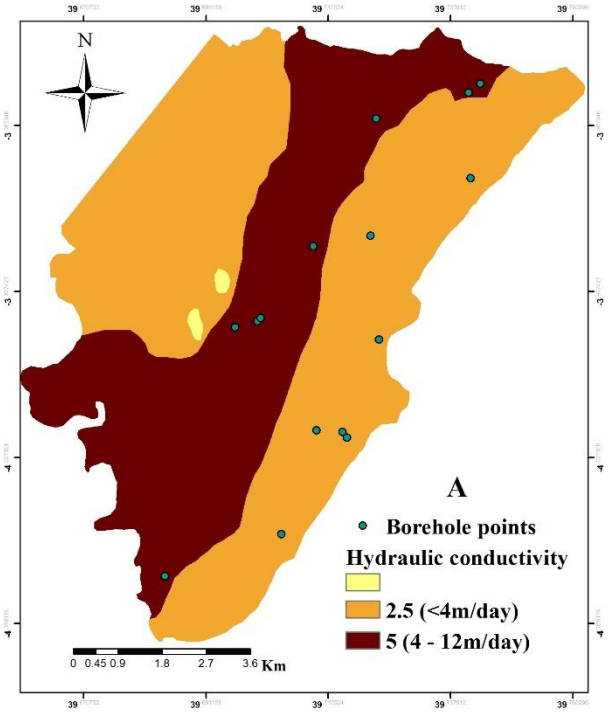

Parameter A (Aquifer hydraulic conductivity)

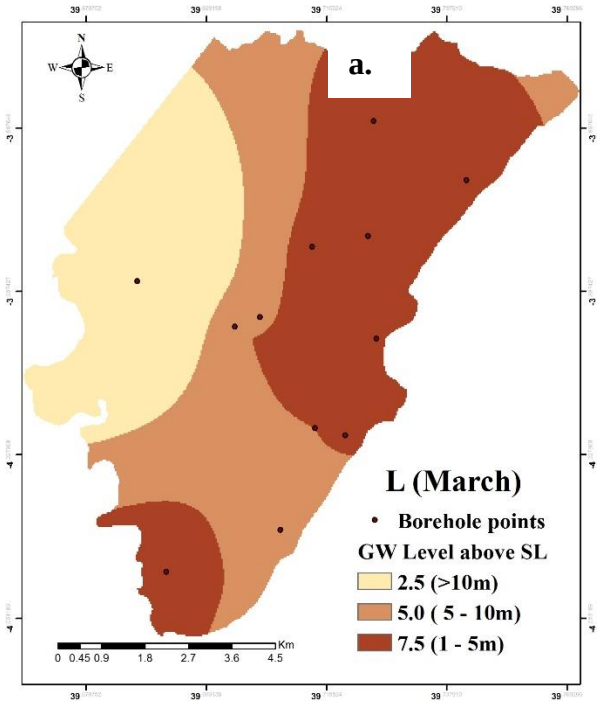

b.

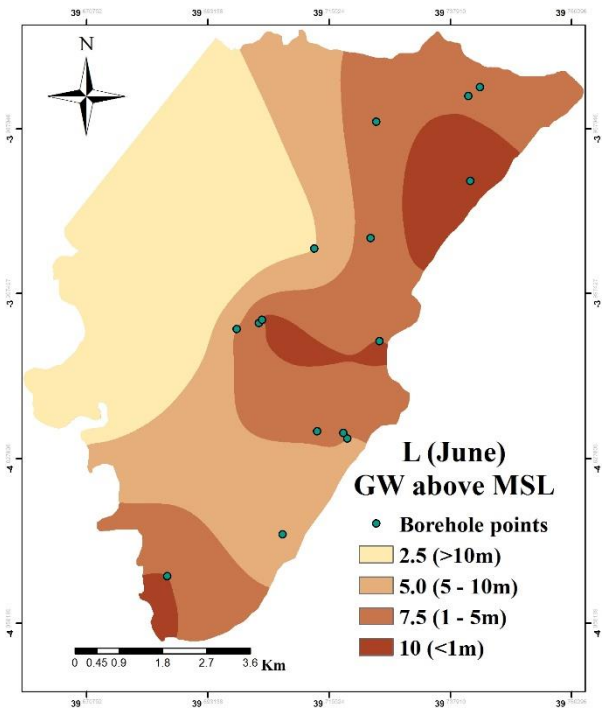

Parameter L (Level of GW above SL in March)

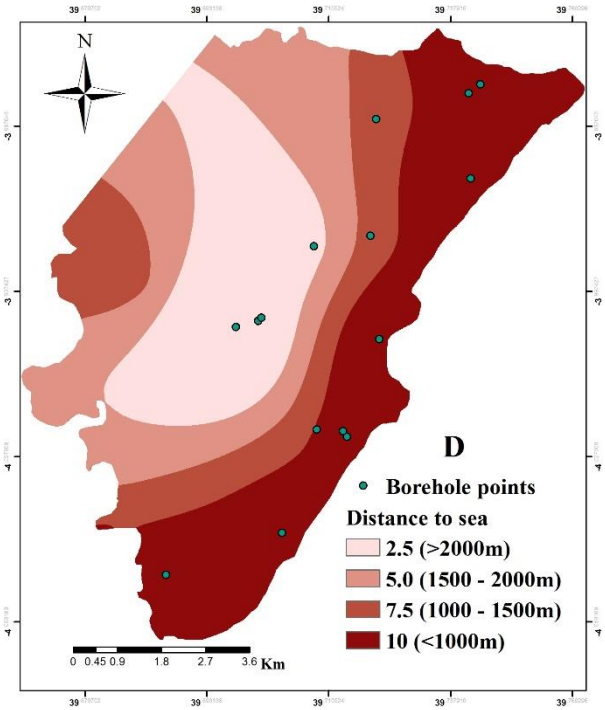

Parameter L (Level of GW above sea level for June)

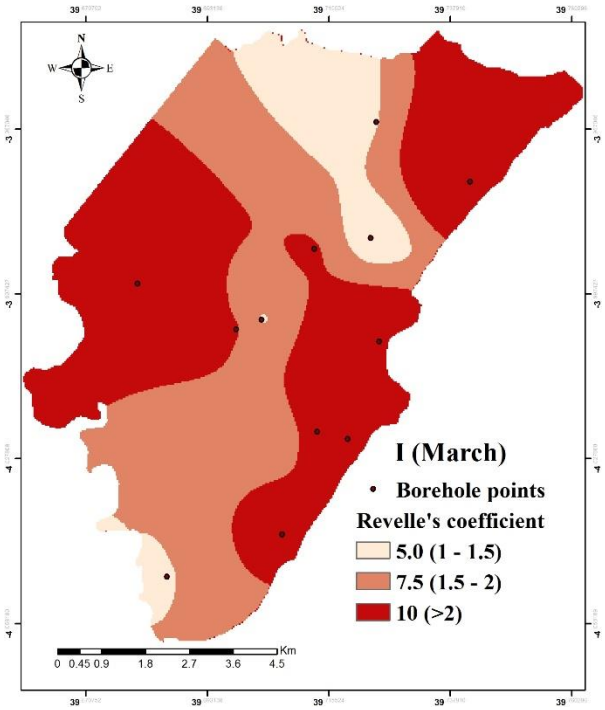

Parameter D (Distance to the shore)

Parameter I- Existing status of SWI (March

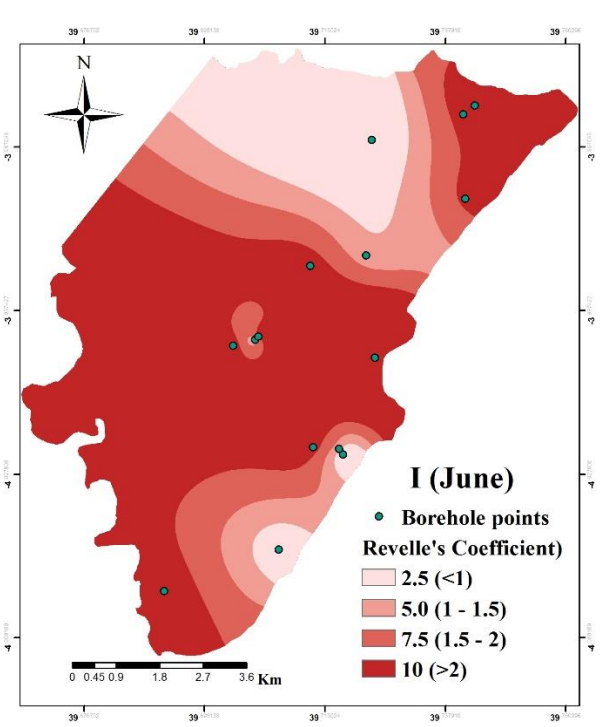

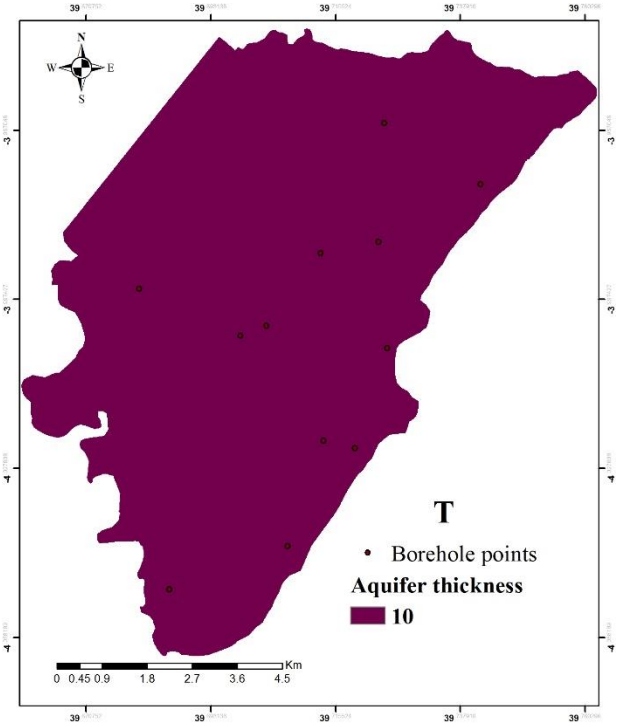

Parameter I- Existing status of SWI (June)

Parameter T: (Thickness of the mapped aquifer)

APPENDIX VIII

LIST OF PUBLICATIONS AND CONFERENCE PROCEEDINGS

Idowu, T. E., Nyadawa, M., & K'Orowe, M. O. (2016). Seawater Intrusion Vulnerability Assessment of a Coastal Aquifer: North Coast Of Mombasa, Kenya as a Case Study. *Int. Journal of Engineering Research and Application*, *6*(8, (Part -3)), 37–45. ISSN: 2248-9622

Idowu, T. E., Nyadawa, M., & K'Orowe, M. O. (2016). Assessment of Groundwater Salinity and Impact of Seawater Intrusion on a Coastal Aquifer –North Coast of Mombasa as the Case Study. In: Alain L.F (ed), Proceedings of *2016 Fourth International Annual Conference, Society for Advancement of Science in Africa.* In view for publication by Cambridge publishers July 2017.